GROWTH, ARCHITECTURE, CELL SEPARATION, ELECTROPHYSIOLOGY AND SUCROSE TRANSPORT OF RIPENING RICE CARYOPSES

A Dissertation

Presented to the Faculty of the Graduate School

of Cornell University

in Partial Fulfillment of the Requirements for the Degree of

Doctor of Philosophy

by

Jordan Oliver Hay

May 2005

GROWTH, ARCHITECTURE, CELL SEPARATION, ELECTROPHYSIOLOGY AND SUCROSE TRANSPORT OF RIPENING RICE CARYOPSES

Jordan Oliver Hay, Ph.D.

Cornell University 2005

Rice (*Oryza sativa* L.) life cycle and yield depend on the partitioning of assimilated carbon to ripening caryopses. Structural and functional aspects of this important process were investigated. First, spatiotemporal dynamics of ripening were assessed. Panicle fresh weight accumulation was maximum after three weeks and had a maximum rate after twelve days. Panicle architecture and ripening asynchrony were reduced to the form of an annotated panicle array. This format permitted a quantitative, computational approach to panicle consensus generation, data analysis and graphical display. Next, the separability of caryopsis tissues was assessed. The caryopsis coat was mechanically isolated from most of the embryonic tissues and facially separated into outer and inner coats from within the tube cell layer. Pectolyase Y-23 compromised adhesion between the maternal nucellus and embryonic aleurone and between endosperm cells. Viable protoplasts were prepared from approximately 10% of the isolated endosperm cells. Low protoplast yield was correlated with low viability of the isolated cells. Third, the mechanism of sucrose uptake by the aleurone was studied. The sucrose concentration-dependence of uptake rate had a nonsaturable component and a relatively small saturable component. Finally, electrophysiology of the caryopsis coat was assessed. Membrane potentials of the aleurone and nucellus were approximately −60 mV and −80 mV, respectively, and invariable over a range of bath conditions. Sucrose negligibly depolarized the aleurone membrane potential. Thus, it was not possible to confirm that the saturable sucrose influx was mediated by a cotransport system. Overall, the work has increased the experimental accessibility of ripening panicles and caryopses for research on the control of carbon partitioning.

BIOGRAPHICAL SKETCH

Jordan Oliver Hay received a degree of Bachelor of Science with a major in Plant Biology from the University of California at Davis on June 19, 1998. His mentors for undergraduate research and teaching included Wendy Silk, Bruno Moulia, Robert Thornton and Judy Jernstedt. The following August he entered a Doctor of Philosophy program in the Field of Plant Biology at Cornell University. He will do postdoctoral research and teaching at Myongji University.

To God Most High, the God of all comfort

Though the fig tree does not bud and there are no grapes on the vines, though the olive crop fails and the fields produce no food, though there are no sheep in the pen and no cattle in the stalls, yet I will rejoice in the Lord, I will be joyful in God my Savior.

Habakkuk 3:17-18

I tell you the truth, unless a kernel of wheat falls to the ground and dies, it remains only a single seed. But if it dies, it produces many seeds.

John 12:24

ACKNOWLEDGMENTS

God enabled everything. Kyoung lovingly helped me a lot at home, lab and the greenhouse. My family and friends were supportive and brought me joy. Many people spent a lot of time and energy to mentor and help me: Roger Spanswick, Susan McCouch and Larry Walker, dissertation; Karl Niklas, Peter Davies, Tom Silva, Carol McFadden, Tyson Sacco, Kathryn Baker, Michael Burgess, Anne Plescia, David Winkler, Carolyn Eberhard, Monica Howland, Sara Jayne Hymes and Virleen Carlson, teaching; Ajay Garg, Jukon Kim, Miguel Pineros and Randy Wayne, research; Fumio Onishi, Andrew Leed, Kim Goodwin, Christy Lee, Aimee Roberts and Bill Thompson, rice culture; Kyoung Hay, Sharon Ciferri, Millicent Maynard and Kelly Craft, outreach; Hairhin Diffloth, Korean; Heewon Chun, Eunha Choi, Tim Huh, James Kim, Yangmin Lee, Hyuck Woo, Shiyong Yoo, Jay Yun, John Sotero, Bill and Janice Arion, Donnie Houston, Aloja and Peyi Airewele, Prince Bhebe, Sven Pedersen, Elizabeth Williams, Michael Corriero, Chip Adams-Compton, Jury and Juheon Choi, Eunsoo and Boknam Jee, Jiyun Hwang and Sojin Lee, Christian discipleship. Thank you everyone!

TABLE OF CONTENTS

LIST OF FIGURES

LIST OF TABLES

CHAPTER 1

REVIEW OF SUCROSE TRANSPORT IN RIPENING CARYOPSES AND RESEARCH OBJECTIVES

Justification of Rice Research

The growth of world population and its dependence on rice for consumption justify rice research. Rice is second only to wheat in terms of land area cultivated (Hoshikawa, 1989). Over half of the world population consumes primarily rice in their diet. The United Nations declared 2004 as International Year of Rice with the slogan "rice is life." Indeed, much rice research has the long-term goal of helping human lives through the improvement of rice. It has been argued that the focus of rice research should be yield (Jennings et al., 1979; Sasaki, 2003). However, in addition to its agronomic importance, rice has gained importance as a model monocot for basic research in plant biology. Some of this research actually makes possible and gives direction for practical rice improvement approaches.

General Background and Thesis

This dissertation is related to the general, physiological principle of assimilate partitioning. For flowering plants such as rice, according to the alternation of generations life cycle, the dominant, heterosporous sporophyte functions to produce spores by meiosis, which then divide by mitosis and give rise to multicellular, heterotrophic gametophytes. The sporophyte retains the megaspores and nourishes the megagametophyte. In terms of desiccation tolerance for life on land, these adaptations are more derived than those of seedless vascular plants, which shed spores into the environment and develop independent, often autotrophic, gametophytes. After double fertilization, the embryo and endosperm, together with the integuments, form the seed. The ovary gives rise to the fruit, which, analogous to the spores of seedless vascular plants, is the unit of dispersal. Seeds and fruit, in general, are also heterotrophic.

Hence, in a division of labor, vegetative, photoautotrophic organs such as leaves support heterotrophic, reproductive ones. Assimilate partitioning makes possible this division of labor. For example, certain tissues assimilate inorganic carbon dioxide into organic sugar, some of this sugar is allocated to the synthesis of the partitioned form, sucrose in the case of rice, and the plant partitions sucrose among different organs by translocating it long distances. Upon arrival, the recipient organs transport sucrose short distances to tissues that can use the sucrose, for example, for the storage of starch. Practically, assimilate partitioning determines the harvest index, or proportion of the plant's dry matter that is edible, and can be modified to increase yield. Endosperm, the main edible portion of the rice plant, grows heterotrophically, stores compounds during maturation and then hydrolyzes them to nourish the growing embryo during germination. Hence, endosperm development depends on assimilate partitioning and transport. Plants transport assimilates such as sucrose primarily via the symplasm, which is sometimes in series with transport via the apoplasm. Hence, transport across membranes is needed. Indeed, the biology of sugar and amino acid transporters is an active field of research (Lalonde et al., 2004).

At the time the topic of this dissertation was proposed, it had recently been demonstrated that sucrose transporters are expressed in ripening panicles (Hirose et al., 1997). However, there was little work on uptake by endosperm and it was unclear what contribution this process made to the control of dry matter partitioning. Furthermore, there were experimental limitations that needed to be overcome. Hence, a major part of this dissertation analyzes the experimental accessibility and mechanism of sucrose uptake by ripening rice endosperm.

What is Caryopsis Ripening?

The rice fruit is a grain (Figure 1). It consists of a seed and parts that physically associate with the seed when it is separated from the plant. This definition of the fruit

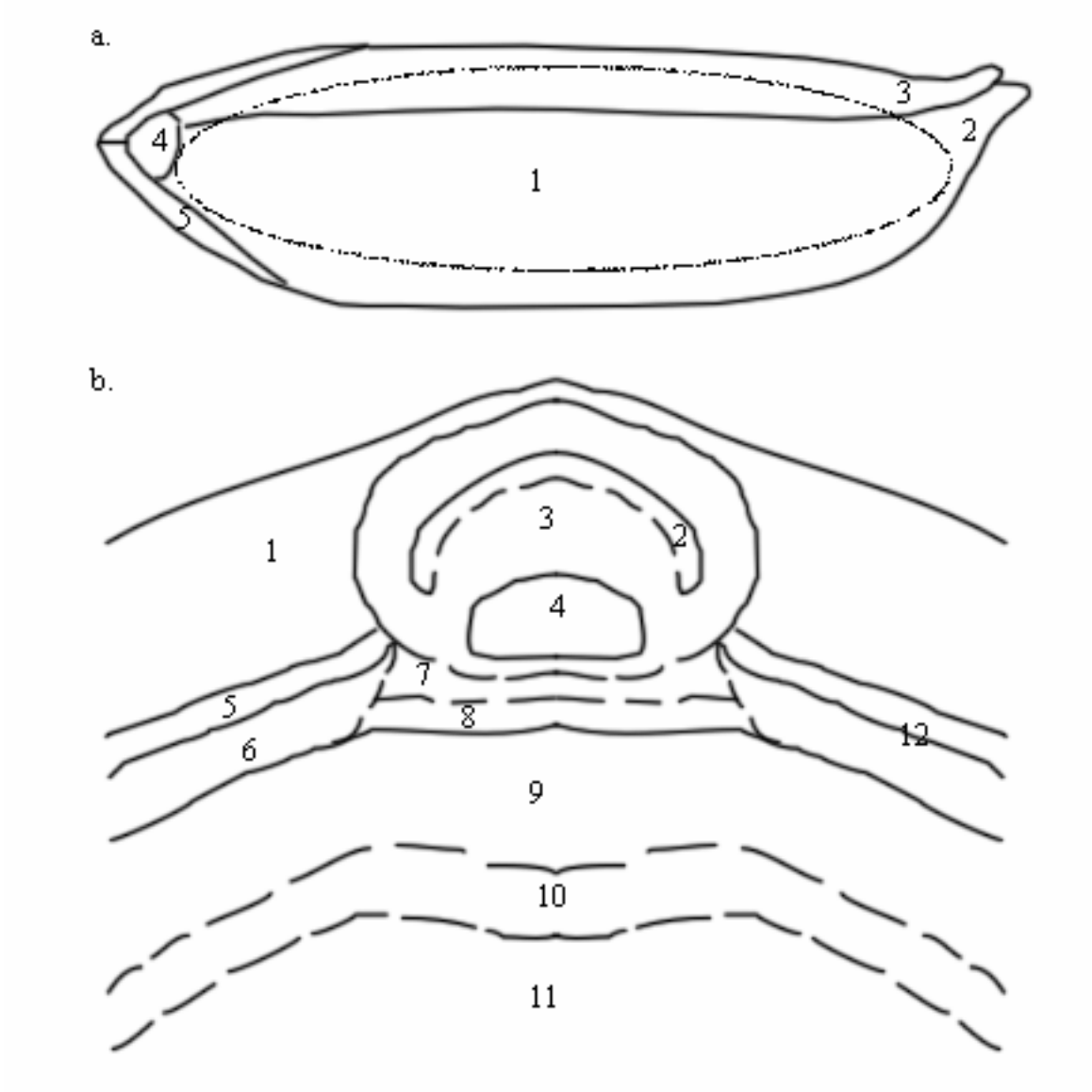

Figure 1 Rice grain structure. Grain morphology (a). The labeled structures of the rice grain are caryopsis (1), lemma (2), palea (3), rachilla (4) and sterile lemma (5). Caryopsis anatomy (b). Diagram is a cross section of palea side of caryopsis and modified from Oparka and Gates (1981b). Labeled tissues are pericarp (1), phloem (2), vascular parenchyma (3), xylem (4), inner integument (5), nucellar epidermis (6), pigment strand (7), nucellar projection (8), aleurone (9), subaleurone (10), inner starchy endosperm (11) and cuticle (12).

includes the caryopsis (seed and pericarp), hull (sterile lemmas, rachilla, lemma, palea) and other parts such as remnants of the androecium.

Ripening is the process of formation of a grain from a spikelet (pedicel, hull, lodicules, stamens, pistil) after the inception of the zygote and primary endosperm nucleus. Hence, initiation, growth and development of spikelet organs as well as pollination and double fertilization lead up to ripening. Ripening, which follows these events, is an integration of many partial processes. This review focuses on sucrose transport within the maternal tissues and endosperm of rice and wheat caryopses.

Endosperm development is a good indicator of the progress of caryopsis ripening. Endosperm transitions through three types: coenocytic, alveolar and cellular (Olsen, 2001). Coenocytic endosperm forms during free-nuclear division of the primary endosperm nucleus. The volume of this endosperm rapidly enlarges in concert with growth of the surrounding maternal tissues. During this time, cells of the maternal tissues elongate and differentiate to form a vascular bundle that will supply the endosperm with sucrose. Alveolar endosperm undergoes cellularization, which involves nuclear division and cell wall formation. Cellular endosperm undergoes cell division and cell differentiation. It metabolizes sucrose into starch, which is deposited in amyloplasts. Caryopses with endosperm at this stage of development are the focus of this review.

Control of Caryopsis Ripening

Caryopsis ripening depends on many complex processes such as morphogenesis, photosynthesis, phloem loading, assimilate translocation, phloem unloading and biochemistry. However, the simple, convenient measure of dry weight exists. Importantly, caryopsis dry weight is only a single component of yield. Other factors such as the number of caryopses that ripen are also important. Caryopsis dry weight is the integral of dry matter accumulation rate over the duration of ripening.

Development of the endosperm and its filling with starch are important features of dry weight accumulation. Wheat caryopsis dry weight positively correlates with number of endosperm cells (Singh and Jenner, 1982). Rice endosperm starch, which accumulates in the amyloplasts of endosperm cells, is the greatest component of caryopsis dry weight (Champagne et al., 2004). The time course of accumulation is similar for wheat endosperm starch and caryopsis dry weight (Jenner and Rathjen, 1977). Hence, endosperm starch storage and dry matter accumulation are almost synonymous.

Because the endosperm is heterotrophic, dry weight accumulation necessitates sucrose uptake and conversion to starch. Rice endosperm starch accumulation rate and sucrose concentration increase with time and reach a maximum nine days after flowering (Singh and Juliano, 1977). Interestingly, wheat starch accumulation rate saturates with regard to sucrose concentration of panicle culture media (Jenner, 1970). Jenner and Rathjen (1972a; 1972b) concluded that the rate of sucrose transport from sites of synthesis to the caryopsis does not limit starch accumulation. These results suggested that either sucrose metabolism or sucrose transport within the caryopsis limits starch accumulation. Transport appeared more limiting because the sucrose concentration at which saturation of endosperm starch accumulation rate occurred was higher for isolated endosperm than cultured panicles. Indeed, Jenner et al. (1991) proposed a saturable model for the rate of sucrose transport to the endosperm via the maternal tissues. Eventually, endosperm starch accumulation rate declines after reaching a maximum. This is not due to decreased supply of sucrose to the caryopsis but instead to processes in the endosperm (Jenner and Rathjen, 1975, 1977).

In conclusion, the caryopsis itself contributes to the control of rate and duration of endosperm starch accumulation. In fact, the conversion of sucrose to starch in ripening endosperm depends on a suite of metabolic and transport partial processes that operate internally and externally to the caryopsis and can each exert a measure of

control over the flux of carbon into the endosperm (Farrar, 1996). Metabolic control analysis (ap Rees and Hill, 1994) can be used, in principle, to quantify the relative contribution each partial process makes to this flux.

Long Distance Transport in the Caryopsis

The rice caryopsis contains phloem that transports assimilates long distances. The mechanism for this involves mass flow driven by a turgor pressure gradient. The chemical nature of these assimilates has been analyzed. Rice translocates assimilated carbon as sucrose (Chino et al., 1987). It has a concentration of approximately 570 mM in the sieve tubes of the uppermost internode one week after panicle emergence (Hayashi and Chino, 1990). Sucrose concentration in the flag leaf sheath phloem increases during caryopsis ripening and is not influenced by starch deposition (Shimada et al., 2004). There are four vascular bundles in the caryopsis of wheat. Three supply the carpel and are broken up during caryopsis elongation. The other one, located parallel to the caryopsis axis and fused with the palea side of the pericarp, differentiates during caryopsis elongation (Lingle and Chevalier, 1985) and facilitates long distance longitudinal transport of assimilates during ripening (Patrick et al., 1991). In rice, the vascular tissues of the caryopsis, rachilla and pedicel are continuous (Zee, 1972). In wheat and barley, the number of sieve elements varies (28-58) along the length of the caryopsis with the fewest sieve elements towards the apex (Lingle and Chevalier, 1985). During caryopsis elongation the single ovule, which fuses to the pericarp, develops into a seed. Rice mutants that do not have anatropous (bent downward) ovules have fully ripened caryopses (Yamaki and Nagato, 2001). Hence, the differentiation of vascular tissue for caryopsis ripening does not require ovule anatropy.

Short Distance Transport through the Maternal Tissues of the Caryopsis

In the caryopsis, the importing phloem is separated a short distance from the endosperm by layers of maternal tissues. As a result, the maternal tissues must transport assimilates that are just unloaded from the phloem to the endosperm. Following the conclusion that transport processes within the caryopsis could contribute to the control of starch accumulation rate in the endosperm (Jenner and Rathjen, 1972a, b), attention was given to the cellular pathway that facilitates the transport of sucrose from phloem to endosperm. Structural features of the cellular pathway were assessed for insight into mechanisms of transport. In wheat, Jenner (1974) proposed a radial transport pathway for sucrose from phloem to endosperm that included passage through the pigment strand, nucellar projection, endosperm cavity and aleurone. Transport steps along this pathway that could possibly rate-limit movement were proposed. The movement of dyes out of the phloem confirmed this cellular pathway and suggested that sucrose moves symplasmically from sieve element to the nucellus, crosses nucellar plasma membranes to the apoplasm and then is taken up by the aleurone and starchy endosperm (Wang et al., 1994). Plasmodesmata diameters and frequencies along the cellular pathway through these maternal tissues are sufficient to accommodate the flux (Wang et al., 1995a). The mobility of tracers with known Stokes radius suggested that these plasmodesmata form aqueous channels approximately 8 nm in diameter (Fisher and Cash-Clark, 2000a).

Similarly, sieve elements, companion cells, vascular parenchyma, pigment strand and nucellus (Figure 1) form a symplasmic domain in rice. Unlike wheat, in addition to radial transport, circumferential movement through the nucellar epidermis is possible (Oparka and Gates, 1981a, b). The nucellar epidermis appears to be specialized for this function. The cells are circumferentially elongated and have

cellulosic wall thickenings that may delay crushing of the cells as the ripening endosperm compresses the maternal tissues (Ellis and Chaffey, 1987).

The mechanism of transport through the maternal tissues is not fully understood. Two possible mechanisms of transport of sucrose through maternal tissue plasmodesmata are diffusion and bulk flow. The driving forces for diffusion and bulk flow are concentration gradient and turgor pressure gradient, respectively (Patrick and Offler, 1996). Sieve element unloading may regulate the rate of conversion of sucrose to starch. This is suggested by the fact that the greatest sucrose concentration drop is between sieve element and adjacent vascular parenchyma (Fisher and Wang, 1993, 1995). This results in a huge turgor differential of approximately 1 MPa (Fisher and Cash-Clark, 2000b). Hence, bulk flow through plasmodesmata may be an important mechanism for sieve element unloading. From studies of multicellular trichomes, it has been proposed that plasmodesmata are negatively sensitive to turgor and operate to control unloading flux (Oparka and Prior, 1992). In wheat, there is a major sucrose concentration drop between sieve element (540 mM) and apoplasm of the maternal/embryonic interface, or endosperm cavity (65 mM), a distance of approximately 1 mm (Fisher and Gifford, 1986). Sucrose concentration gradients between the phloem of rachis, pedicel and caryopsis were not found. At a finer level of spatial resolution, it was shown that sucrose concentration of the maternal tissues decreases from vascular tissue to the endosperm cavity (Fisher and Wang, 1995). From a flux of 6.5×10^{-5} mol/m^2/s the permeability coefficient was estimated to be 6×10^{-6} m/s. It was concluded that diffusion is sufficient to account for transport. In addition, a potential turgor pressure differential of 0.2 MPa between vascular parenchyma and nucellus could be estimated, showing that bulk flow may operate along the transport pathway. However, observations of symplasmic movement of dyes from the nucellus to the vascular parenchyma, against the flow of imported sucrose,

suggests that diffusion is the dominant mechanism of transport (Wang and Fisher, 1994b).

Sucrose Efflux to the Apoplasm by the Maternal Tissues

The sucrose in the maternal tissues of wheat is modeled as a pool totally available for transport to the endosperm (Fisher and Wang, 1993). However, symplasmic discontinuity requires an apoplasmic transport step at this interface (Lalonde et al., 2003). In caryopses of rice and wheat, this step is between the nucellus and endosperm. Sucrose efflux to the apoplasm by the nucellus may be a step that exerts major control on the flux of sucrose into the endosperm. The wall ingrowths of the nucellus of wheat, which increase plasma membrane surface area, are necessary to supply the apoplasm of the maternal/embryonic interface with enough sucrose to keep pace with starch accumulation (Wang et al., 1995a). However, the mechanism of transport across the plasma membrane is not fully understood. Efflux is inhibited by the sulphydryl group modifier *p*-chloromercuribenzene-sulphonic acid (PCMBS), is insensitive to pH, respiratory inhibitors, protonophores, potassium concentration and osmolarity (Wang and Fisher, 1995) and is stimulated by auxin (Darussalam et al., 1998). Hence, transport seems to be passive, protein-mediated and not via pores. In contrast, there is evidence for sucrose efflux via pores in the plasma membranes of pea seed coat cells (Van Dongen et al., 2001). The nucellus is equipped with sucrose transporters and proton pumps but has only proton pumping activity (Bagnall et al., 2000). Sucrose transporters could theoretically facilitate efflux (Borstlap and Schuurmans, 2004). However, this remains to be demonstrated.

Sucrose Uptake by the Endosperm

Symplasmic discontinuity requires sucrose retrieval by the endosperm (Lalonde et al., 2003). Sucrose encounters the aleurone first in the pathway of uptake. In wheat, there is a large resistance to transport in the aleurone apoplasm (Wang et al.,

1994) probably as a result of the properties of aleurone cell walls (Bacic and Stone, 1981a, b). This suggests an importance for transport across plasma membranes of the aleurone. However, the aleurone alone is not sufficient to support the required rate of sucrose retrieval (Niemietz and Jenner, 1993). Plasma membrane surface area of aleurone plus subaleurone is sufficient to accommodate the radial flux of sucrose from the aleurone to the starchy endosperm, and, furthermore, the density of plasmodesmata is also sufficient (Wang et al., 1995b). There is no evidence for longitudinal movement of sucrose in the endosperm (Patrick et al., 1991). The protonophore carbonylcyanide-m-chlorophenyl hydrazone (CCCP) and PCMBS inhibit uptake by the aleurone but not starchy endosperm (Wang et al., 1995b). This suggests that sucrose transporters in the outer endosperm mediate sucrose uptake.

Sucrose Transporters

Sugar transporters, such as those for sucrose, belong to the major facilitator superfamily (Pao et al., 1998) and are essential for the transport of assimilates from autotrophic sources to heterotrophic sinks (Bush, 1999). Interestingly, thirty out of 269 genes preferentially expressed during rice grain ripening were various transporters (Zhu et al., 2003). Expression analysis of sucrose transporters has supported transporter-mediated flux of sucrose across the plasma membrane of endosperm cells during caryopsis ripening of many species (Hirose et al., 1997; Aoki et al., 1999; Weschke et al., 2000; Aoki et al., 2002).

Spatial patterns of expression suggest an important role for sucrose transporters in both maternal and embryonic tissues of the caryopsis. Sucrose transporters are in the plasma membranes of the maternal nucellus and embryonic aleurone (Furbank et al., 2001). Five sucrose transporters are expressed in the ripening grain (Aoki et al., 2003). Antisense expression of the rice sucrose transporter gene *OsSUT1* impairs ripening and germination but not the activity of source leaves

(Ishimaru et al., 2001; Scofield et al., 2002). Indeed, temporal patterns of OsSUT1 expression correlate well with the dynamics of caryopsis weight (Hirose et al., 1997; Furbank et al., 2001; Hirose et al., 2002). In addition to caryopsis tissues, this sucrose transporter is expressed in companion cells of the embryo (Matsukura et al., 2000). OsSUT2-5 seem to be more important during the early stages of ripening. However, there are times when there is overlap in the expression of all five genes (Aoki et al., 2003). Clearly, more work is needed to understand how each of these transporters is functioning.

The thermodynamics of sucrose transport is well understood. Sucrose transporters are directed inwardly across the plasma membrane. The change in free energy for the transport is positive. Energy required for the transport comes from ATP hydrolysis that is catalyzed by proton pumps, which concentrate protons to the outside of the plasma membrane. The driving force for sucrose transport is the electrochemical potential (μ) difference for protons:

$$\mu_{H^+}{}^{in} - \mu_{H^+}{}^{out} = RT \ln([H^+]^{in}/[H^+]^{out}) + F(\psi^{in} - \psi^{out})$$

where R is the gas constant, T the absolute temperature, F the faraday and ψ the electrical potential. Sucrose transporters couple sucrose transport to energetically favorable proton transport in the same direction. The maximum ratio of inside and outside sucrose concentrations is dependent on the ratio of proton concentrations and the membrane potential (Buckhout and Tubbe, 1996). Importantly, proton pumps, together with sucrose transporters and sucrose binding protein, are expressed in the vascular parenchyma, nucellus, aleurone and subaleurone (Bagnall et al., 2000; Furbank et al., 2001). The nucellus and aleurone/subaleurone have strong proton pumping activity. However, only uptake by the aleurone increases the pH of the surrounding medium and is inhibited by PCMBS. This suggests that the aleurone takes

up sucrose by cotransport with protons and the maternally expressed transporters have a different function.

Research Objectives

The long-term goal of this research was to assess the contribution of sucrose transport steps to the control of carbon flow into the endosperm of the ripening rice caryopsis. The major hindrance to this objective was the lack of suitable experimental systems to assess sucrose efflux by the maternal tissues and retrieval by the endosperm. Four objectives and rationales were defined. First, a system for growing rice year-round in the greenhouse was needed for the continuous supply of ripening grains. Second, tissue isolation methods were needed because there is not an apoplasmic cavity that separates endosperm and maternal tissues in the rice caryopsis. Third, an experimental system to assess the kinetics of sucrose uptake by aleurone protoplasts was needed to identify the mechanism(s) of sucrose retrieval across the plasma membrane of the aleurone cells and to determine kinetic constants useful in computing flux control coefficients by metabolic control analysis. Fourth, electrophysiological methods were needed to record aleurone membrane potentials and directly assess the activity of sucrose/proton cotransporters.

CHAPTER 2

GROWTH ANALYSIS OF RICE GRAIN PRODUCTION

Abstract

Plant organ development demonstrates the significance of carbon partitioning, an integration of many partial processes that vary in time and space over much of the structural hierarchy. Temporal dynamics of organ development for a system of continuous greenhouse production of rice (*Oryza sativa* L. cv. Jefferson) were observed. Curves were fit to temporal changes in vegetative and reproductive organ number and fresh weight. Emergence of leaves and tillers was linear with time. The first five panicles emerged over a period of ten days. Panicle fresh weight accumulation was nonlinear. Maximum fresh weight accumulation rate occurred after twelve days and maximum fresh weight after three weeks. These results were illustrative of whole plant carbon partitioning being a central process of rice plant growth and ripening.

Introduction

The manner by which photosynthetically assimilated carbon is allocated within the whole rice plant, partitioning, is apparent by the growth dynamics of new organs. The rice panicle illustrates this. The panicle differentiates, grows and emerges from sheathing leaves. Following emergence, it gradually bends under its own self-weight. Clearly, the panicle is an example of a sink that depends primarily on outside sources for the supply of assimilates that are used in respiratory, biosynthetic and storage processes. Sinks such as ripening caryopses eventually become sources that supply other sinks. The endosperm of the caryopsis supplies the growing embryo. Hence, the relationship between source and sink is central to the life cycle and an understanding of how it is regulated is essential for rice yield improvement.

For any study of partitioning during the ripening phase, it is necessary to grow plants to maturity. Therefore, an understanding of the growth and development of the whole plant is essential. The objective of this study was to establish a continuous system of rice grain production for investigations of carbon partitioning between panicle and ripening caryopses. Changes in vegetative and reproductive morphology were assessed. Methods included greenhouse production of *Oryza sativa* L. cv. Jefferson (McClung et al., 1997) and analysis of leaf, tiller and panicle development.

How much dry matter a plant accumulates over a time period is the integral of the growth rate and is related to yield by the harvest index (Yoshida, 1972). Along these lines, partitioning between a panicle and its ripening caryopses should not be studied in isolation. Indeed, partitioning is an integration of processes across vegetative and reproductive parts of the whole plant. The regulation of these processes is being dissected largely at the molecular level.

Meristematic activity of phytomers, vegetative units of axillary bud, internode, node and leaf (Nemoto et al., 1995), regulates partitioning to above ground vegetative sinks. Branching and leaf emergence occur during vegetative growth. The regulatory gene *MONOCULM1* is expressed in leaf axils and is required for the differentiation of tiller branch meristems (Li et al., 2003). Leaf differentiation rate is regulated by PLASTOCHRON1 (Itoh et al., 1998), a cytochrome P450 expressed in leaf primordia (Miyoshi et al., 2004).

Reproductive sinks originate from the differentiation of a panicle inflorescence meristem at the shoot apex. Next is the differentiation of panicle branch meristems and floral meristems, which is regulated by *LAX1* and *FZP2* (Komatsu et al., 2001). Differentiation of the panicle and its parts determines yield capacity, which, in terms of growth analysis is a function of the number of panicles, the number of

spikelets/panicle, the percent of spikelets that form ripened grains and the weight per grain (usually expressed on the basis of 1,000 grains; Matsushima, 1967).

Panicle differentiation is generally photoperiod-sensitive and induced under short days (Vergara and Chang, 1985). The time from initiation to emergence can also be photoperiod-sensitive (Yin and Kropff, 1998). Quantitative inheritance of a number of genes forms the basis for the timing of panicle differentiation. Numerous quantitative trait loci have been mapped and genes have been identified (Yano et al., 2001). Photoperiodic control of panicle differentiation involves photoreceptors, circadian clock proteins, mediators for the clock and integrators (Izawa et al., 2003). Phytochromes are required photoreceptors (Izawa et al., 2000). Hd1, a zinc finger transcription factor encoded by the rice ortholog of *CO*, is expressed diurnally and acts as an output of the circadian clock (Yano et al., 2000; Izawa et al., 2002). Output from the circadian clock that is coincident with long days inhibits flowering in rice (Hayama and Coupland, 2004). Hd1 regulates downstream genes, such as *Hd3*, which induces flowering under the proper photoperiod (Kojima et al., 2002). The rice ortholog of *LFY, RFL*, is expressed in the inflorescence meristem during the early stages of differentiation, not in panicle branch or floral meristems, suggesting that unlike *LFY, RFL* does not induce floral meristem differentiation (Kyozuka et al., 1998). *LFY* is a floral integrator and induces *Arabidopsis* inflorescence differentiation under long days (Izawa et al., 2003). Interestingly, overexpression of *LFY* in rice causes early heading (He et al., 2000).

A number of important processes occur in source leaves. These include diffusion of carbon dioxide from the air to mesophyll plastids, reduction of carbon dioxide in the stroma, export to the cytosol of organic carbon product or mobilized starch for the synthesis of sucrose and transport of sucrose to sites of phloem loading. Photophosphorylation is sustained by the recycling of inorganic phosphate released

during sucrose synthesis back to the stroma (Paul and Foyer, 2001), a process mediated by the triose phosphate/phosphate translocator (Wang et al., 2002).

After heading, many processes coordinate starch storage in the ripening caryopses. These include transport of sucrose, the main translocated carbohydrate (Fukumorita and Chino, 1982; Chino et al., 1987), across plasma membranes. Rice grains have invertases, some which are bound to the cell wall (Sung and Huang, 1994). Cell wall invertase activity and expression of the cell wall invertase gene *OsCIN1* in the caryopsis is maximal during the very early stages of ripening when the caryopsis is elongating (Hirose et al., 2002) suggesting that the transport of hexoses may contribute to caryopsis growth. Nevertheless, sucrose transporters are required because antisense expression of the sucrose transporter *OsSUT1* impairs ripening (Scofield et al., 2002). After sucrose uptake, conversion to hexose nucleotides is mediated by cytosolic sucrose synthase, production of hexose phosphate by UGPase (Abe et al., 2002), production of sugar nucleotides by AGPase, transport across the amyloplast membranes by a translocator and starch synthesis by enzymes in the stroma (James et al., 2003). AGPase, of which there are two isoforms, is mainly in the cytosol of the rice endosperm compared to the amyloplast (Sikka et al., 2001). Water stress increases the activities of sucrose synthase and starch synthesis enzymes (Yang et al., 2003). A kinase regulates sucrose synthase and is needed for starch accumulation (Asano et al., 2002). When AGPase activity in wheat and rice was increased by transgenic expression of a maize gene that encodes a modified subunit, percent ripening increased (Smidansky et al., 2002; Smidansky et al., 2003). Constitutive antisense expression of a gene that encodes a plastid adenylate kinase increases the level of adenylates, ADP-glucose, starch and yield in potato (Regierer et al., 2002).

There is much evidence for hormonal regulation of caryopsis ripening. Auxin is transported in rice phloem (Yokota et al., 1994). Abscisic acid, like water stress,

increases partitioning to ripening grains (Yang et al., 2001) while ethylene inhibits it (Yang et al., 2004). Root-derived cytokinin promotes endosperm cell division and dry matter accumulation (Yang et al., 2000; Yang et al., 2002).

Materials and Methods

Rice Culture

Oryza sativa L. cv. Jefferson was grown in greenhouse 2A at Kenneth Post Laboratory, Cornell University, Ithaca, NY, USA. Temperature settings were 30°C during the day and 25°C during the night. Supplementary lighting (12 hr/day) was provided by 400 watt high pressure sodium lamps. Only reverse osmosis water was used. Every week twelve pots (ITML 8" Royal Standard) were filled with moistened potting soil (Metromix 360) amended with Sprint iron chelate (1 g/pot), Osmocote (1 g/pot) and Peters Excel 20-10-20 liquid fertilizer (300 ml/pot, 200 ppm N) and arranged in four trays kept full with water. Two grains were planted 1 cm deep at the center of each pot. Three weeks later, the weaker seedling in each pot was discarded and weekly application of liquid fertilizer (same as basal application) to the soil commenced.

Reproductive Measurements

Twelve treatments of 0, 4, 6, 8, 10, 12, 14, 16, 18, 20, 24 and 28 days after heading before harvest were randomly assigned to the first heading tillers. The criterion used to assign a heading date to a single panicle was the appearance of any portion of the panicle above the flag leaf sheath that morning. If two or more tillers on the same plant headed within the same 24-hour period, the heading order was determined by the extent of panicle emergence. In the morning of the heading date, panicles were excised just below the neck node and immediately weighed. The same was done for the second through fifth heading tillers.

Third-order polynomials were fit to average fresh weights by polynomial regression using the least-squares method (Matlab). The equations and their first derivatives were evaluated for all days after heading. Time of occurrence of maximum fresh weight and fresh weight accumulation rate were determined from the appropriate root of the first and second derivative, respectively.

Vegetative Measurements

Tillers were counted on each plant once a week. The seedling after emergence was considered to have one tiller. Leaves of the main stem and first tiller (branch) were also counted as they emerged each day. A leaf was judged ligulated when its blade joint, the joint between the blade and sheath, was level with or above the blade joint of the leaf below. The coleoptile and first leaf, which does not have a blade joint, were not counted.

Results

One-week-old seedlings had one leaf that emerged from its surrounding sheath (Figure 2). This was termed a visible leaf. Subsequently, the blade joint of the leaf emerged and the leaf was termed a ligulated leaf. Leaves higher up on the stem emerged in series the same way. By the time the second leaf was visible, the first leaf was ligulated. There was a linear relationship between number of emerged leaves (both visible and ligulated) and days after seeding (approximately 4 days/leaf). The emergence rate of visible leaves was greater than that for ligulated leaves. Leaves of the first tiller emerged after two weeks and when the main stem had more than three visible leaves. Leaves of the first tiller appeared at a greater rate than those on the main stem. One-month-old seedlings had a main stem with over five visible leaves, two more than the first tiller had.

For the first two weeks, only the main stem was visible on the plant (Figure 3). Thereafter, tillers started to emerge. Tiller emergence over time was linear. The time

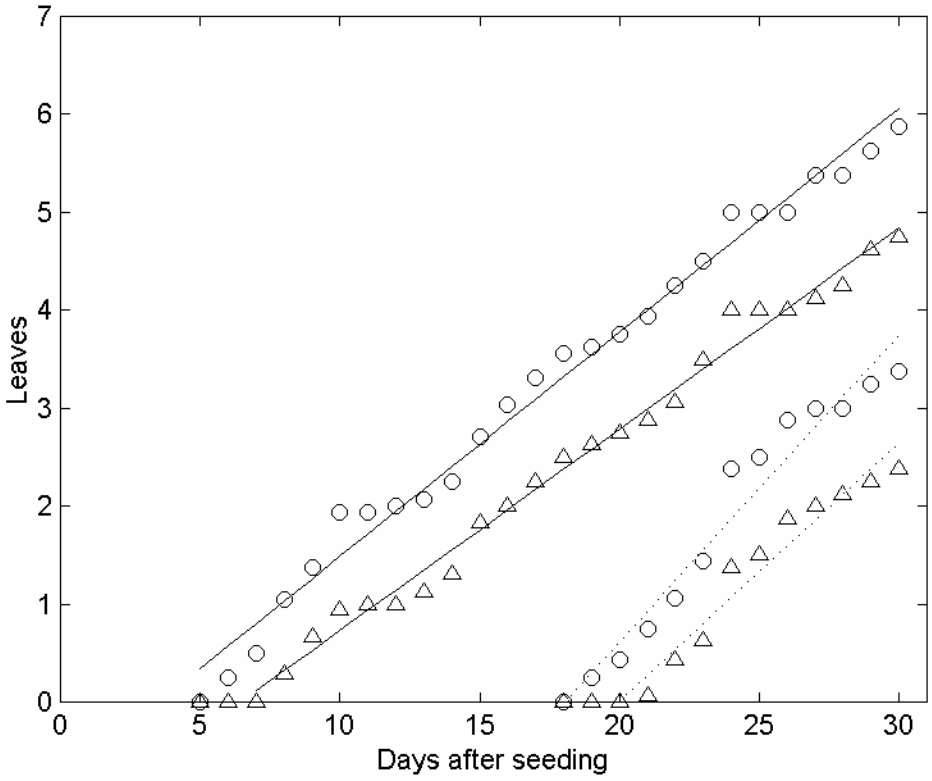

Figure 2 Relationship between number of leaves and days after seeding for *Oryza sativa* L. cv. Jefferson. Symbols are average number of visible leaves (○) and ligulated leaves (△). For days after seeding ≤ 23, 16 replicates were averaged. For days after seeding > 23, 8 replicates were averaged. The straight lines are least-squares fits to main stem leaves (–) and first tiller leaves (·). From left to right, the fitted equations are $y = 0.229x - 0.798$, $y = 0.205x - 1.322$, $y = 0.313x - 5.638$ and $y = 0.263x - 5.247$ and R^2 values are 0.987, 0.989, 0.955 and 0.950.

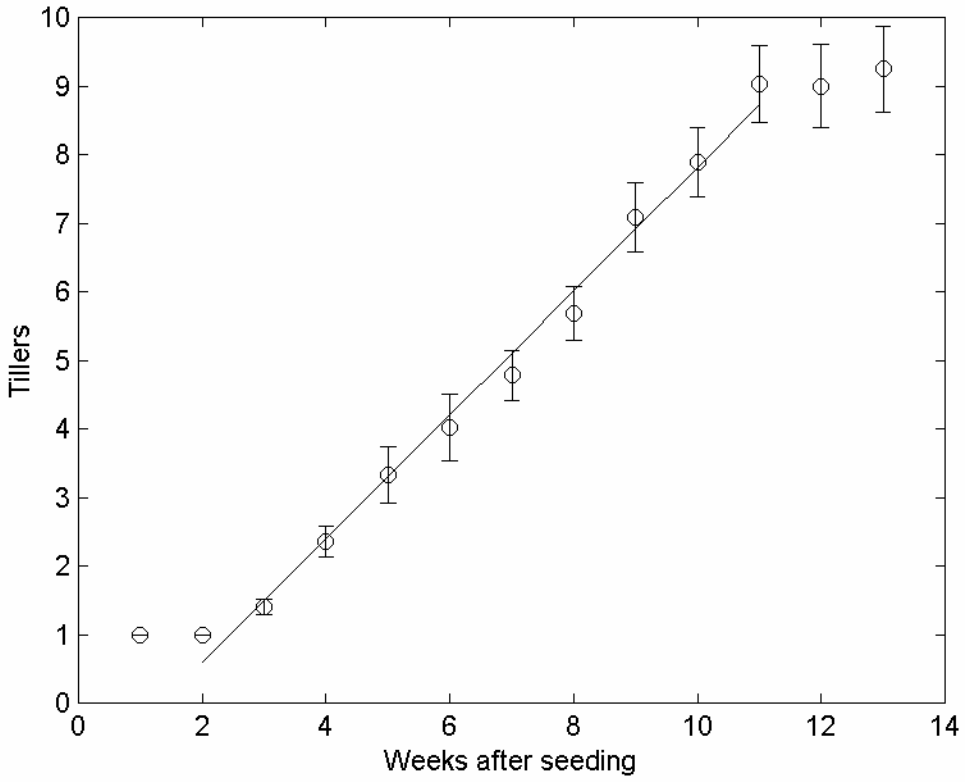

Figure 3 Relationship between number of tillers and weeks after seeding for *Oryza sativa* L. cv. Jefferson. The main stem was counted as a tiller. Bars are the 95% confidence interval of a mean of 72 replicates. The line is a least-squares fit to the central ten data points. The fitted equation is $y = 0.904x - 1.216$ and R^2 value is 0.992.

between consecutive tillers was 7.7 days. Plants had five tillers (including the main stem) after six weeks and reached a maximum of nine after ten weeks.

The first emergence of a panicle on a plant occurred over seventy days after seeding (Figure 4). It took over five more days for the second panicle to emerge. Emergence of the third through fifth panicles was linear with time with a panicle emerging every 1.6 days.

Panicle fresh weight decreased slightly immediately after emergence, increased as much as fourfold and then decreased again (Figure 5). Panicles reached a maximum fresh weight accumulation rate 12.7 days after heading (Figure 6) and a maximum fresh weight 22.9 days after heading (Figure 5).

Discussion

This system of rice production ensures a constant supply of rice at all growth stages. Although there was limited control over environmental variables such as temperature and light intensity, the results were replicated adequately to obtain satisfactory measures of statistical variation. Germination and emergence occur within a week after imbibing a grain (Figure 2; Figure 3). The optimal temperature for germination is 30-32°C (Hoshikawa, 1989). Planting two grains per pot and selecting the stronger seedling ensures that each pot has a healthy seedling. Healthy seedlings are the key to successful rice production (Hoshikawa, 1989). Ways to promote seedling health include sowing high-density grains, keeping plants free of disease, increasing root growth by promoting oxygen availability and administering proper fertilizer (Matsushima, 1967). Iron chelate ensures that young plants do not develop chlorosis. Rice seedlings are very prone to iron deficiency because relative to other grasses, they secrete a smaller amount of phytosiderophores (Mori et al., 1991).

Emergence of a leaf blade is followed by that of its blade joint (Figure 2). The growth zone is at the base of the leaf. Interestingly, the emergence rate of visible

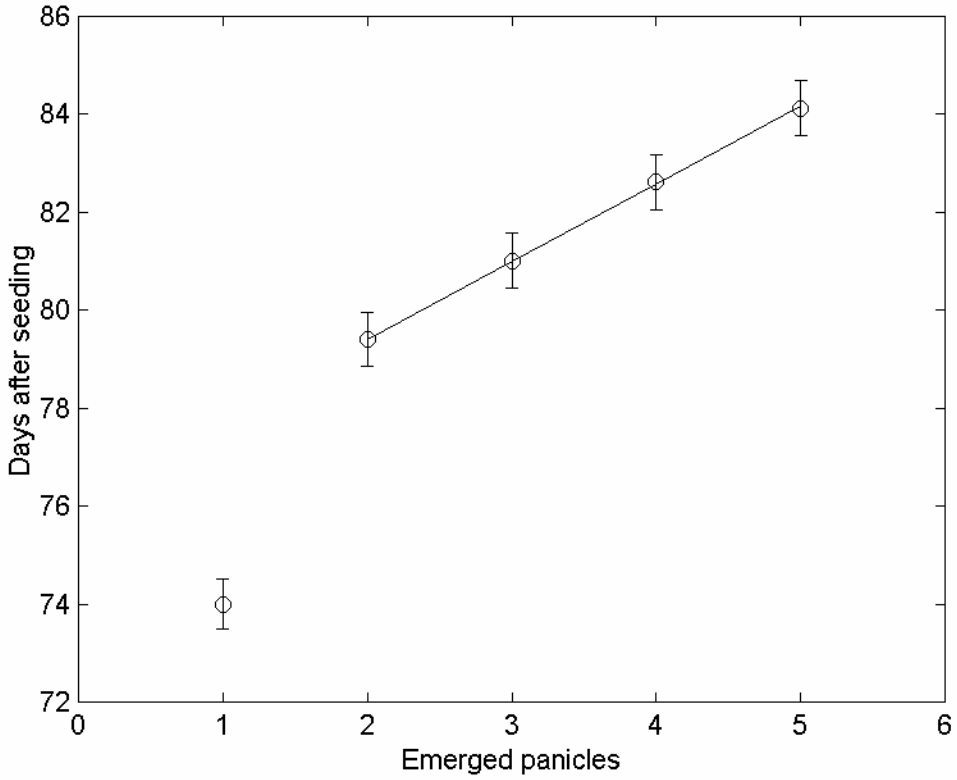

Figure 4 Relationship between days after seeding and number of emerged panicles for *Oryza sativa* L. cv. Jefferson. Bars are the standard error of a mean of 245 replicates. The line is a least-squares fit to four data points. The fitted equation is $y = 1.579x + 76.26$ and R^2 value is 1.000.

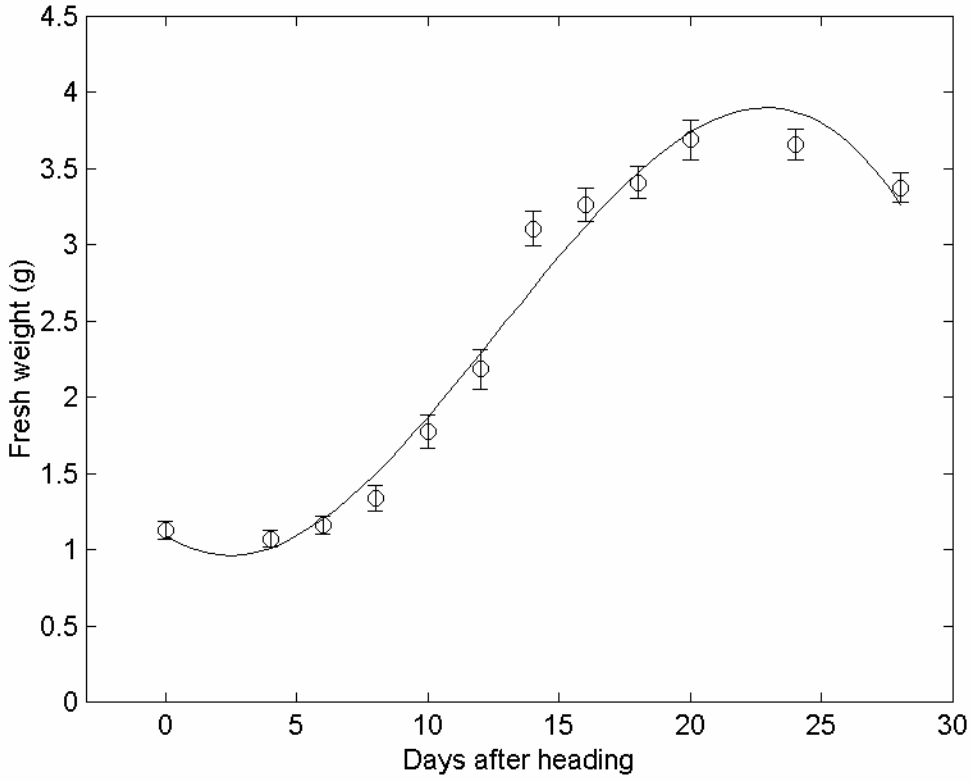

Figure 5 Relationship between panicle fresh weight and days after heading for *Oryza sativa* L. cv. Jefferson. Symbols are average fresh weights for panicles 1-5. Bars are the standard error of a mean of 15 replicates (0-12 days after heading) and 115 replicates (14-28 days after heading). The fitted polynomial equation (–) is $y = -0.000684x^3 + 0.0260x^2 - 0.114x + 1.10$ and R^2 is 0.978. Time of maximum fresh weight is 22.9 days after heading.

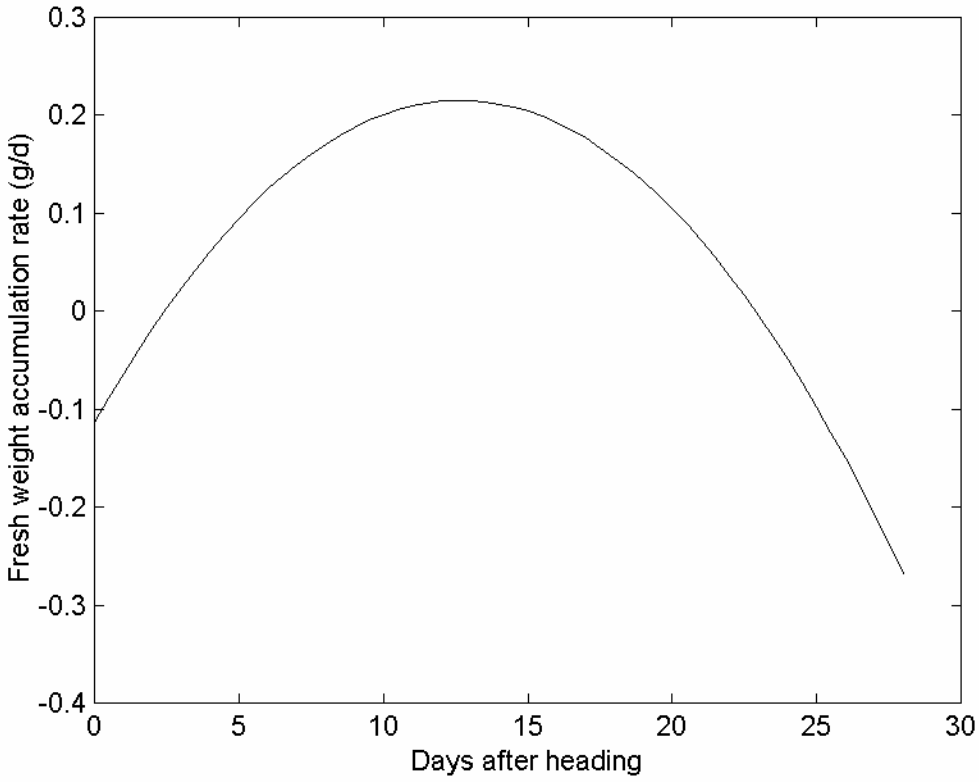

Figure 6 Relationship between panicle fresh weight accumulation rate and days after heading for *Oryza sativa* L. cv. Jefferson. Curve is first derivative of fitted polynomial in Figure 5. Time of maximum fresh weight accumulation rate is 12.7 days after heading.

leaves is greater than that for ligulated leaves. As a result, the time it takes for a blade joint to reach the level of its subtending blade joint increases with order of leaf emergence. This is consistent with the fact that leaves, except for the last few, increase in length with order of emergence (Tivet et al., 2001). Leaf emergence rates are consistent with the first tiller having a greater rate than the main stem (Nemoto et al., 1995). The number of ligulated leaves on the main stem is useful for assigning vegetative growth stages to a rice plant (Klepper et al., 1982; Counce et al., 2000). Leaf emergence and leaf initiation are synchronous (Nemoto et al., 1995). Thirty days after seeding corresponds to less than half way through the vegetative stage since there are fewer than five ligulated main stem leaves (Figure 2) compared to more than ten leaves at maturity.

Tiller emergence, like leaf emergence, is linear over time (Figure 3). The lag in tiller emergence is expected since axillary buds differentiate and emerge after the differentiation of four and seven more leaves respectively (Nemoto et al., 1995). However, tiller emergence rate is approximately half that of leaves. Since only the first five tillers to bear panicles were used per plant, almost half of the total tillers per plant were not used. The number of tillers can be controlled by a variety of methods such as nutrient application (Matsushima, 1967).

The first panicle emerges 74 days after seeding and by 10 days later, all five panicles have emerged (Figure 4). Panicle emergence is not correlated with the order of tiller emergence; that is, the panicle of the main stem does not emerge first (Hoshikawa, 1989). From the data presented here, it is not possible to associate emerged panicles with specific tillers. The rate of emergence for the last three panicles is 4.9 times greater than that of tiller emergence. The first panicle emerges around the time when the maximum number of tillers is reached. Panicles differentiate approximately 30 days before heading and the most active stage of microsporogenesis

is ten days before heading, around the time when the blade joints of the flag leaf and leaf below are in the same vertical position (Matsushima, 1967). Extrapolation of the relationship between ligulated leaves and days after seeding suggests that panicle differentiation occurs when there are seven blade joints visible on the main stem, a time when tillers are still emerging. Hence, reproductive and vegetative growth overlap.

The initial decrease in panicle fresh weight (Figure 5) is likely because the panicles on the heading date are very moist. During this time, the flag leaf sheath encloses most of the panicle. Panicles dry out when they emerge and are exposed to air (Hoshikawa, 1989). The duration of fresh weight decrease, probably less than four days, is very short and may correspond to the time it takes for a panicle to emerge completely. Panicles took more than a day, on average, to emerge. However, panicles can fully emerge on the heading date (Hoshikawa, 1989).

Panicle fresh weight accumulation is nonlinear (Figure 5). Accumulation of grain dry weight, but not grain fresh weight, was reported as sigmoidal (Hoshikawa, 1989). Panicle dry weight accumulation is sigmoidal and is best fit with Richard's function (Sadasivam et al., 1990). Ripening of grains is asynchronous so the growth curves of superior and inferior grains can be different (Zhu et al., 1988). Asynchronous ripening may contribute to the sigmoidal accumulation of panicle fresh weight. The time of maximum panicle fresh weight accumulation rate and fresh weight occurs approximately 13 and 23 days after heading, respectively. Hence, fresh weight accumulation is most active around two weeks after heading and ceases around three weeks after heading. Caryopsis ripening is greatly responsible for the increase in weight. Water and assimilates are delivered to each ripening caryopsis from the panicle via a dorsal vascular bundle (Oparka and Gates, 1981b). During this time, the caryopsis increases in length, width and girth (Hoshikawa, 1993) within the hull,

which places a limit on caryopsis expansion. Most assimilates come from leaf photosynthesis and storage reserves in the leaf sheath and stem. Before panicle emergence, the sheath of the second leaf below the uppermost leaf stores starch, which is mobilized to the ripening caryopses after panicle emergence. In agreement, relatively high expression of starch synthesis genes occurs before panicle emergence and that of sucrose synthesis and transporter genes after (Hirose et al., 1999).

Given that the fresh weight increase of panicles is nonlinear, it is challenging to the find the time of maximum fresh weight accumulation rate. This was done by finding the root of the second derivative of fresh weight as a function of time. Panicles reached a maximum rate close to two weeks after emergence. During this time, the sink activity of the panicle is very high and other vegetative parts of the shoot redistribute fixed carbon to it (Okawa et al., 2002). Sucrose concentration and starch accumulation rate are maximal nine days after flowering (Singh and Juliano, 1977). Sucrose transporter expression (Furbank et al., 2001) and ABA concentration (Kato and Takeda, 1993) reach a maximum around this time.

Panicle fresh weight decreases again three weeks after emergence (Figure 5). Grain fresh weight is mostly water during the initial stages after flowering and water content of grains decreases asymptotically to 20% after flowering (Hoshikawa, 1989; Horigane et al., 2001). Grain fresh weight decreases close to maturity. Water leaves the ripening caryopsis via the dorsal vascular bundle. Suberized cell wall linings of the pigment strand delineate apoplasmic pathways for water movement from endosperm to the dorsal vascular bundle (Oparka and Gates, 1982). Close to maturity there is a narrow channel of water in the core of endosperm, which may be involved with embryo water relations, since it is continuous with the location of the embryo (Horigane et al., 2001).

In conclusion, the dynamics of rice growth and development are manifested by the emergence of leaves, tillers and panicles and dramatic increase in panicle fresh weight. One question that arises is how panicle weight varies in both time and space. Asynchronous flowering (Vergara and Chang, 1985) then needs to be considered. Another question is what role sucrose transporters play in regulating mass transport to the panicle. For this, caryopsis anatomy and useful experimental systems need consideration.

CHAPTER 3

COMPUTATIONAL ANALYSIS OF THE ARCHITECTURE AND ASYNCHRONY OF RICE CARYOPSIS RIPENING

Abstract

Caryopses of a rice panicle ripen asynchronously, a phenomenon in part determined by panicle architecture. It was expected that ripening asynchrony and architecture could be descriptively and algorithmically modeled because of the constraints imposed by maximum degrees of branching. Branching architecture and time-dependent, qualitative grain densities of panicles from *Oryza sativa* L. cv. Jefferson were reduced to the form of annotated one-dimensional arrays. These annotated panicle arrays were algorithmically assessed for node-dependent yield components, aligned for consensus generation and plotted. The number of secondary (2°) branches and percent ripening greatly varied with node and the latter with time. The results suggest that a computational approach is useful for descriptive modeling of panicle morphogenesis and asynchronous ripening.

Introduction

The differentiation of rice panicle architecture is related to yield capacity, a function of number of panicles, spikelets/panicle, percent of spikelets that form ripened grains and the grain weight (Matsushima, 1967). Spikelets flower and ovaries begin ripening at different times. Hence, asynchronous ripening superimposed on rachis branching architecture determines the spatial dynamics of panicle ripening. Panicle architecture varies widely among varieties. Yamagishi et al. (2003) identified the number of organs and branching pattern as two principal components that explained 71.8% of the variation. Few varieties had high scores for both components.

The rice panicle has an architecture that is based typically on three levels of lateral branching (Xu and Vergara, 1986; Takeoka et al., 1993; Komatsu et al., 2001).

Primary (1°) branches arise spirally from the nodes of the rachis and 2° branches arise alternately from 1° branch nodes. Spikelets borne on pedicels arise terminally or alternately from the nodes of branches (Figure 7). Komatsu et al. (2001) have classified the panicle meristems that coordinate this architecture into four types. The primary inflorescence meristem gives rise to bract primordia and lateral branch meristems and then degenerates. Branch meristems give rise to lateral branch meristems and spikelet meristems and do not degenerate. Instead, they transition to terminal spikelet meristems. The gene *LAX1* is required for the differentiation of lateral meristems and *FZP2* for spikelet meristems. *LAX1* also regulates determinate rachis branch growth (Komatsu et al., 2001). Spikelet meristems give rise to the hull and floret primordia.

Several other genes are related to panicle architecture. *PLASTOCHRON1* codes for a cytochrome P450 that is highly expressed in bract primordia and results in elongated bracts and axillary shoots instead of 1° branches when mutated (Miyoshi et al., 2004). Pleiotropic effects of *An-4* include an increase in 1° branch length and 2° branches/1° branch which results in an increase of spikelets/panicle (Sato et al., 1996). *Ur-1* increases the number of spikelets/panicle by increasing both 2° branches/1° branch and spikelets/2° branch (Murai and Iizawa, 1994; Murai et al., 2002).

Hormones regulate panicle architecture. Gibberellic acid increases number of 1° branches and spikelets but decreases number of 2° branches and spikelets. Whether or not spikelets/panicle increases is dependent on variety and is correlated with an increase in volume of the inflorescence meristem at initiation (Mu and Yamagishi, 2001). Number of 1° branches, but not necessarily 2° branches and total number of spikelets, is correlated with diameter of the dome of the inflorescence meristem that is increased with duration of the vegetative phase (Kobayasi et al., 2001). Dome

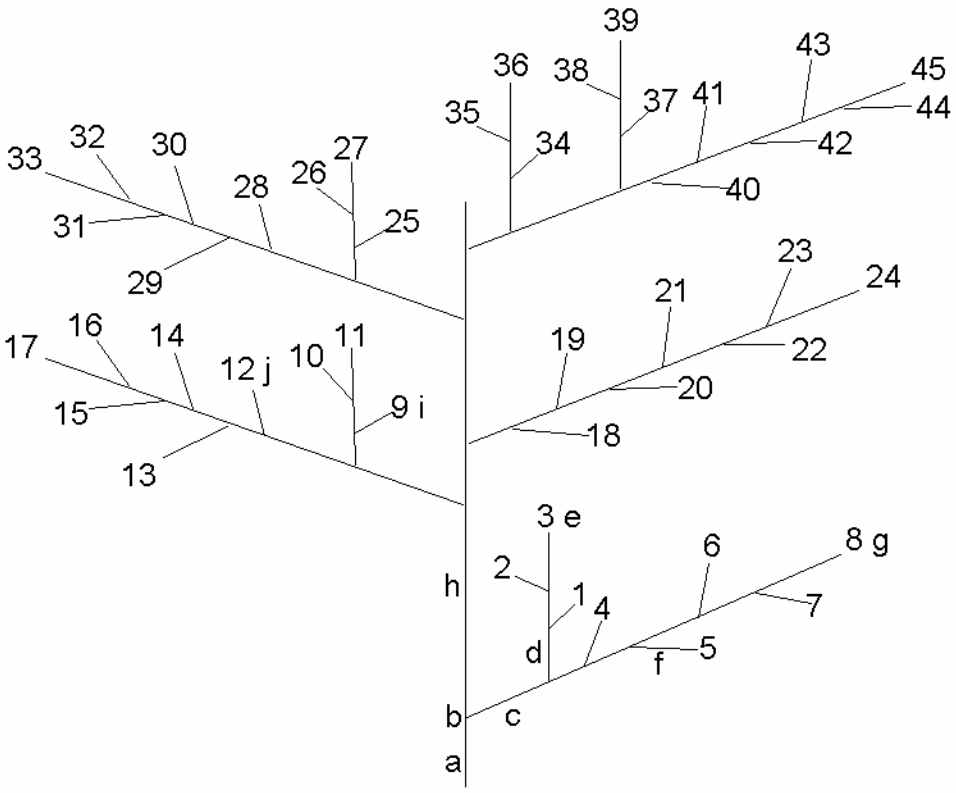

Figure 7 Manual drawing of panicle architecture for *Oryza sativa* L. cv. Jefferson. The first five rachis nodes of a panicle are shown. Numbers represent spikelets/grains in acropetal order. Letters indicate peduncle (a), first rachis node (b), 1° branch (c), 2° branch (d), apical 2° spikelet/grain (e), pedicel (f), apical 1° spikelet/grain (g), rachis (h), basal 2° spikelet/grain (i) and basal 1° spikelet/grain (j).

diameter and the aforementioned panicle traits also increase with nitrogen application for some varieties (Koller et al., 2002).

Differentiation and development of the panicle involves sequential events that take place before emergence from the flag leaf sheath. Panicle differentiation commences with the differentiation of an encircling bract primordium, which eventually subtends the first 1° branch, from the inflorescence meristem (Xu and Vergara, 1986). Sequential differentiation and subsequent development of 1° branch, 2° branch and spikelet primordia encompass early panicle development which lasts approximately 20 days and has reached completion in panicles as large as 1.5 cm (Matsushima, 1967). Differentiation of multiple primordia on a branch and development of each primordium, but not the asynchrony of development, is strictly acropetal. Spikelet differentiation refers to spikelet meristems that arise in acropetal sequence from a branch meristem, and spikelet development refers to spikelet meristems that give rise to spikelet organ primordia in an acropetal manner. However, counterintuitively, the apical spikelet (Figure 7) begins development first, the basal one second, and the rest follow in an acropetal sequence. Although branch differentiation is acropetal, the asynchrony of branch development is basipetal (Xu and Vergara, 1986).

Flowering and ripening are also asynchronous, the order being generally basipetal, like the order of branch development. Superior (towards the top of the panicle) grains begin ripening before inferior ones. Superior grains are less prone to sterility and abortion (Xu and Vergara, 1986), factors that decrease percent ripening, a parameter proportional to yield (Matsushima, 1967). Assimilates are first partitioned to the superior grains (Okano and Kono, 1993). These grains accumulate more dry matter and have greater specific gravity (Mohapatra et al., 1993), which is proportional to the caryopsis/grain volume (Matsushima, 1967).

Superior and inferior grains differ in many respects. Inferior caryopses commence endosperm development after a lag period of four days and have fewer endosperm and inner integument cells (Ishimaru et al., 2003). Superior grains have a greater hull and endosperm weight and concentration of total soluble sugars, amylase and protein at maturity (Mitra and Bera, 2003). Superior grains have higher dry weight accumulation, starch accumulation, water accumulation and subsequent dehydration (Mohapatra et al., 1993). Superior grains have a higher rate of ABA accumulation during early to mid-ripening (Tsukaguchi et al., 1999). Inferior grains during ripening dry out later and less than superior grains (Mohapatra et al., 1993).

Photoassimilates from the flag leaf and two penultimate leaves in high yielding varieties supply the ripening panicle (Mohapatra et al., 2004). There is evidence that supply of assimilates to the inferior grains is not limiting. Inferior grains have higher concentrations of sucrose and free amino acids throughout ripening (Mohapatra et al., 1993) and a lower activity of sucrose synthase (Patel and Mohapatra, 1996). Application of ethylene inhibitors promotes their ripening (Mohapatra et al., 2000).

Quantitative studies on spatial variation in panicle ripening are lacking. Most work has been on the asynchrony of flowering and comparisons between superior and inferior grains. Manual drawings of panicle architecture (Figure 7) are commonly encountered in the literature. These drawings are used to map flowering dates or show the locations of the grains that were studied. However, a desirable alternative is a computational, descriptive model for a panicle that can be used to analyze and display its basic architecture. The objective of this study was to develop a format for storing information on branching architecture together with basic information about each spikelet/grain such as whether it sinks in water. Methods included the systematic arraying of spikelets/grains on a well plate, data input and analysis using algorithms written in Matlab.

Materials and Methods

Panicle Harvesting

Six sets of panicles were harvested. Set 1, set 2 and set 3 each contained five panicles that emerged first on a plant and were harvested 10, 15 and 20 days after heading, respectively. Set 4, set 5 and set 6 each contained 8 panicles that emerged first, third and fifth, respectively, and were harvested at maturity. Set 7 designated the combination of sets 1-6 (39 panicles). Before use, panicles were dried out at room temperature until reaching a constant weight.

Panicle Architecture Modeling

Spikelets/grains were systematically detached from panicle branches and arrayed in acropetal order (Figure 7) in wells of plates from left to right and bottom to top. Some wells were left empty. Empty well sequences (Table 1) represented steps between branches. Threes were assigned to the empty wells. Each spikelet/grain was assigned a score for sinking in water. Ones represented grains that sank and twos represented spikelets/grains that floated. The numbers were entered into Excel and the resulting panicle array (Figure 8) was saved as a tab delimited text file.

The panicle array was imported into Matlab and converted to an annotated panicle array (Figure 9) by bordering spikelet/grain scores with numbers to designate what branch the spikelets/grains were from. See ***Functions for Creating the Annotated Panicle Array***, page 124. Numbering of rachis nodes and border notations were defined as follows. Multiples of ten were used to indicate the border of 1° spikelets/grains. Multiples of ten plus increments of one indicated the border of 2° spikelets/grains. For example, the borders for 1° spikelets/grains of the first rachis node (spikelets/grains 4-8 in Figure 7) were 10, for those of the second rachis node (spikelets/grains 12-17) 20, and so on. The borders for 2° spikelets/grains of the first 2° branch of the first rachis node (spikelets/grains 9-11) were 11.

Table 1 Relationship between panicle architecture of *Oryza sativa* L. cv. Jefferson and panicle array. Types of steps taken when spikelets/grains of a panicle are arrayed in acropetal order, examples (refer to Figure 7) and the number of empty wells used to encode the steps are listed.

Step from	Step to	Example	Empty wells
Spikelet/grain	Acropetal spikelet/grain (same branch)	1→2	0
Apical 2° spikelet/grain	Basal 1° spikelet/grain (same rachis node)	3→4	1
Apical 2° spikelet/grain	Basal 2° spikelet/grain (same rachis node)	36→37	2
Peduncle or apical 1° spikelet/grain	Basal 1° spikelet/grain (next rachis node)	17→18	3
Peduncle or apical 1° spikelet/grain	Basal 2° spikelet/grain (next rachis node)	8→9	4

1	1	2	2	2							
3	3	3	1	1	1	1	1	2	3	3	3
3	3	2	1	2	3	1	1	1	1	1	1
3	2	2	2	3	2	1	1	1	1	3	3
2	2	2	3	1	1	1	1	1	3	3	3
1	1	1	3	3	3	3	2	2	2	3	3
2	2	2	3	3	2	2	2	3	2	2	2
3	2	2	2	2	2	1	3	3	3	3	2
2	2	3	3	2	2	2	3	3	2	2	2
3	2	2	1	2	1	3	3	3	3	2	2
2	2	3	3	2	2	2	3	3	2	2	2
2	2	2	2	2	2	1	3	3	3	3	2
3	3	2	2	2	2	3	3	2	2	2	3
2	2	2	3	2	2	1	2	2	1	3	3
3	3	2	2	2	3	3	2	2	2	3	3
2	**2**	**2**	**3**	**2**	**2**	**2**	**2**	**2**	**1**	3	3
2	**2**	**2**	**3**	**3**	**3**	**3**	**2**	**2**	**2**	**3**	**3**
2	**3**	**3**	**3**	**3**	**2**	**2**	**2**	**3**	**2**	**2**	**2**
2	**2**	**2**	**3**	**3**	**3**	**2**	**2**	**2**	**2**	**2**	**2**
2	**3**	**3**	**3**	**3**	**2**	**2**	**2**	**3**	**2**	**2**	**2**
3	**3**	**3**	**3**	**2**	**2**	**2**	**3**	**2**	**2**	**2**	**2**

Figure 8 Panicle array for *Oryza sativa* L. cv. Jefferson. Spikelets/grains were arrayed in acropetal order into the wells of plates from left to right and bottom to top. Numbers were assigned to wells. Threes indicate empty wells according to Table 1. Ones indicate grains that sink in water. Twos indicate spikelets/grains that float in water. Figure 7 is a manual drawing of the bold portion of the array.

11	**2**	**2**	**2**	***11***	**10**	**2**	**2**	**2**	**2**
2	***10***	***21***	**2**	**2**	**2**	***21***	***20***	**2**	**2**
2	**2**	**2**	**2**	***20***	***30***	**2**	**2**	**2**	**2**
2	**2**	**2**	***30***	***41***	**2**	**2**	**2**	***41***	***40***
2	**2**	**2**	**2**	**2**	**2**	***40***	***51***	**2**	**2**
2	***51***	***52***	**2**	**2**	**2**	***52***	***50***	**2**	**2**
2	**2**	**2**	**1**	***50***	*61*	2	2	2	*61*
62	2	2	2	*62*	*63*	2	2	2	*63*
60	2	2	1	2	2	1	*60*	*71*	2
2	2	2	*71*	*72*	2	2	2	*72*	*70*
2	2	2	2	2	2	1	*70*	*81*	2
2	2	*81*	*82*	2	2	2	*82*	*83*	2
2	2	*83*	*80*	2	2	1	2	1	*80*
91	2	2	2	2	*91*	*92*	2	2	2
92	*93*	2	2	2	*93*	*90*	2	2	2
2	2	1	*90*	*101*	2	2	2	2	*101*
102	2	2	2	*102*	*100*	2	2	2	1
1	1	*100*	*111*	2	2	2	*111*	*112*	2
2	2	*112*	*110*	1	1	1	1	1	*110*
121	2	2	2	*121*	*120*	2	1	1	1
1	*120*	*131*	2	1	2	*131*	*130*	1	1
1	1	1	1	*130*	*140*	1	1	1	1
1	2	*140*	*150*	1	1	2	2	2	*150*

Figure 9 Annotated panicle array for *Oryza sativa* L. cv. Jefferson. The panicle array in Figure 8 was annotated. The annotated panicle array is read from left to right and top to bottom. Borders are in italics. The panicle has 15 nodes. Primary spikelets/grains are at every node. Secondary spikelets/grains are at every rachis node except rachis nodes 3, 14 and 15. Figure 7 is a manual drawing of the bold portion of the array.

Annotated panicle arrays were displayed graphically as panicle plots (Figure 10) by drawing shapes that represented spikelets/grains and connecting them by lines that represented rachis branches. See ***Function and Scripts for Drawing the Panicle Plot***, page 128. Spikelet and branch vestiges as well as quantitative information on shape were not considered.

Annotated panicle arrays were mined for data using algorithms written in Matlab. See ***Functions for Analyzing the Annotated Panicle Array***, page 125. For instance, the number of nodes could be simply determined by finding the array maximum, dividing it by ten and rounding down the answer to a whole number (numnodes.m, page 126). The number of spikelets/grains could be found by counting the ones and twos (ns.m, page 126).

Annotated panicle arrays were aligned by aligning borders. See ***Functions for Aligning Annotated Panicle Arrays***, page 131. Borders not present in all the arrays and zeros were added into arrays as necessary. For instance, the alignment of 10 2 2 1 2 10 20 1 1 2 2 20 and 10 2 2 2 10 is 10 2 2 1 2 10 20 1 1 2 2 20 and 10 2 2 2 0 10 20 0 0 0 0 20. To generate a consensus array, a spikelet/grain was assigned to a position if a 1 or 2 was present at that position in at least 50% of the aligned panicle arrays. A grain that sank in water was assigned to a position if there was a 1 at that position in at least 50% of the aligned panicle arrays. For instance the consensus of the alignment 10 1 2 2 10, 10 2 2 0 10, 10 1 1 0 10, 10 2 2 0 10, 10 1 1 0 10, 10 2 2 2 10 is 10 1 2 10.

Results

Panicles on average had over ten rachis nodes and a maximum of one 1° branch per node (Table 2). Panicles sometimes did not have a 1° branch at the first rachis node (junction between peduncle and rachis). There were more 2° branches than 1° branches and fewer 2° spikelets than 1° spikelets. Secondary branches had

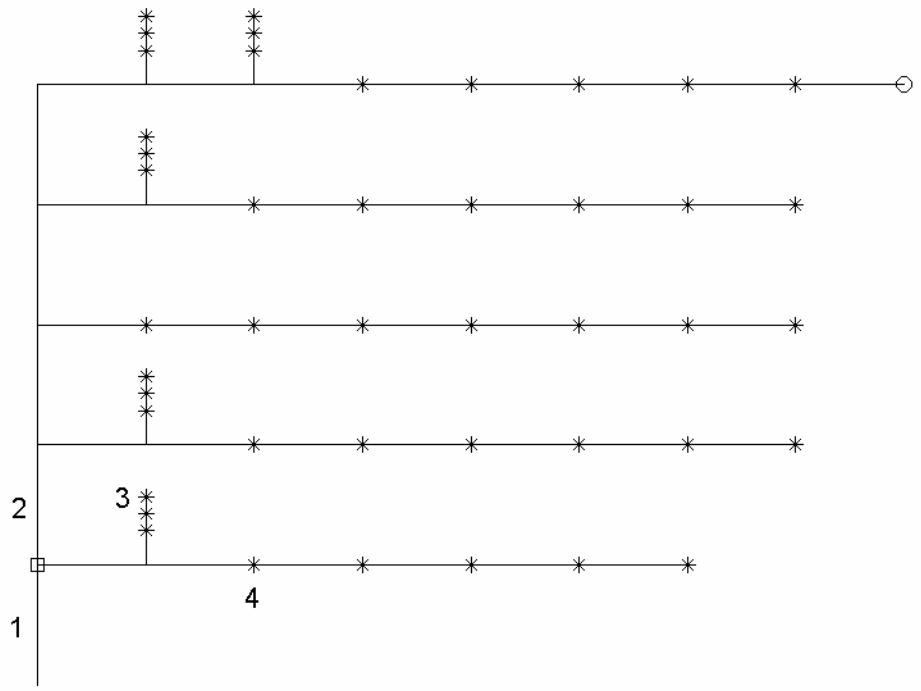

Figure 10 Panicle plot for *Oryza sativa* L. cv. Jefferson. The bold portion of the annotated panicle array in Figure 9 is plotted. Symbols indicate spikelets/grains that float in water (*), grains that sink in water (○) and the first rachis node (□). Numbers indicate peduncle (1), rachis (2), 2° spikelet/grain (3) and 1° spikelet/grain (4). Figure 7 is a manual drawing of this plot.

Table 2 Panicle architecture traits for *Oryza sativa* L. cv. Jefferson. Averages (μ) and 95% confidence intervals (±) are listed. See Panicle Harvesting, page 34, for description and sample size of each panicle set.

Panicle set		1	2	3	4	5	6	7
Rachis nodes	μ	16.00	16.20	14.20	15.00	13.88	13.25	14.59
	±	0.88	2.04	1.62	0.89	0.54	1.40	0.51
Spikelets	μ	186.20	177.80	163.60	145.38	133.88	117.75	149.08
	±	26.77	17.19	30.28	8.94	8.61	18.77	9.40
1° spikelets	μ	96.40	95.60	84.40	86.38	78.75	74.00	84.49
	±	6.43	13.36	10.77	5.99	3.97	9.47	3.64
1° branches	μ	15.80	16.20	14.00	15.00	13.75	13.13	14.49
	±	0.56	2.04	1.52	0.89	0.39	1.37	0.50
1° spikelets/ 1° branch	μ	6.10	5.90	6.02	5.76	5.72	5.63	5.82
	±	0.33	0.26	0.22	0.13	0.17	0.22	0.08
2° spikelets	μ	89.80	82.20	79.20	59.00	55.13	43.75	64.59
	±	23.45	11.36	23.39	5.53	7.72	12.04	6.60
2° branches	μ	28.80	25.80	24.60	19.25	17.88	14.75	20.79
	±	6.54	3.21	7.43	1.66	2.16	3.73	1.96
2° spikelets/ 2° branch	μ	3.11	3.18	3.22	3.06	3.08	2.94	3.08
	±	0.10	0.06	0.09	0.05	0.09	0.13	0.04

approximately half the number of spikelets as 1° branches. Earlier emerging panicles had more spikelets than later emerging ones (Table 2).

The consensus panicle plot generated from the alignment of 39 annotated panicle arrays (set 7) showed similar trends in architecture (Figure 11). There were 15 nodes on the rachis. Number of total spikelets, 1° spikelets and 2° spikelets varied with node as did 2° branches. The maximum number of 1° spikelets for a node was six. There were typically three spikelets on a 2° branch. The maximum number of 2° branches for a node was two. Nodes 5-11 had the greatest number of spikelets and had two 2° branches instead of one or none. The first and last two rachis nodes did not have 2° branches.

Nodal distribution of average spikelet number was similar to the consensus panicle plot. Spikelets were more frequent on the middle nodes of the rachis (Figure 12) with a maximum at nodes 6-7. This was the case also for 2° spikelets (Figure 13) and 2° branches (Figure 14). Primary spikelets varied little with rachis node (Figure 15), the maximum being close to six spikelets. Panicle spikelet number was thus greatly correlated with number of 2° branches on a panicle.

Spikelets and some grains did not sink in water. Removing the hull was the only possible way to differentiate between spikelet and grain in this case. Whether a grain sank or not depended on the progress of caryopsis ripening. As the caryopsis grows, the air enclosed by the hull is displaced.

Consensus panicles of set 1 (Figure 16), set 2 (Figure 17) and set 3 (Figure 18) were similar in architecture. There were as many as three 2° branches at a rachis node. For set 2, the upper two rachis nodes did not have 2° branches. Set 3 had one less rachis node than set 1 or set 2, which both had 16 nodes. They differed greatly in the number of grains that sank in water (dense grains). Consensus panicles from 10 days after heading did not have any dense grains (Figure 16). Panicles from 15 days after

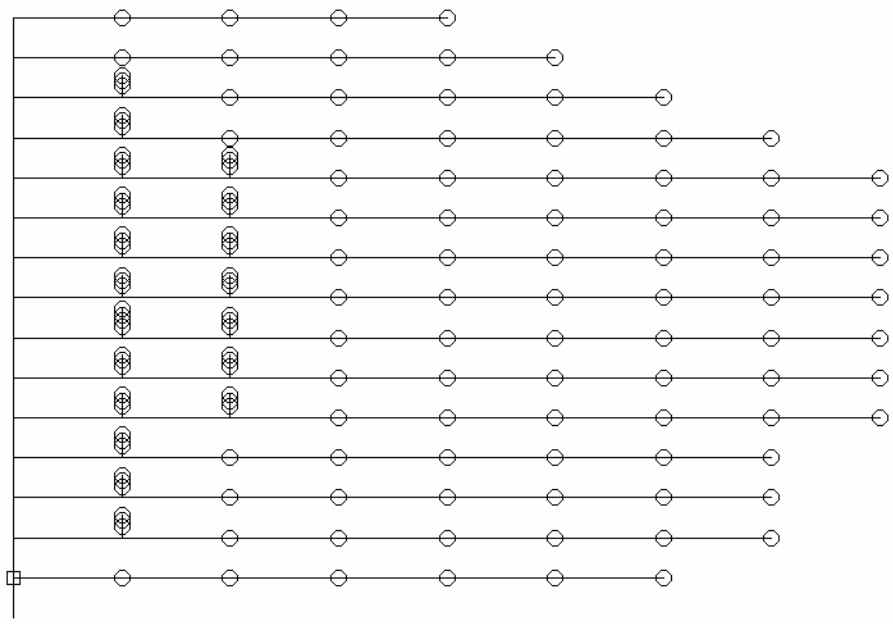

Figure 11 Consensus panicle plot for *Oryza sativa* L. cv. Jefferson. Panicles are from set 7. Symbols indicate spikelets (○) and the first rachis node (□).

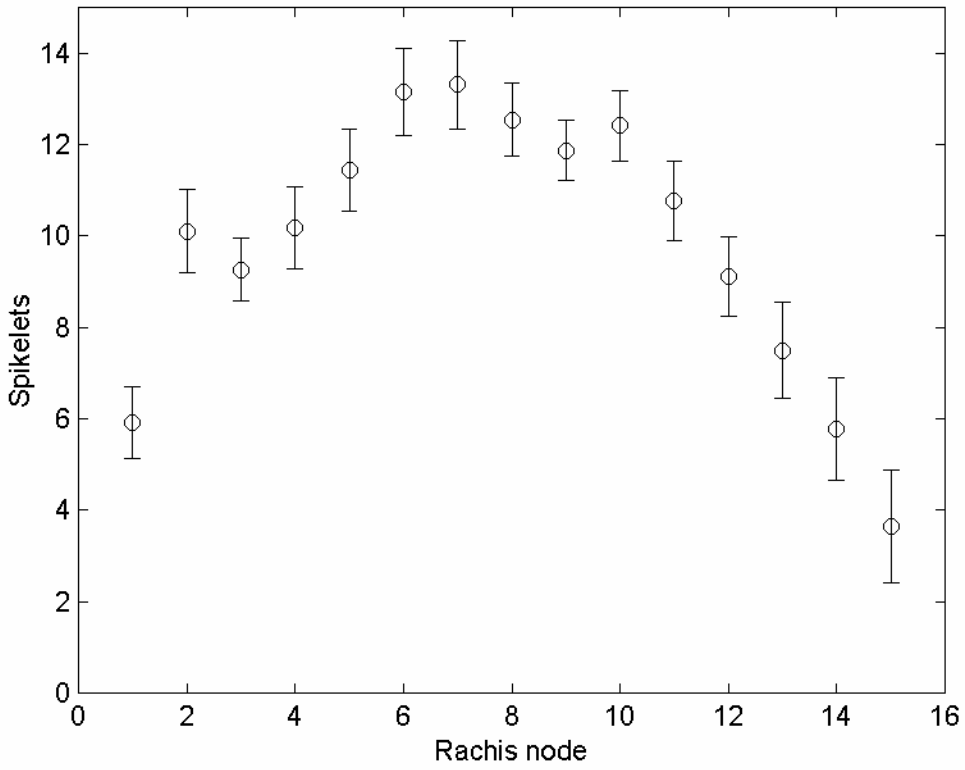

Figure 12 Relationship between number of spikelets and rachis node for *Oryza sativa* L. cv. Jefferson. Bars are the 95% confidence interval of a mean for the first 15 nodes of panicles in set 7.

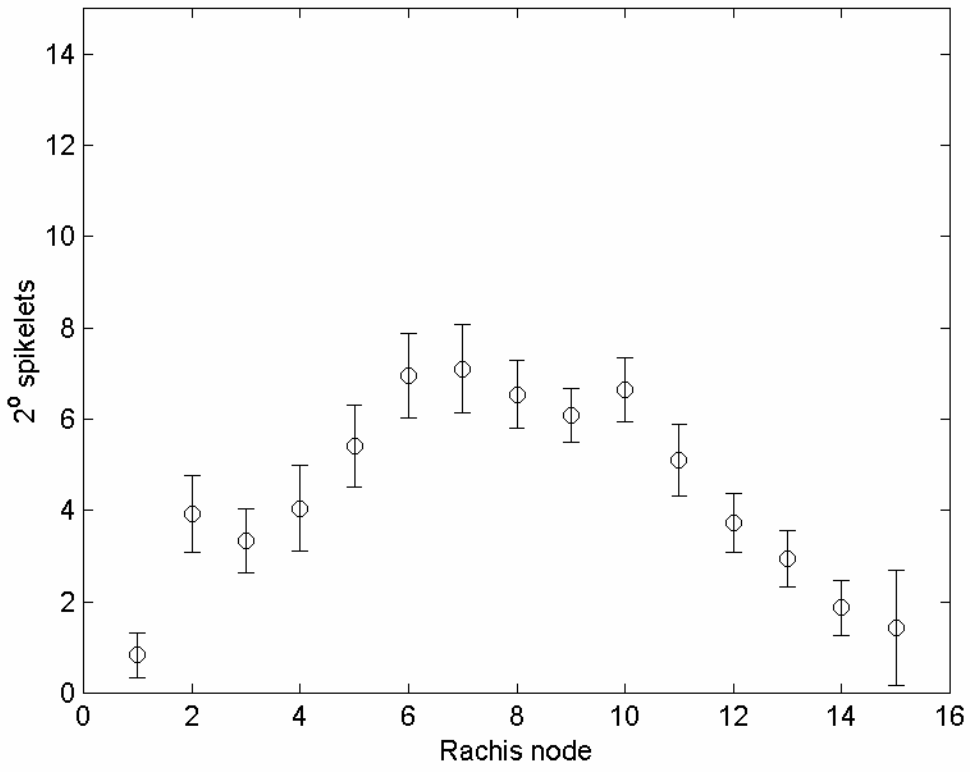

Figure 13 Relationship between number of 2° spikelets and rachis node for *Oryza sativa* L. cv. Jefferson. Bars are the 95% confidence interval of a mean for the first 15 nodes of panicles in set 7.

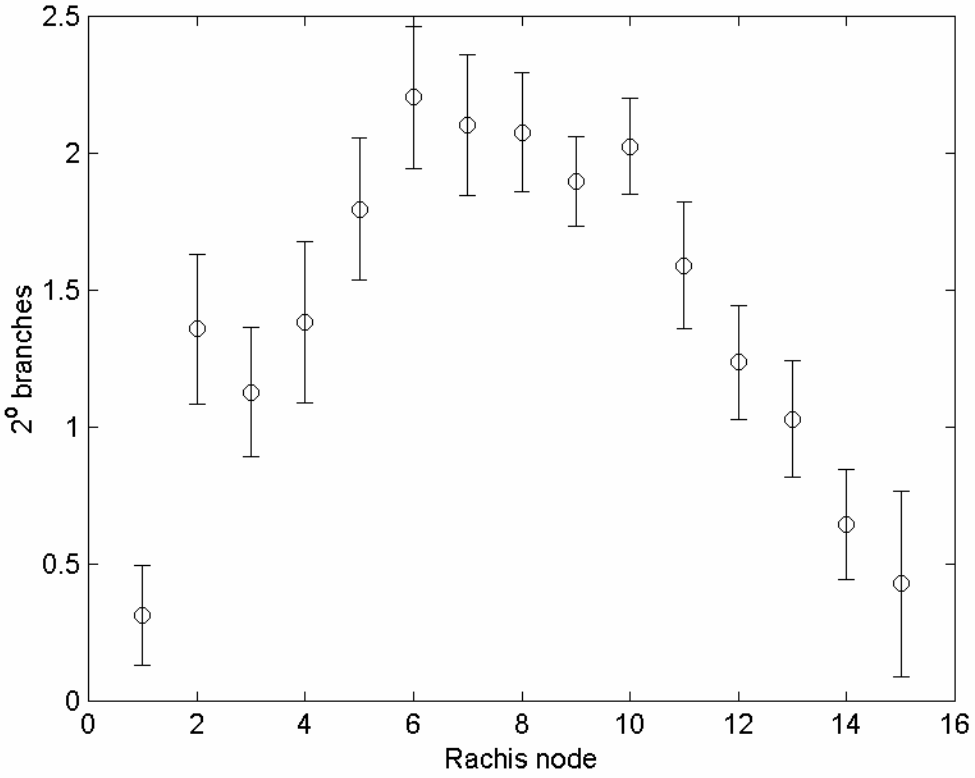

Figure 14 Relationship between number of 2° branches and rachis node for *Oryza sativa* L. cv. Jefferson. Bars are the 95% confidence interval of a mean for the first 15 nodes of panicles in set 7.

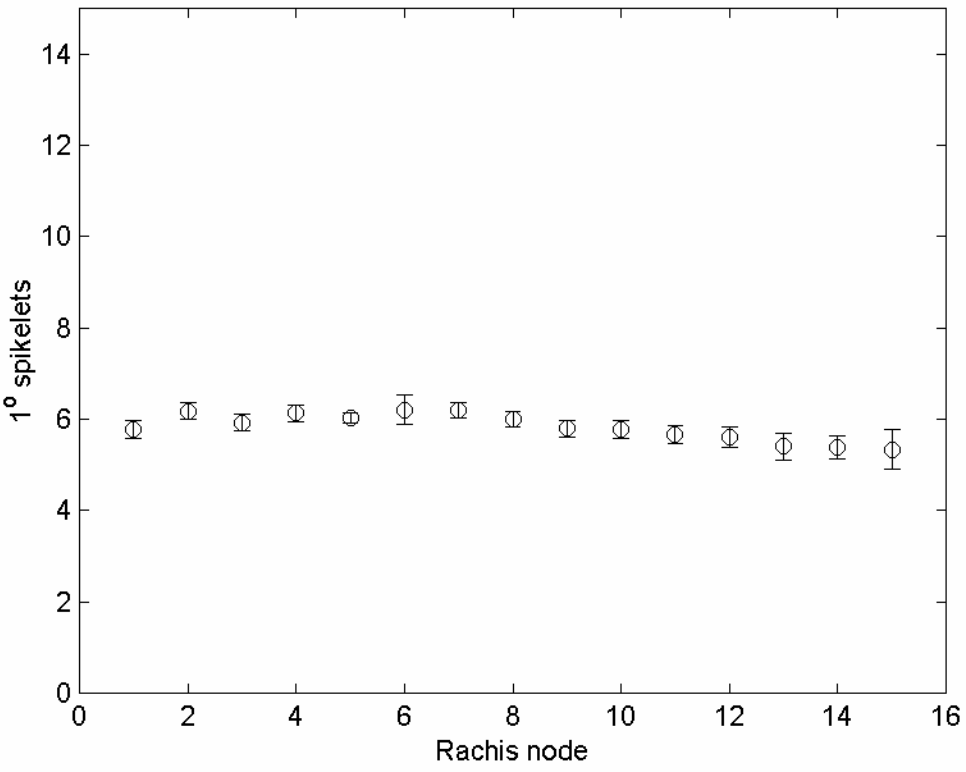

Figure 15 Relationship between number of 1° spikelets and rachis node for *Oryza sativa* L. cv. Jefferson. Bars are the 95% confidence interval of a mean for the first 15 nodes of panicles in set 7.

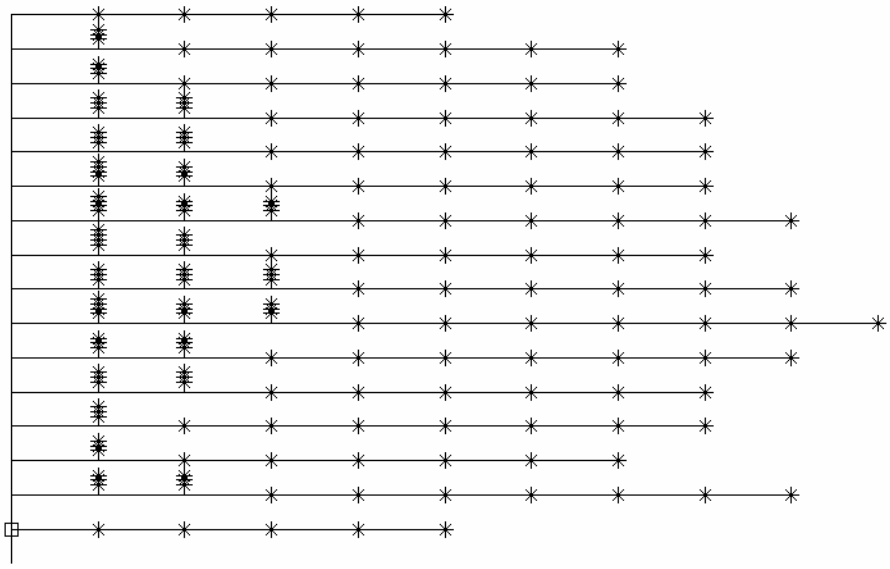

Figure 16 Consensus panicle plot for *Oryza sativa* L. cv. Jefferson 10 days after heading. Panicles were from set 1. Symbols indicate spikelets/grains that float in water (*) and the first rachis node (□).

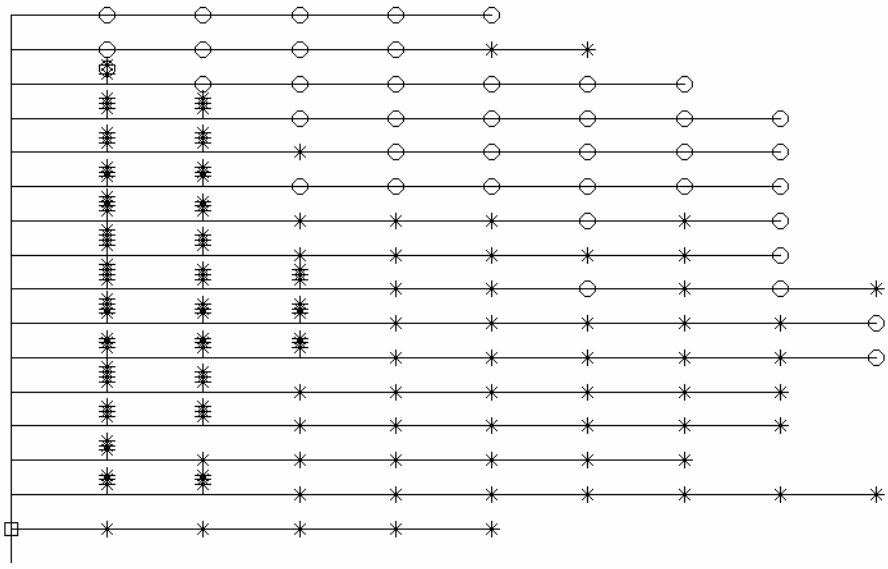

Figure 17 Consensus panicle plot for *Oryza sativa* L. cv. Jefferson 15 days after heading. Panicles were from set 2. Symbols indicate spikelets/grains that float in water (*), grains that sink in water (○) and the first rachis node (□).

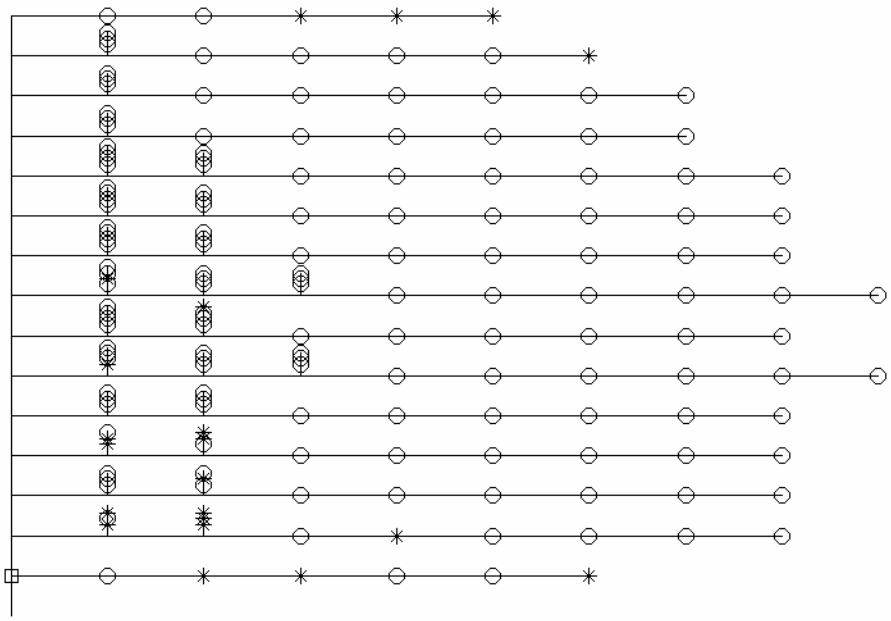

Figure 18 Consensus panicle plot for *Oryza sativa* L. cv. Jefferson 20 days after heading. Panicles were from set 3. Symbols indicate spikelets/grains that float in water (*), grains that sink in water (○) and the first rachis node (□).

heading had a minority of spikelets/grains that were dense (Figure 17). Almost all the spikelets/grains were dense at 20 days after heading (Figure 18).

The frequency of dense grains was correlated with days after heading at all nodes except for node 14 (Figure 19). On average, for 20 days after heading, greater than 50% of spikelets/grains at every node were dense. Set 1 and set 2 panicles did not have any dense grains at the lower nodes. Set 1 had more nodes that lacked dense grains than set 2 did. The nodal distribution of frequencies of all dense grains (Figure 19) followed the pattern of 1° grains (Figure 20) more than 2° grains (Figure 21). For all days after heading, dense grains were more frequent on upper nodes.

Discussion

Panicle development involves three orders of acropetal, lateral branching. Primary rachis branch meristems arise from the inflorescence meristem, 2° branch meristems and lateral spikelet meristems from 1° branch meristems, and lateral spikelet meristems from 2° branch meristems. Phyllotaxy generated by the inflorescence meristem is spiral and that by the branch meristems is alternate. The inflorescence meristem eventually degenerates, while the branch meristems transition to terminal spikelet meristems. As a result, each node can be assigned to a single branch or spikelet. Rachis internodes are sometimes very short, causing a pseudo-opposite branching pattern.

The annotated panicle array (Figure 9) is a versatile format for the storage of panicle architectural data. Advantages include its storage of both branching pattern and a spikelet/grain trait of interest. While only a qualitative trait was tested here, the model can be applied to quantitative traits, such a grain weight, instead of sinking versus floating. The other advantage is that the annotated array is easily extracted for data and manipulated by algorithms.

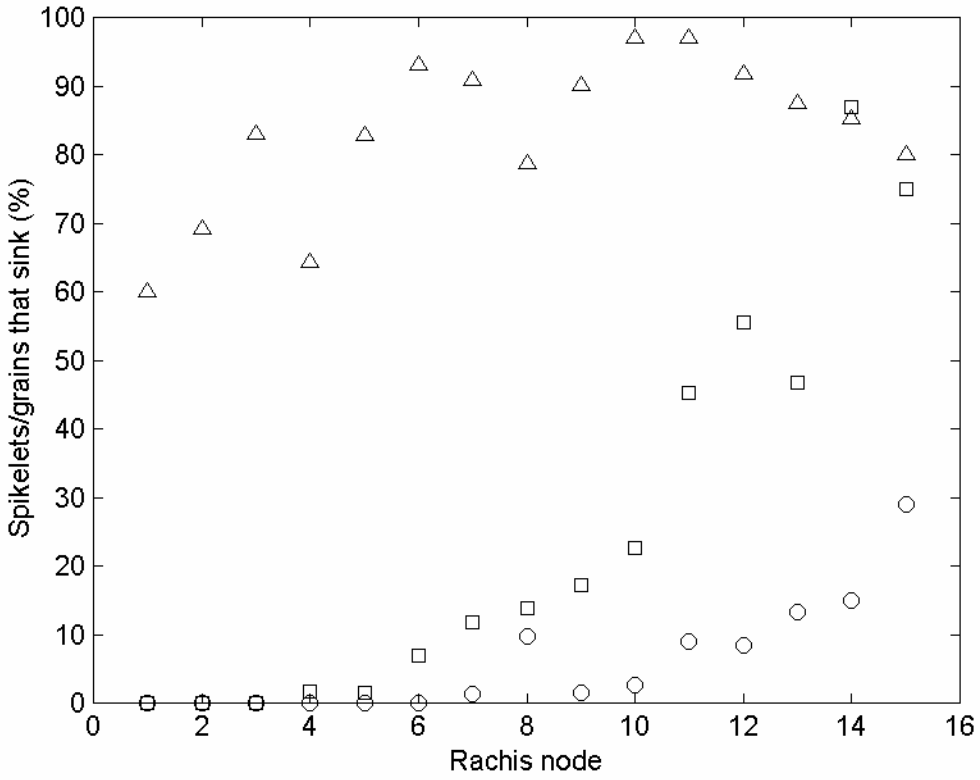

Figure 19 Relationship between spikelets/grains that sink and rachis node for *Oryza sativa* L. cv. Jefferson. Symbols are averages for panicle set 1 (○), set 2 (□) and set 3 (△).

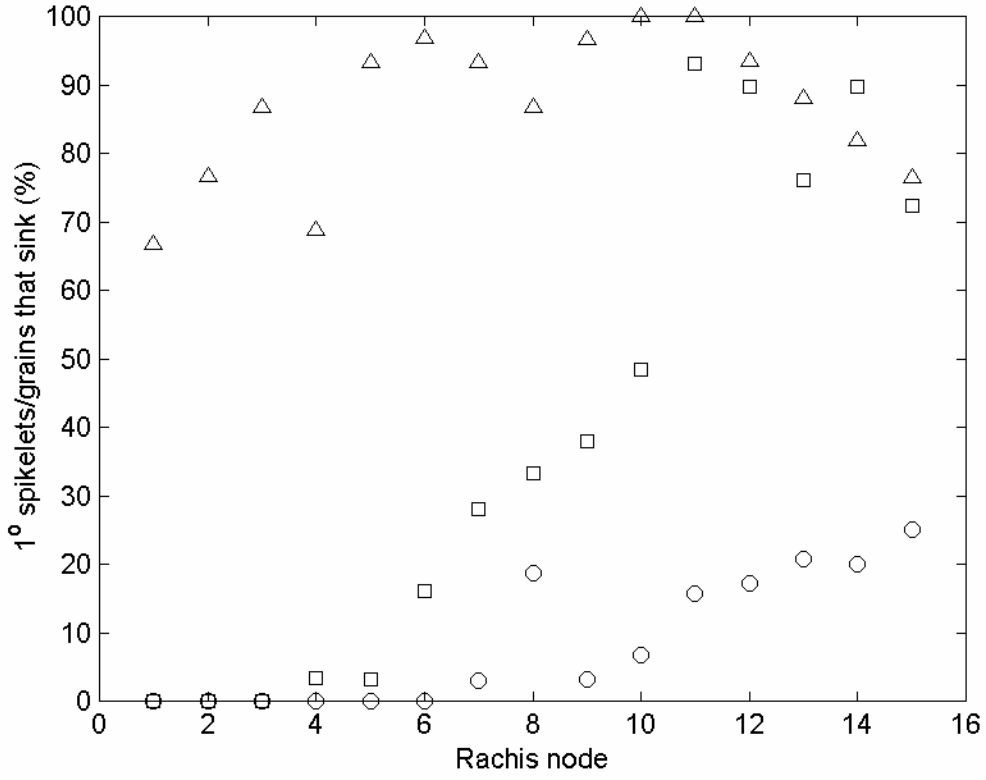

Figure 20 Relationship between 1° spikelets/grains that sink and rachis node for *Oryza sativa* L. cv. Jefferson. Symbols are averages for panicle set 1 (○), set 2 (□) and set 3 (△).

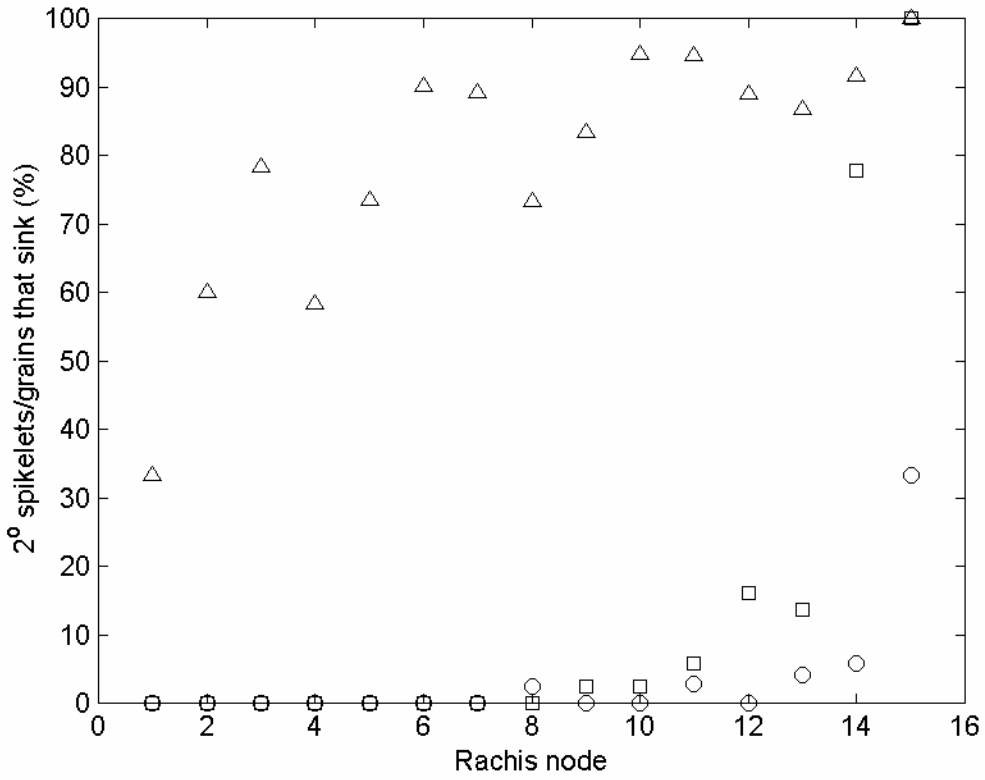

Figure 21 Relationship between 2° spikelets/grains that sink and rachis node for *Oryza sativa* L. cv. Jefferson. Symbols are averages for panicle set 1 (○), set 2 (□) and set 3 (△).

Graphical representations of panicles (Figure 11) are simple, two dimensional maps of spikelet/grain positions relative to each other. Each can be represented by a symbol that represents a qualitative trait (Figure 17). If quantitative traits are of interest, values can be assigned to each position. Since there is plant to plant variation in panicle architecture, defining a consensus from aligned annotated panicle arrays is appropriate. The alignment involves an acropetal alignment of branches. With this alignment, scores can be computed as percent of paired spikelets. However, it may be also possible to implement more complex alignments and scores using dynamic programming algorithms analogous to those used for polymer sequence alignments or three dimensional structural alignments analogous to those used for folded polypeptide alignments.

The basic branching architecture of the panicles is standard, though tertiary branches are possible. Coordinated activity of the panicle meristems is responsible for this morphology. One 1° branch occurs at each node. However, rachis internodes can be very short, making it difficult sometimes to assign an acropetal order to 1° branches. For instance, during ideal growth conditions during the panicle differentiation stage, two or three 1° branches are commonly found near the neck node (Matsushima, 1967). In contrast, 1° branches are sometimes lacking on the neck node. Vestiges of organs are commonly seen on panicles. Proximal 1° branches degenerate more frequently than distal ones (Matsushima, 1967). Except for 1° branch vestiges at neck nodes, vestiges were ignored in the model. Hence, it needs to be emphasized that the nodal distributions may not accurately represent differentiation. Nodal distributions, especially for 2° branches and spikelets can be different when vestiges are taken into account (Kobayasi and Imaki, 1997).

The distribution of yield components was as expected for rice. Secondary branches are more numerous but shorter, containing fewer spikelets. Panicles can be

morphologically classified on the basis of which nodes have the most 2° spikelets (Takeoka et al., 1993). Jefferson has 2° branches associated more with the middle nodes of the rachis (Figure 11).

Asynchronous ripening produces the observed nodal distributions of dense grains and changes with days after heading. Primary grains ripen before 2° grains. The trend of ripening across the whole panicle is generally basipetal. It is known that the apical 1° spikelet flowers first and then the rest of the 1° spikelets open in acropetal order (Xu and Vergara, 1986). The pattern of ripening is supposed to follow flowering. However, there was no evidence for the basal 1° spikelet being dominant over the middle ones. Another, surprising finding is the lack of dense grains at some positions toward the apex of the panicle at 20 and 15 days after heading (Figure 17; Figure 18). These are the spikelets that flower early on and would be expected to be dominant.

In conclusion, a framework has been established to study ripening on a more global scale. The temporal and spatial variation of grains that sank in water was established. Interesting questions arise such as what genes and proteins regulate this asynchrony of ripening. The computational methods provide an efficient framework to approach this problem. For instance, gene expression and protein levels could be quantified for each spikelet/grain on the panicle at different times after emergence. The results could be analyzed as a function of rachis node or in terms of position on the consensus panicle. Hence, these methods could lead to a better understanding of the molecular basis for how panicle ripening varies in both space and time.

CHAPTER 4

COMPOSITION OF THE CARYOPSIS COAT OF RIPENING RICE

Abstract

The ripening rice caryopsis contains maternal tissues that supply nutrients to the embryonic endosperm where storage compounds are biosynthesized and deposited. Because of tissue adhesion, the compositions of parts that result from caryopsis dissection are not clear unless carefully defined. The objective of this study was to assess the extent to which the caryopsis could be dissected by mechanical means. Caryopsis coats were isolated, by removing as much embryonic tissue from caryopses as possible, and microscopically characterized. Complete separation of endosperm and maternal tissues was only possible during the very early stages of ripening. During mid-ripening, in centripetal order, the pericarp, inner integument, nucellus, aleurone and a patchy subaleurone adhered to each other. Of these tissues, only the pericarp and inner integument could be mechanically separated. However, microscopic inspection of regions lateral to the dorsal vascular bundle revealed that the separation was incomplete because tube cells of the pericarp adhered to the inner integument. These results suggested that the caryopsis coat can be subdivided into two parts, referred to here as inner and outer coats, and illustrated how, in the context of caryopsis dissection, especially during ripening when several cell types are living, terms such as seed coat, pericarp and aleurone layer can be confusing.

Introduction

The structure of a sink governs to a certain extent the route by which unloaded nutrients move through it. Complex anatomy can restrict investigations of nutrient transport in sinks (Fisher and Oparka, 1996). The ripening rice caryopsis, a fruit with one seed, is a prime example of this.

The bulk of the caryopsis is the seed. One of the anatomical complexities is the structural relationship between the seed and its fruit. During ripening, the outer integument degenerates and the inner integument fuses to the inner surface of pericarp, or tube cell layer (Hoshikawa, 1993). As a result, it is challenging to separate the seed, which takes up nutrients and deposits storage compounds, from the rest of the fruit, which supplies the seed.

The caryopsis is composed of several concentric maternal and embryonic tissues from the core of inner starchy endosperm centrifugally to the outer epidermis of the pericarp (Hoshikawa, 1993). Following symplasmic unloading from sieve element/companion cell complexes of the dorsal vascular bundle (Figure 1), nutrients move radially and circumferentially through maternal tissues before reaching the aleurone, the outer surface of the embryonic endosperm that abuts the maternal nucellus (Oparka and Gates, 1981b). Therefore, the nucellus must release nutrients and the aleurone take them up. The second anatomical complexity has to do with the structural nature of this maternal/embryonic interface. The aleurone adheres to the maternal tissues during dissection and prevents simple separation.

These two problems of inner integument/pericarp and aleurone/nucellus adhesion hinder tissue-specific assessments of nutrient transport. Aleurone layers with attached maternal tissues (Phillips and Paleg, 1970) and caryopsis segments have been adopted for studies of aleurone secretion from mature caryopses. Since maternal tissues die at maturity (Hoshikawa, 1993) and the endosperm, except for the aleurone, undergoes programmed cell death (Young and Gallie, 2000), the aleurone is the only living tissue in these systems, which lack the embryo. However, during ripening these systems contain several living tissues in addition to the aleurone. Clearly, new experimental systems are needed.

Experimental techniques for separating caryopsis tissues may facilitate investigations of transport along this pathway. The objective of this study was to assess the extent to which caryopsis tissues could be mechanically separated. Ripening caryopses from *Oryza sativa* L. cv. Jefferson were dissected and component parts characterized by light microscopy.

Materials and Methods

Caryopsis Dissection and Macroscopic Characterization of the Caryopsis Coat

Grains from panicles with green hulls and green caryopses ten to fourteen days after heading were removed from the rachis branches. The hull, stigma and stamens were removed. The lateral side of the caryopsis was cut lengthwise halfway through. The starchy endosperm and embryo were removed from the caryopsis coat. Vortexing caryopsis coats in aqueous suspension released more starch. The amount of starch in solution was determined by adding I_2KI and measuring the absorbance at 580 nm. The inner and outer caryopsis coats were separated by applying light pressure to the caryopsis coat and swirling it in a puddle of water on a hard surface. Coats were stained with 0.5% I_2 1% KI and viewed with the naked eye.

Microscopic Characterization of the Caryopsis Coat

The inner surface of isolated caryopsis coats was rubbed gently under running water. Wet mounts of whole inner and outer coats were prepared and viewed *en face*. Cross sections (1-mm thick) of caryopsis coats, inner coats and outer coats embedded in wax were viewed with an underwater objective. Stains were used at the following concentrations: 0.005% Fast Green, 0.5% I_2 1% KI and 0.01% fluorescein diacetate (FDA) in DMSO diluted a hundred fold. Specimens were microscopically visualized as described above under bright field and fluorescence illumination.

Results

Endosperm Adhered to the Caryopsis Coat

Dissection removed the embryos and most of the milky and doughy endosperm from caryopses. Caryopsis coats that weighed 7.9 ± 0.2 mg (n = 30) and had a surface area of approximately 30 mm^2 remained. Endosperm adhering to the inner surface, was visible to the naked eye, and turned black after exposure to I_2KI (Figure 22). Vortexing removed some of this endosperm. Starch in solution more than doubled after five seconds and leveled off thereafter (Figure 23).

The Caryopsis Coat was Frontally Separable

A green outer coat could be easily separated from both caryopses and caryopsis coats (Figure 22). Lateral regions were easier to separate than dorsal regions. Frontal views of inner and outer coat surfaces showed that the dorsal vascular tissue and lateral tube cell layer partitioned between both coats. Inwardly and outwardly adhered tissues were distributed to inner and outer coats respectively (Figure 24).

Patches of Subaleurone Covered the Aleurone

Frontal views confirmed that adhered endosperm was exposed on the inner surface of inner coats. Outwardly adjacent maternal cells were often exposed at edges. The aleurone formed a continuous layer 1,875 ± 121 cells/mm^2 (n = 10) and was covered by patches of subaleurone (Figure 24). Both tissues appeared heterogeneous in the number of cells thick.

Cross sections showed quantitatively that the dorsal aleurone and subaleurone were thicker compared to lateral regions and that the subaleurone was thinner than the aleurone (Figure 25). Variation in thickness of the lateral portions of the nucellus was not as great. The subaleurone inwardly covered only portions of the aleurone cross section (typically less than half of it) while the nucellus covered it completely.

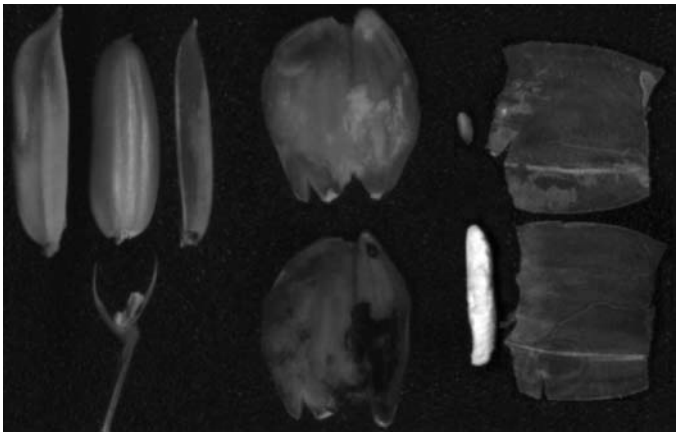

Figure 22 Dissection of the ripening grain of *Oryza sativa* L. cv. Jefferson. From left to right and top to bottom: lemma, caryopsis, palea, caryopsis coat, embryo, inner caryopsis coat, pedicel and rest of hull, caryopsis coat stained with I_2KI, starchy endosperm and outer caryopsis coat. The caryopsis coat, approximately 30 mm^2, is that which remains of the caryopsis after as much embryonic tissues are removed as possible. Inner and outer coats result from facial separation of the caryopsis coat. Note that the inner and outer coats with conspicuous horizontal dorsal vascular bundles are rotated 90° relative to the caryopsis coat.

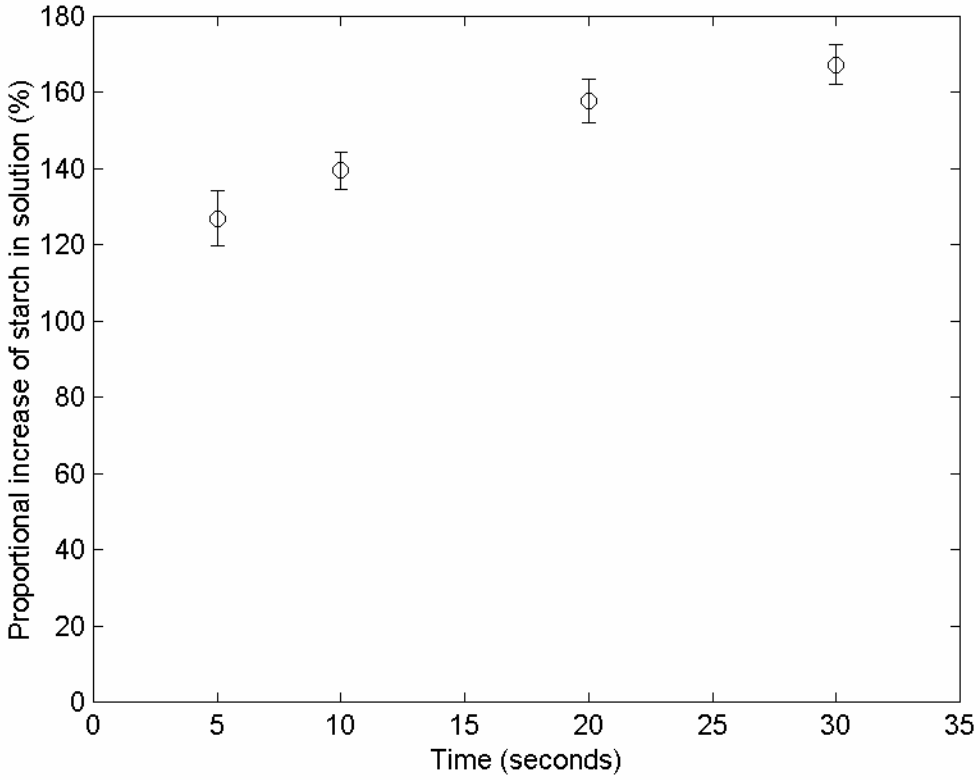

Figure 23 Effect of vortexing time on the amount of free starch in incubation medium containing ripening caryopsis coats of *Oryza sativa* L. cv. Jefferson. Caryopsis coats were isolated by mechanically removing embryonic tissues from caryopses. Amount of free starch was determined by measuring the absorbance of aqueous caryopsis suspensions to which I_2KI was added. Bars are the standard error of a mean of three replicates.

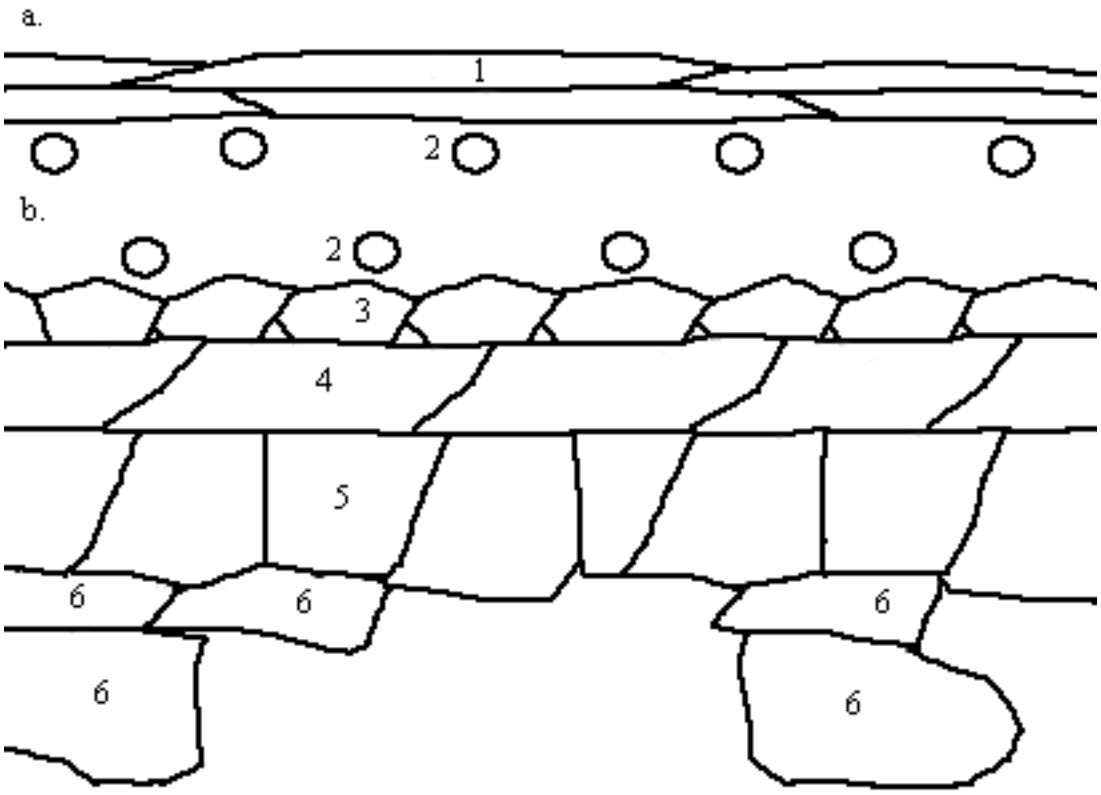

Figure 24 Distribution of tissues resulting from mechanical isolation and facial separation of the ripening caryopsis coat of *Oryza sativa* L. cv. Jefferson. Cross section of tissues lateral to the dorsal vascular bundle are shown. Separation occurs in the tube cell layer. Outer coat (a). Outer tissues such as the outer epidermis are not shown. Labeled cells are from the cross cell layer (1) and inner epidermis of the pericarp, or tube cell layer (2). Inner coat (b). Labeled cells are from the tube cell layer (2), inner integument (3), nucellar epidermis (4), aleurone (5) and outer starchy endosperm, or subaleurone (6). Maternal cells are 1, 2, 3 and 4. Embryonic/endosperm cells are 5 and 6. Cells of the seed are 3, 4, 5 and 6. Pericarp cells are 1 and 2.

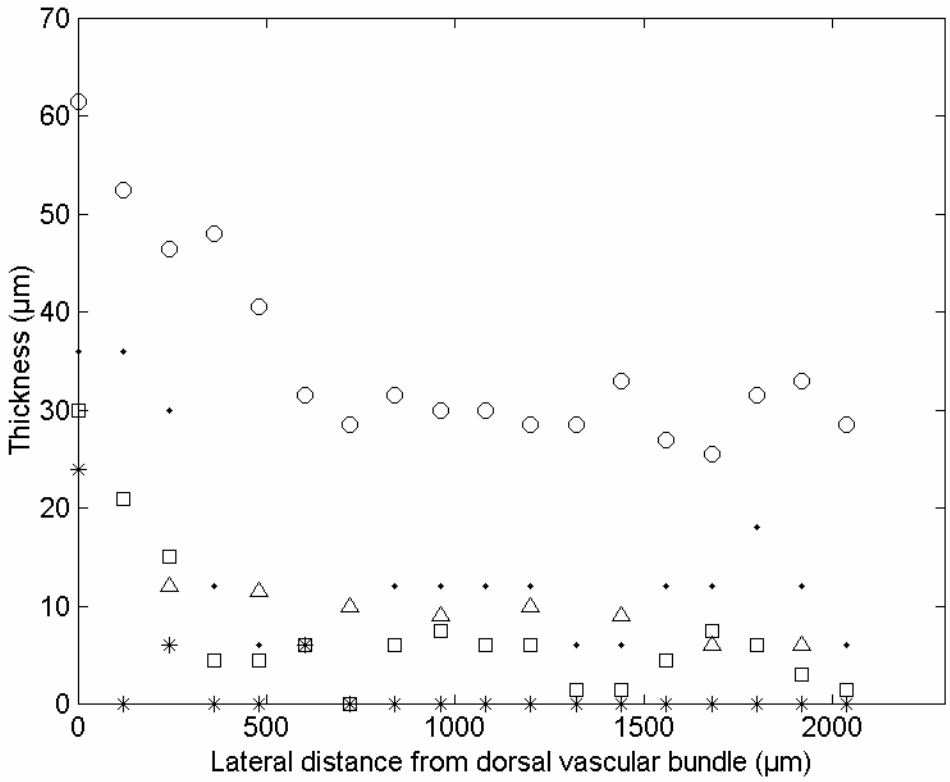

Figure 25 Relationship between thickness of the aleurone, subaleurone and nucellar epidermis and lateral distance from the dorsal vascular bundle of the ripening caryopsis coat of *Oryza sativa* L. cv. Jefferson. Symbols are aleurone average (n = 4, ○), subaleurone average (n = 4, □), subaleurone maximum (·), subaleurone minimum (*) and nucellar epidermis average (n = 2, △).

Staining Made the Subaleurone More Discernable

Application of Fast Green and I_2KI to caryopsis coats made the subaleurone more easily discernable. Subaleurone cells were chromophilic to Fast Green and chromogenic (developed black coloration) in I_2KI. Green and black coloration varied in intensity among subaleurone cell layers and for the most part co-localized to individual subaleurone cells. Subaleurone cells were more chromophilic and less chromogenic the closer they were to the aleurone. The aleurone was not chromogenic in I_2KI and chromophobic to Fast Green; however, double staining caused the aleurone, especially the embryo-surrounding region, to be slightly chromophilic.

Isolated caryopsis coats had a few cell types that fluoresced in FDA. Organelles of the subaleurone were brightly fluorescent in FDA giving the subaleurone a speckled appearance. Conversely, the aleurone displayed a homogeneous fluorescence that was very weak. Visible from the outer surface of inner coats were patches of brightly fluorescent inner integument cells.

Endosperm and Maternal Tissues Did not Adhere Early on in Ripening

For caryopses that just finished elongation, dissection removed the embryo and milky endosperm. The caryopsis coat that resulted had a slick inner surface. Endosperm visible to the naked eye did not adhere to the inner surface. Microscopic inspection showed that nucellus was exposed on the inner surface of these coats. Separation of the caryopsis coat into inner and outer coat was much more difficult.

Discussion

Caryopsis dissection (Figure 22) is not always sufficient to fully separate embryonic and maternal tissues. This is illustrated after the early stages of ripening, when the embryonic aleurone adheres tightly to the maternal nucellus (Figure 24). The term caryopsis coat, as defined here, is that which remains after as much embryonic tissue as possible is mechanically removed from the caryopsis. Hence, depending on

the stage of ripening at which it is isolated, it includes maternal tissues with or without adhering embryonic tissues. In contrast, in the context of caryopsis cross sections, the same term has been defined to include only the maternal tissues (Bechtel and Pomeranz, 1977). The ability to fully separate the aleurone and nucellus early on in ripening suggests that an active process of wall cross-linking (Fry, 1986) is responsible for the adherence of these two tissues and is not complete until after the caryopsis finishes elongation. Later in ripening, the failure of mechanical isolation may be because the aleurone and subaleurone are very thin (Figure 25) and tightly adhered to the nucellus. However, mechanical separation of aleurone and maternal tissues of imbibed barley by using a blender is reported by Taiz and Jones (1971).

The caryopsis coat is frontally separable after the early stages of ripening (Figure 22). Because inner and outer coats are thinner and more transparent, it is possible to inspect microscopically their surfaces and underlying layers without any sectioning. Using this technique, tube cells and vascular tissue are obvious on the surface of both inner and outer coats. Hence, separation of the caryopsis coat occurs dorsally within the dorsal vascular tissue, also called the ovular vascular trace (Krishnan and Dayanandan, 2003), and laterally within the tube cell layer (Figure 24). The tube cell layer has many intercellular spaces, which form when the caryopsis increases in girth (Hoshikawa, 1993). This may explain why separation is favored there and why ease of separation increases with lateral position. That the caryopsis coat is not easily divided early on in ripening suggests that the aleurone, when tightly adhered to the nucellus, favors separation. The aleurone, with its large thickness relative to the maternal tissues (Figure 25), especially in the dorsal region, suggests that the aleurone, when stuck to the nucellus, contributes greatly to the stiffness of the inner coat. Another possibility is that maternal tissues, such as the tube cell layer, have not yet reached a state of differentiation that is favorable for separation. The fact that

the tube cell layer would be expected to have more intercellular spaces after the caryopsis finishes elongation is consistent with this.

The composition of each coat can be inferred given the locations of separation and descriptions of caryopsis anatomy by Hoshikawa (1993). For example, subaleurone, aleurone, nucellus, inner integument and tube cell layer assign to lateral regions of the inner coat and tube cell layer, cross cell layer and outer epidermis to the outer coat (Figure 24). The outer coat is composed entirely of maternal tissues of the ripening ovary wall (pericarp), while the inner coat is composed of endosperm, maternal tissues of the seed (inner integument and nucellus) and pericarp (tube cells). Hence, the anatomical terms aleurone layer, seed coat and pericarp are extremely confusing when not clearly defined in the context of caryopsis dissection and tissue adherence. This study suggests that the terms inner coat and outer coat are useful alternatives because they are based on mechanical criteria. The inner and outer coats (Figure 22) are defined as those structures that result after facial separation of the caryopsis coat.

The aleurone has a heterogeneous topography. One contributing factor is that endosperm-surrounding aleurone is more granular than embryo-surrounding aleurone (Bechtel and Pomeranz, 1977). The other is that patches of cells inwardly adhere to the endosperm-surrounding aleurone (Figure 25). These cells are of the outer starchy endosperm, and hence referred to as subaleurone. Within multi-layered subaleurone patches, concentration of Fast Green-stained protein declines inwardly while that of I_2KI-stained starch declines outwardly. Similar gradients related to protein and starch storage have been demonstrated. The outer endosperm is specialized for protein storage (Ellis et al., 1987). The subaleurone and inner starchy endosperm stain most intensely with protein indicators and starch indicators respectively (Krishnan et al., 2001). Compared to those of the inner starchy endosperm, subaleurone amyloplasts

and starch granules are smaller and protein bodies more concentrated (Hoshikawa, 1993). The level of endosperm-specific expression of reporter genes under the control of glutelin and prolamin promoters is stronger in the subaleurone (Qu and Takaiwa, 2004).

The aleurone and nucellus, technically, must adhere to each other *de novo* after the early stages of ripening. This adhesion would not result from cell plate formation during cytokinesis, which is more common (Jarvis et al., 2003). Aleurone initials are the peripheral cells that result from the first round of mitosis and cytokinesis during endosperm cellularization. Outer periclinal walls of aleurone initials are derived from the central cell wall of the embryo sac (Brown et al., 1996). The embryo sac is surrounded by a multi-layered nucellus of which the inner cells degenerate after double fertilization (Hoshikawa, 1993). In wheat this cell death is programmed (Domínguez et al., 2001). In rice, inner nucellus degeneration commences before and completes after aleurone differentiation (Ishimaru et al., 2003). This suggests that the cells of the aleurone abut and tightly adhere to those of the outer nucellus after both cell types are differentiated. The regulation of this adhesion is not fully understood. It is not known whether adherence at the maternal/embryonic interface is important in the regulation of nutrient release and uptake or for cell-to-cell signaling.

In conclusion, adhesion among tissues within the caryopsis coat is a major factor that limits the extent to which the caryopsis coat can be dissected. Mechanical isolation of the maternal/embryonic interface is not always feasible. This complicates tissue-specific application of experimental techniques to assess transport steps. Outer and inner caryopsis coats were mechanically separable. In this study, the compositions of the inner and outer coats are clearly defined in terms of their component cell types. A similar approach would be very important to interpret gene expression, enzyme activity, transport, etc. in the context of structures that result from dissection.

Enzymatic separation of the maternal/embryonic interface may be a good alternative to mechanical isolation when aleurone and nucellus unyieldingly adhere. Isolated cells and protoplasts of maternal and embryonic origin may provide good experimental systems to assess sucrose efflux and uptake.

CHAPTER 5

ENZYMATIC MACERATION OF CARYOPSIS COAT CELLS

Abstract

In the ripening caryopsis of rice, storage of carbohydrates, proteins and lipids in the endosperm depends on uptake by the aleurone of assimilates that are released from the nucellus. Investigation of mechanisms of transport at this interface is complicated because of adherence between the aleurone and nucellus. The extent to which enzymes could be used to separate caryopsis tissues was investigated. Caryopsis coats were isolated by dissection and endosperm cells exposed on the inner surface were macerated with Pectolyase Y-23. Manual shearing after a very short incubation time freed the endosperm and exposed the nucellus. Longer incubation time was required for greater separation of endosperm cells. Yield of endosperm cells increased linearly with the number of coats and reached a maximum after an hour. The proportion of cells that were viable, as determined by plasmolysis and vital staining, was approximately 10%. Subaleurone cells contributed less than 25% to the yield. These results suggest that pectin polymers are needed for adherence between the aleurone and nucellus and that enzymatic maceration is useful for separating this interface.

Introduction

The rice caryopsis maternal/embryonic interface is that across which nutrients move during ripening. It is composed of maternal nucellus to the outside and embryonic aleurone to the inside. When isolation of the aleurone from caryopses is attempted mechanically, the aleurone can stick to maternal tissues (Phillips and Paleg, 1970). Although it is possible to mechanically free the aleurone (Taiz and Jones, 1971), in some cases, as in ripening rice, it unyieldingly adheres to the nucellus after the early stages of ripening (Chapter 4). Enzymatic tissue maceration followed by cell isolation

(Zaitlin, 1959; Zaitlin and Coltrin, 1964; Takebe et al., 1968) may be a useful alternative to mechanical isolation via dissection.

Aleurone cells have been enzymatically isolated from imbibed grains (Taiz and Jones, 1971; Eastwood, 1977; Hooley, 1982). Sometimes the cells were isolated because enzyme preparations meant for protoplast isolation did not completely remove the cell wall.

Pectin degrading enzymes are specifically useful for maceration and cell isolation and have been employed on a number of fruits and vegetables (Nakamura et al., 1995). The objective of this study was to isolate aleurone cells in good yield from ripening rice caryopses and, in the process, expose the nucellar half of the maternal/embryonic interface. Caryopsis coats were isolated, exposed to Pectolyase Y-23, and manually sheared. Viability and composition of the resulting cell suspension were characterized.

Materials and Methods

Enzymatic Maceration of Caryopsis Coats

Isolated caryopsis coats were collected (200/hr, 10-20/ml) in ice-cold incubation medium (IM). IM contained 600 mM mannitol, 1 mM KCl, 1 mM $MgCl_2$, 1 mM $CaCl_2$ and 1 mM MES and was adjusted to pH 6 with NaOH (about 1 mM). Caryopsis coats in IM were transferred to a 50-ml conical centrifuge tube, vortexed for 30 seconds, transferred to a Buchner funnel, and then rinsed with water. The coats were transferred to IM with 0.1% Pectolyase Y-23 (Seishin Pharmaceutical) and incubated for 1.5 hours. Coats were transferred back to IM and manually sheared. The cell suspension was transferred to nylon mesh (105 μm) and the filtrate collected.

Microscopic Characterization of Cells

Cells were stained in suspension with Fast Green, I_2KI and FDA at concentrations previously listed (Microscopic Characterization of the Caryopsis Coat,

page 58). The nucellus was stained with 0.05% Janus Green. Cells were suspended in pure solutions of KCl. Concentrations and dimensions of cells in suspension were determined with a Neubauer hemacytometer and an ocular micrometer, respectively.

Results

Enzymatic Maceration Separated Endosperm and Maternal Tissues

Manual shearing of caryopsis coats after five minutes of incubation in Pectolyase Y-23 exposed the nucellus on the inner surface except for a few regions still covered by aleurone. Maternal tissues remained largely intact. The nucellus was chromogenic in Janus Green.

Cells of the endosperm were observed in suspension. Only a portion of cells passed through the nylon mesh. Cell yield was dependent on incubation time and the number of caryopsis coats. The greatest number of cells was isolated when caryopsis coats were incubated for at least 60 minutes (Figure 26). Cell yield was linear with the number of coats incubated per volume of IM. Approximately 56,000 cells were isolated per caryopsis coat (Figure 27). Some maternal tube and cross cells (Figure 24) were also observed in suspension.

Aggregation, Viability and Plasmolysis Varied Among Endosperm Cells

Endosperm cells were commonly observed still attached to each other in aggregates (Figure 28). Cell aggregates were fewer than single cells, contained the majority of cells and almost always had fewer than five cells (Figure 29).

Aleurone and subaleurone cells exposed to Fast Green and I_2KI were distinguishable also in suspension. Subaleurone cells were chromophilic to Fast Green and chromogenic in I_2KI. They contributed less than 25% to the yield of isolated endosperm cells and had a greater product and ratio of length and width (Table 3). Cytoplasmic granules released by subaleurone cells were commonly observed.

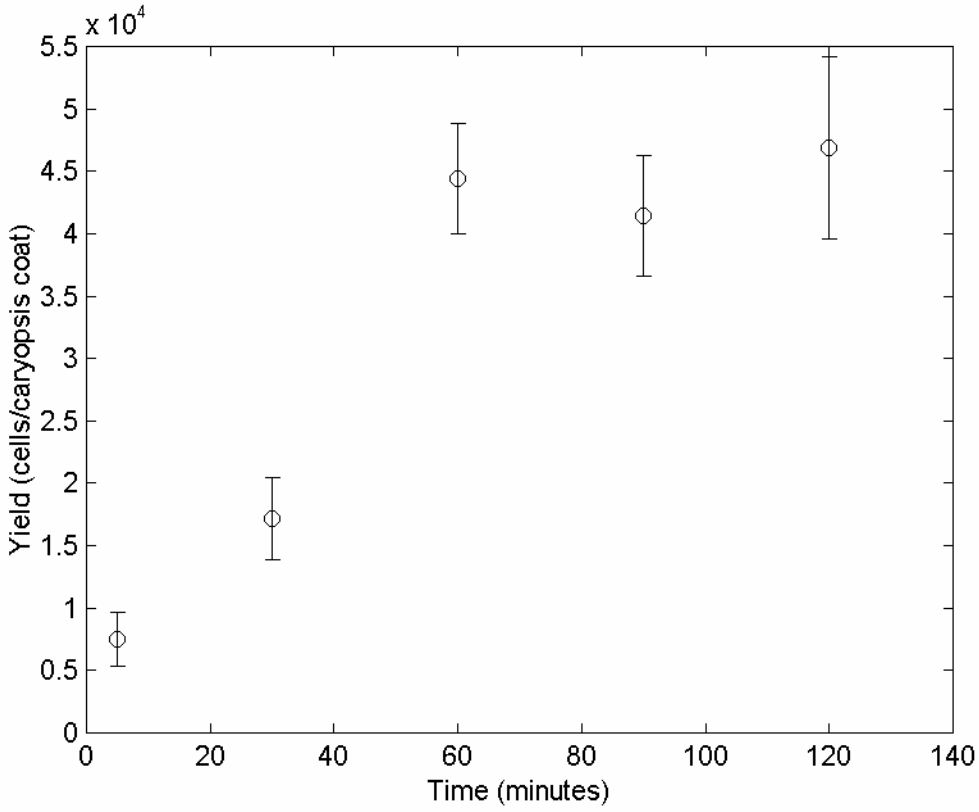

Figure 26 Effect of time of exposure to Pectolyase Y-23 on yield of endosperm cells isolated from the inner surface of ripening caryopsis coats of *Oryza sativa* L. cv. Jefferson. Caryopsis coats were isolated from 10-14 days-after-heading panicles, incubated in 0.1% Pectolyase Y-23 for different times and then subjected to gentle shear force. The resulting cell suspension was filtered through nylon mesh (105 µm) before cells were counted. Bars are the standard error of a mean of three replicates.

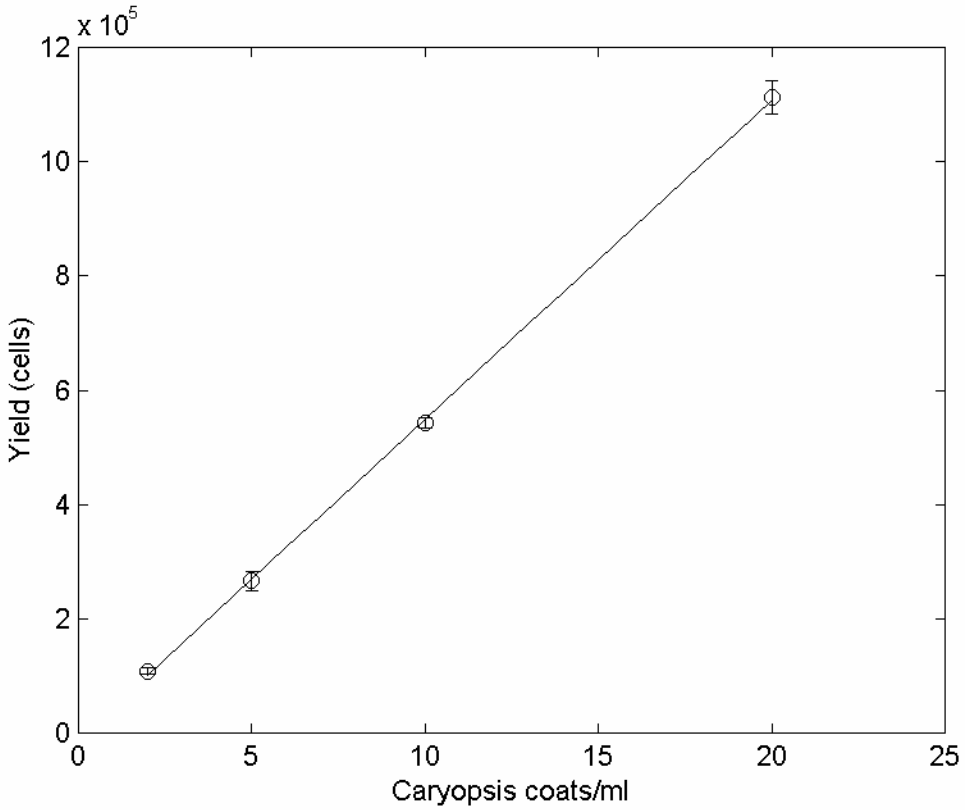

Figure 27 Effect of the number of isolated caryopsis coats per volume of incubation medium on yield of endosperm cells isolated from the inner surface of ripening caryopsis coats of *Oryza sativa* L. cv. Jefferson. Coats were incubated in Pectolyase Y-23 for 90 minutes before shearing. Bars are the standard error of a mean of three replicates. The line is a least-squares fit. The fitted equation is $y = 55921x - 10230$ and R^2 value is 1.000.

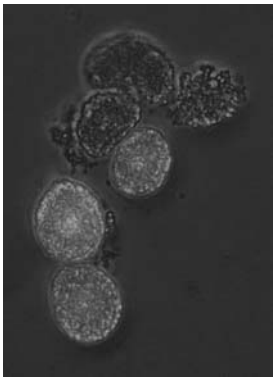

Figure 28 Aggregates of endosperm cells isolated from the inner surface of ripening caryopsis coats of *Oryza sativa* L. cv. Jefferson. Cells were vitally stained with FDA. Light-shaded cells displayed a bright green fluorescence.

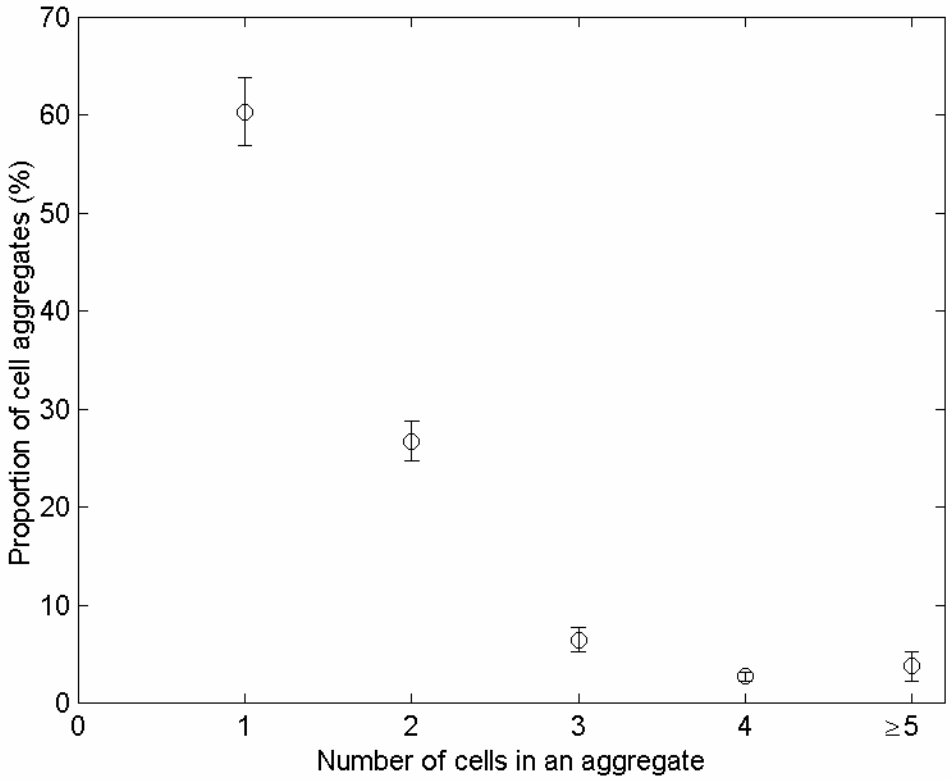

Figure 29 Proportion of endosperm cell aggregates of various sizes after the isolation of cells from the inner surface of ripening caryopsis coats of *Oryza sativa* L. cv. Jefferson. Bars are the standard error of a mean of nine replicates.

Table 3 Proportion and dimension of cells that stained with Fast Green, I_2KI or FDA after they were isolated from the inner surface of ripening caryopsis coats of *Oryza sativa* L. cv. Jefferson. Means and standard errors are listed.

	Fast Green-chromophobic (aleurone)	Fast Green-chromophilic (subaleurone)	I_2KI-chromogenic (subaleurone)	Fluorescent in FDA
Proportion of cells (%), n = 8	78.7 ± 1.6	21.3 ± 1.6	15.0 ± 1.1	9.7 ± 2.3
Cell length x width (mm^2), n = 20	604 ± 44	1,005 ± 167	1,513 ± 188	Not measured
Cell length/width, n = 20	1.3 ± 0.07	1.6 ± 0.1	1.4 ± 0.06	Not measured

Some separated endosperm cells (about 10%) fluoresced in FDA (Table 3). The fluorescence of aleurone cells in suspension seemed more obvious than that of the aleurone of caryopsis coats. Some cells within a clump fluoresced while others did not (Figure 28). Tube and cross cells did not fluoresce.

Some separated endosperm cells plasmolyzed appreciably when exposed to pure KCl solutions greater than 200 mM (Figure 30). These cells appeared shriveled up and were fluorescent when also exposed to FDA. The proportion of cells showing this characteristic increased with higher concentrations of KCl and reached a maximum of approximately 15% around 800 mM.

Discussion

Pectolyase Y-23 activity macerates the aleurone and compromises tight adhesion between the aleurone and nucellus (Figure 26). This enzyme preparation contains endopolygalacturonase and endopectinylase (Nishimura et al., 1987), fungal endohydrolases that separate plant cells by the depolymerization of pectins (Ishii, 1976). Pectins are components of the cell wall matrix and are found in the middle lamella across which cells adhere and form tissues. Pectic polymers of rice endosperm contain galacturonic acid and rhamnose in their main chain (Shibuya and Nakane, 1984). *De novo* cell adherence requires the formation of cross-links between walls (Fry, 1986). Pectin cross-linking and cell adhesion is disrupted in cells with a mutation in a pectin glucuronyltransferase gene (Iwai et al., 2002). *De novo* adherence of pollen tube and stylar epidermis also requires a pectic polymer (Mollet et al., 2000) and the lipid transfer-like protein SCA (Park et al., 2000). Interestingly, the lipid transfer protein LTP-ne is specifically expressed in the outer layer of barley nucellus a few days after pollination (Chen and Foolad, 1999).

Enzymatic maceration enables complete separation of endosperm and maternal tissues. However, care needs to be taken during shearing to minimize contamination of

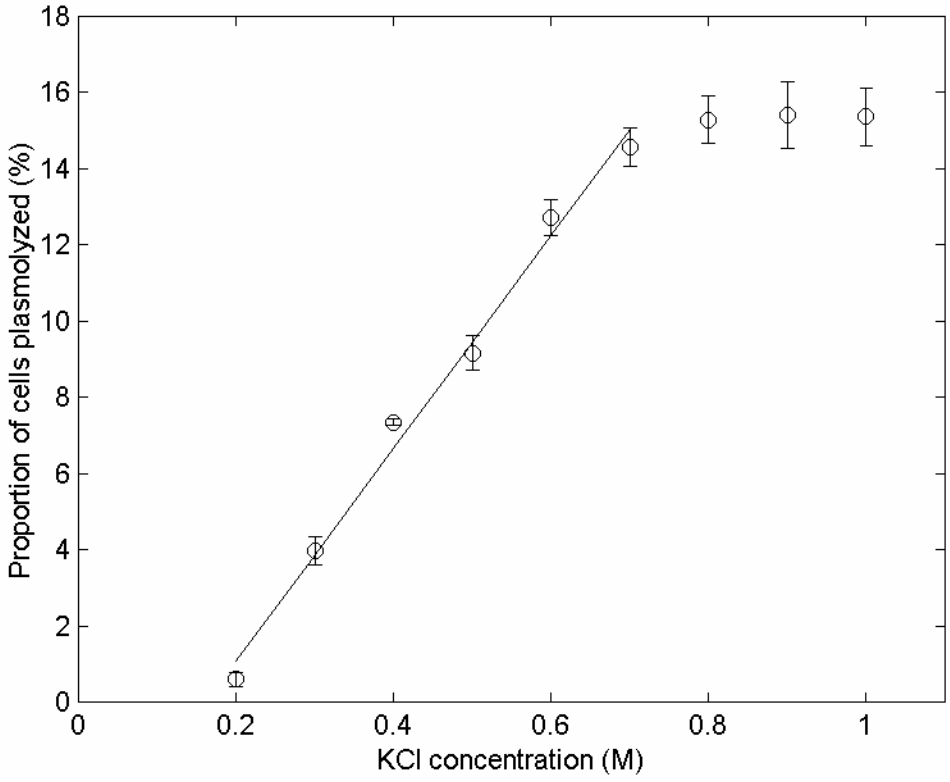

Figure 30 Effect of KCl concentration on the plasmolyzed proportion of endosperm cells isolated from the inner surface of ripening caryopsis coats of *Oryza sativa* L. cv. Jefferson. Bars are the standard error of a mean of three replicates. The line is a least-squares fit to six data points. The fitted equation is $y = 27.974x - 4.531$ and R^2 value is 0.991.

the endosperm fraction by maternal tube and cross cells. This method for separation is useful because the nucellus and aleurone of rice are not separated *in vivo* by an endosperm cavity like in wheat, which has been taken advantage of experimentally to assess transport of assimilates (Wang et al., 1993). Furthermore, from our experience, mechanical separation of the maternal/embryonic interface in rice is not possible after the early stages of ripening, making enzymatic isolation a useful alternative. Another way around the problem of endosperm and maternal tissue adherence is the isolation of protoplasts (Sadasivam and Gallie, 1994), which are sometimes confusingly referred to as isolated cells (Smirnova et al., 1989).

Enzymatic separation of cells within the adhered endosperm is incomplete (Figure 29). Cells of the aleurone divide anticlinally as the caryopsis increases in girth (Olsen, 2001), so most adherence between cells is a result of cytokinesis followed by mitosis. Compared to separation of the nucellus and adhered endosperm, much more time is needed to separate endosperm cells enough to pass through the filter. This suggests that aleurone cells adhere more strongly to each other than to the nucellus.

The viable proportion of separated endosperm cells is only approximately 10% (Table 3). Although edge cells are likely to get damaged (Cochrane, 1994), it is unlikely that dissection is the main cause of viability loss. Furthermore, it is unlikely that Pectolyase Y-23 toxicity is responsible (Basham and Bateman, 1975). Low viability may result from osmotic damage to cells during the maceration process (Bateman and Basham, 1976). The speckled appearance of the subaleurone exposed to FDA suggests that the fluorescent product that results after cleavage of FDA by esterase accumulates in organelles. It is possible that the plasma membrane containing these organelles is not intact. Hence, viability of separated cells in suspension may actually be overestimated. However, the maximum percentage of cells plasmolyzed (Figure 30) supports that the estimate of viability is in the correct range.

Aleurone and subaleurone cells are discernable in stained suspensions. A cell is judged to be from the aleurone if it is chromophobic to Fast Green and not chromogenic in I_2KI. Consistent with their patchy coverage of the aleurone, subaleurone cells represent the minority. Given the yield of isolated endosperm cells per coat (Figure 27), the aleurone proportion of cells, the area of the isolated coat and the cell density of the aleurone, an estimated 80% of the aleurone cells pass through the filter. Isolation efficiency, viability and the relatively low number of aleurone cells in rice compared to other caryopses like barley are major factors that require maceration of many coats to obtain good yield of viable cells. Easily removable milky or doughy outer endosperm aids dissection of the caryopsis. However, since dissection is very time consuming, development of an apparatus for high throughput isolation of coats from ripening caryopses is desirable. There are reports of such devices for imbibed grains of wheat and barley (Phillips and Paleg, 1970; Murthy, 1989).

In conclusion, the problem of tight adhesion between the aleurone and nucellus is circumvented by enzymatic maceration and isolation of the cells exposed on the inner surface of isolated caryopsis coats. Two new experimental systems result, isolated aleurone cells and caryopsis coats free of embryonic tissues. Since it is possible to separate inner and outer caryopsis coats, embryonic-cell-free inner coats are also possible. Now that the maternal/embryonic interface is separable after the early stages of ripening, mechanisms of transport can be assessed for each half separately. Embryonic-cell-free inner coats would still have inner integument cells and patchy coverage of adhered pericarp cells such as tube and vascular cells. Embryonic-cell-free caryopsis coats may actually be more useful to assess transport by the nucellus specifically because the maternal tissues outwardly adjacent to the nucellar epidermis would be bordered on both sides by a cuticle. In any case, though the exposed nucellus reacts with Janus Green, indicating mitochondrial activity, integrity

of the nucellus plasma membranes needs to be assessed. The cells do not test positive for viability with exposure to FDA. However, this could be due to a lack of esterase activity instead of plasma membrane damage. The major drawback of the isolated aleurone cell system is the low viability of cells. With only approximately 10% viable, preparation of protoplasts from isolated cells followed by protoplast purification may be desirable.

CHAPTER 6

ISOLATION OF CARYOPSIS COAT PROTOPLASTS

Abstract

Protoplast isolation is a useful approach to isolate cell types. The ripening caryopsis of rice has a complex sink structure with both maternal and embryonic cell types. It was expected that protoplasts of the embryonic endosperm and maternal tissues could be isolated. Enzymatic cell wall degradation was employed to isolate protoplasts. Sequential cell and protoplast isolation was most effective for the aleurone exposed on the inner surface of isolated caryopsis coats. Protoplast isolation was optimal in incubation medium (IM) with 0.6 M mannitol. Maximum protoplast yield from isolated cells exposed to 1% cellulase was achieved after 90 minutes. Most protoplasts were 20-30 μm in diameter and between the densities of 40% and 60% Percoll incubation medium (PIM). Only approximately 10% of isolated cells yielded protoplasts. Low protoplast yield was correlated with low viability of isolated cells. Results suggested that it is possible to quickly isolate protoplasts from the aleurone in high enough yield for protoplast uptake studies. Giant aleurone protoplasts and maternal protoplasts were isolated from caryopsis coats after simultaneous exposure to cellulase and Pectolyase Y-23 for eight hours. Giant protoplasts had diameters greater than ten times normal. Maternal protoplasts were small, and some were vacuolated. These results suggested that the aleurone is prone to spontaneous protoplast fusion and that protoplast isolation from the maternal tissues requires unique conditions.

Introduction

The ripening rice caryopsis is a sink with a complex structure composed of several cell types of both embryonic and maternal origin. Of particular interest are the cells of the nucellus and endosperm aleurone because they make up the maternal/embryonic interface. Plasmodesmata accommodate symplasmic transport

throughout the maternal nucellus and embryonic aleurone but not between them (Oparka and Gates, 1981a). Hence, nutrients must cross both maternal and embryonic plasma membranes before they are used in the biosynthesis and deposition of endospermic storage compounds.

Mechanisms of nutrient transport in the ripening rice caryopsis are difficult to assess at the tissue level because of tissue adherence. Suitable procedures for isolating the aleurone and nucellus are lacking. Protoplast isolation may be a useful approach, because protoplasts, by lacking walls, can be separated from other protoplasts and used to assess transport mechanisms at the plasma membrane.

Enzymatic digestion of cell walls is the preferred method of protoplast isolation. In contrast to other methods such as laser microsurgery (Kurkdjian et al., 1993; De Boer et al., 1994) and mechanical cutting (Trebacz and Schonknecht, 2000), it yields numerous protoplasts from the tissue and does not require that the cells be able to plasmolyze substantially (Cocking, 1972).

Plasmolysis is typically the first step for protoplast isolation. Lacking cell walls, protoplasts easily burst in hypotonic solutions. Thus, plasmolysis is important for the prevention of cell death associated with wall degradation (Cocking, 1972). Plasmolysis prior to enzyme treatment can also prevent cell death associated with maceration (Bateman and Millar, 1966). Cell types differ in the effect that plasmolysis has on the physical relationship between the plasma membrane and cell wall (Oparka, 1994). Embryonic cells that lack vacuoles and have dense protoplasm do not necessarily show separation between the cell wall and plasma membrane during the osmotic loss of water when bathed in hypertonic solution (Lee-Stadelmann and Stadelmann, 1989). This may be true for the embryonic aleurone.

Caryopsis protoplasts that have been isolated are mostly of aleurone origin. Aleurone protoplasts are similar in physiology and ultrastructure to cells of intact

tissue (Hillmer et al., 1990). These protoplasts have been mostly used for the study of hormone-regulated secretion of hydrolases, a process that is important for seed germination. The starting material for protoplast isolation is typically imbibed caryopses in which the aleurone and embryo (easily removed) are the only living tissues. Fewer studies have employed aleurone protoplasts for studies during caryopsis ripening.

Aleurone protoplasts have been isolated from germinating seeds of barley (Taiz and Jones, 1971), oat (Hooley, 1982), and rice (Sadasivam and Gallie, 1994), ripening seeds of wheat (Entwistle et al., 1988; Keeling et al., 1989; Niemietz and Jenner, 1993; Díaz, 1994), maize (Echeverria et al., 1985), and barley (Díaz, 1994), and cultured endosperm from maize (Felker et al., 1991).

The importance of aleurone protoplasts is seen in their many applications. Applications include uptake and transient expression of transgenes (Lee et al., 1989; Gopalakrishnan et al., 1991; Díaz, 1994; Sadasivam and Gallie, 1994; Suzuki et al., 2002), investigations of hormone signal transduction in the context of secretion (Jacobsen et al., 1985; Gilroy and Jones, 1994; Suzuki et al., 2002) and cell death (Bethke et al., 1997; Bethke et al., 1999; Bethke and Jones, 2001), isolation and studies of organelles (Echeverria et al., 1985; Bethke et al., 1996; Davies et al., 1996), electrophysiology (Heimovaara-Dijkstra et al., 1994; Van Duijn and Heimovaara-Dijkstra, 1994) and uptake studies (Felker et al., 1991; Niemietz and Jenner, 1993; Wright and Oparka, 1994).

There are two main methods for enzymatic protoplast isolation, sequential cell and protoplast isolation and direct isolation from tissue (Cocking, 1972). One objective of this study was to assess the effectiveness of these approaches for the yield of enough aleurone protoplasts from ripening caryopsis coats to conduct sucrose uptake experiments.

Aleurone cells are connected by numerous plasmodesmata (Oparka and Gates, 1981a) and spontaneous fusion of protoplasts can result during their enzymatic isolation. Spontaneous fusion results from expansion of plasmodesmata (Withers and Cocking, 1972), although plasmolysis is thought to break plasmodesmata (Cocking, 1972). Another objective of this study was to assess the effect of spontaneous fusion on protoplast yield and to isolate giant aleurone protoplasts.

There are few, if any, reports on the isolation of maternal protoplasts from caryopses. This is expected because most work is on mature caryopses which have dead maternal cells (Hoshikawa, 1993). Furthermore, since protoplast isolation protocols need to be optimized for each tissue (Cocking, 1972), maternal tissues probably require different conditions than the aleurone. The final objective of this study was to isolate maternal protoplasts from ripening caryopses.

Standard methods for protoplast isolation were used. These included enzymatic digestion of cell walls, density centrifugation and vital staining.

Materials and Methods

Aleurone Protoplast Isolation

Protoplasts were isolated using a modification of the cell isolation procedure previously described (Enzymatic Maceration of Caryopsis Coats, page 70). The only difference was that caryopsis coats were sheared in IM containing 1% Onozuka RS cellulase and incubated for another 1.5 h. Protoplast viability and measurements were determined using the same methods as for isolated cells.

Protoplast Density Estimation

PIM with Percoll at various percentages of the total volume was prepared and the pH was adjusted with HCl. PIM overlaid with an equal volume of protoplast suspension was centrifuged for 5 minutes. The bench top centrifuge (Dynac) was equipped with a swing out bucket rotor, and was attached to a variable

autotransformer (Powerstat) set at 80. After centrifugation, the protoplasts in the pellet were resuspended with a transfer pipette and counted.

Protoplast Purification

Protoplasts in IM were settled by gravity and resuspended in 2 ml of IM. Protoplasts were overlaid on 1 ml 20% PIM that was overlaid on 80% PIM. Protoplasts were centrifuged for 5 minutes. The band at the lower interface was collected, resuspended in 5 ml of IM, and centrifuged for 5 minutes. Centrifugation was as previously described (Protoplast Density Estimation, page 85). Protoplasts were resuspended in 1 ml IM.

Giant Aleurone Protoplast and Maternal Protoplast Isolation

Caryopsis coats were incubated in IM with Pectolyase Y-23 and cellulase for up to eight hours. The coats were then gently sheared in IM without enzymes.

Results

The aleurone was exposed on the inner surface of isolated caryopsis coats. Protoplasts were isolated from the aleurone when it was exposed to cell wall degrading enzymes (Figure 31). Shearing caryopsis coats exposed to Pectolyase Y-23 or cellulase alone yielded very few or none protoplasts. Coats exposed to both enzymes yielded more protoplasts. Simultaneous exposure to the enzymes followed by shearing yielded more protoplasts than sequential exposure followed by shearing. Caryopsis coats that were exposed to Pectolyase Y-23, sheared, and then exposed to cellulase yielded the most protoplasts compared to all other protocols.

Some isolated endosperm cells in suspension when exposed to cellulase gave rise to spherical protoplasts (Figure 32). Protoplast yield increased linearly with time of exposure to cellulase and leveled off close to 10,000 protoplasts/caryopsis coat after 90 minutes.

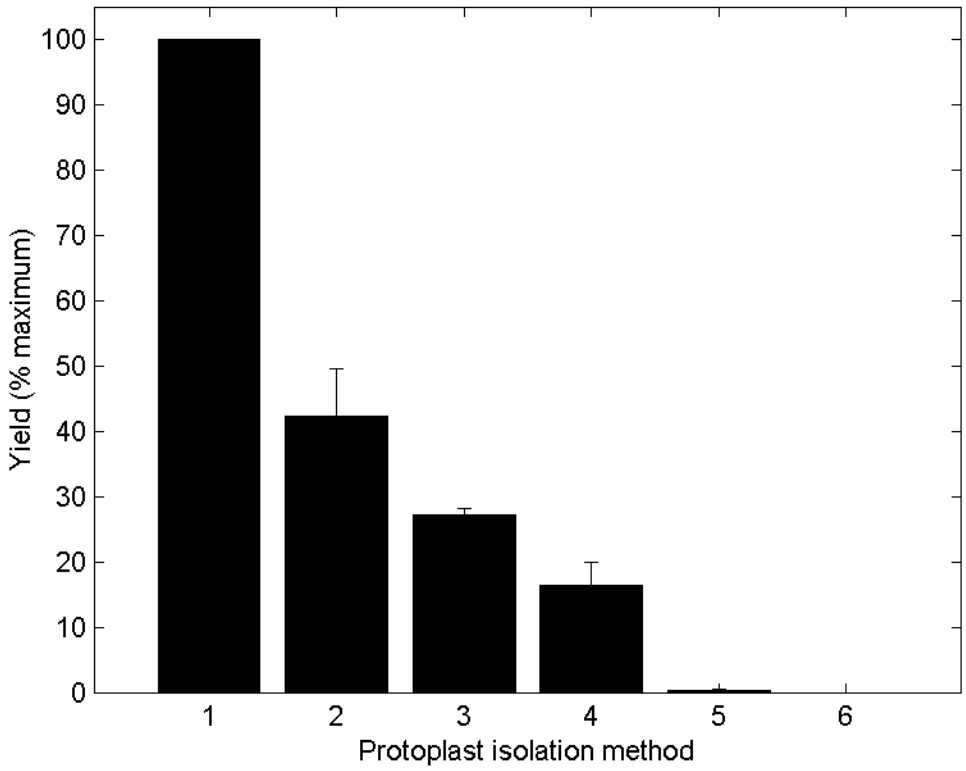

Figure 31 Effect of protoplast isolation method on yield of endosperm protoplasts from ripening caryopsis coats of *Oryza sativa* L. cv. Jefferson. The methods are: Pectolyase Y-23, shear, cellulase (1); Pectolyase Y-23 and cellulase, shear (2); Pectolyase Y-23, cellulase, shear (3); cellulase, Pectolyase Y-23, shear (4); cellulase, shear (5), Pectolyase Y-23, shear (6). Pectolyase Y-23 and cellulase concentrations were 0.1% and 1% respectively. Enzyme treatments were for 90 minutes. Bars are the standard error of a mean of three replicates. Preparation of protoplasts from cell suspensions, method 1, was most effective.

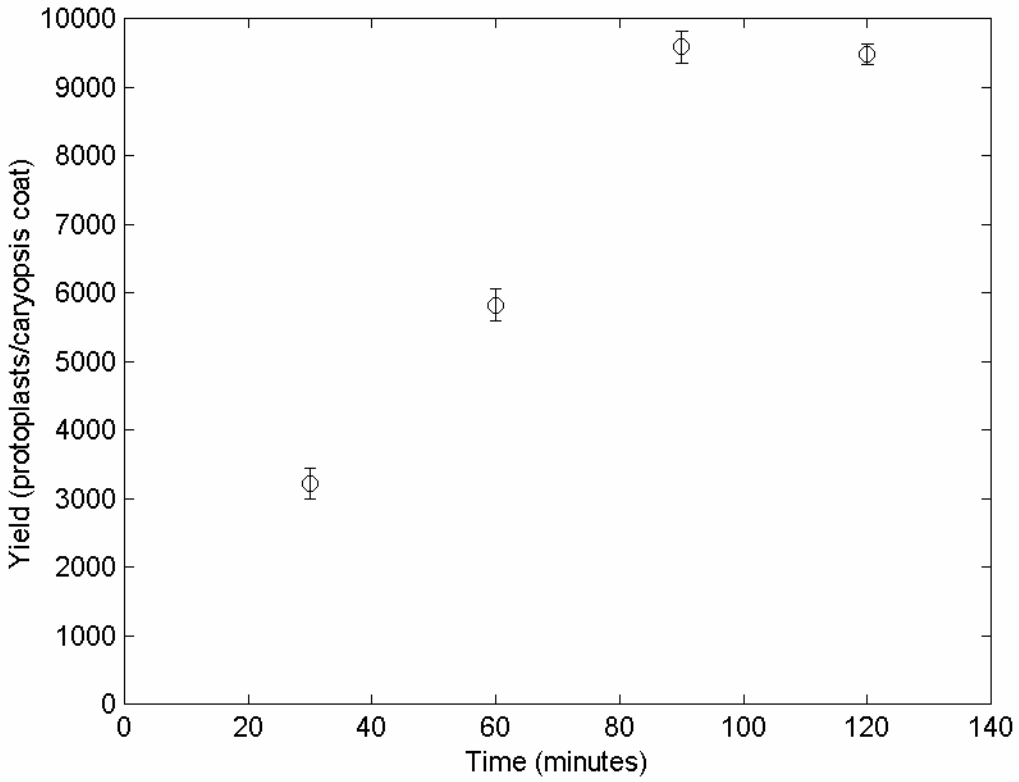

Figure 32 Effect of cellulase incubation time on yield of endosperm protoplasts from ripening caryopsis coats of *Oryza sativa* L. cv. Jefferson. Caryopsis coats were isolated from 10-14 days-after-heading panicles, incubated in 0.1% Pectolyase Y-23 for 90 minutes, transferred to 1% Onozuka RS cellulase, and then subjected to gentle shear force. The resulting cell suspension was filtered through 105-µm nylon mesh and incubated for different times before completely spherical protoplasts, regardless of viability and endosperm cell type, were counted using a hemacytometer. Bars are the standard error of a mean of four replicates.

Protoplast yield varied with IM mannitol concentration (Figure 33). Yield increased with an increase in mannitol concentration from 400 to 600 mM and decreased between 600 and 800 mM. Cells of intact aleurone did not show appreciable plasmolysis in mannitol concentrations up to 800 mM.

Protoplasts were spherical. Protoplast contents were granular and appeared identical to aleurone cells in intact tissue. Most of the protoplasts were between 20 and 30 μm in diameter (Figure 34).

The number of protoplasts isolated was approximately one-tenth the number of isolated cells (Figure 35). The decrease in yield between protoplasts and purified protoplasts was not very great. The greatest change in viability was between cells and protoplasts. Purified protoplasts were over 90% viable. Cells were approximately 10% viable (Figure 35).

The number of protoplasts that were centrifuged to the pellet varied with the Percoll concentration of PIM on which the protoplasts were overlaid (Figure 36). Yield decreased as the concentration of Percoll increased. All protoplasts sank in IM. The majority of protoplasts did not float in PIM ≤40%. Between 40% and 60% PIM, there was a large increase in protoplasts that floated. Almost all the protoplasts floated in 80% PIM.

When inner caryopsis coats were mounted in IM with cellulase and under a cover slip, granular protoplasm was released from cells. The granules sometimes flowed across the surface of the underlying maternal tissues to the edges of the caryopsis coat.

Fusion of juxtaposed endosperm protoplasts during isolation was observed with the light microscope. Isolated endosperm cells were aggregated and still attached to each other by common cell walls. Some protoplasts within the same aggregate were seen to fuse with each other.

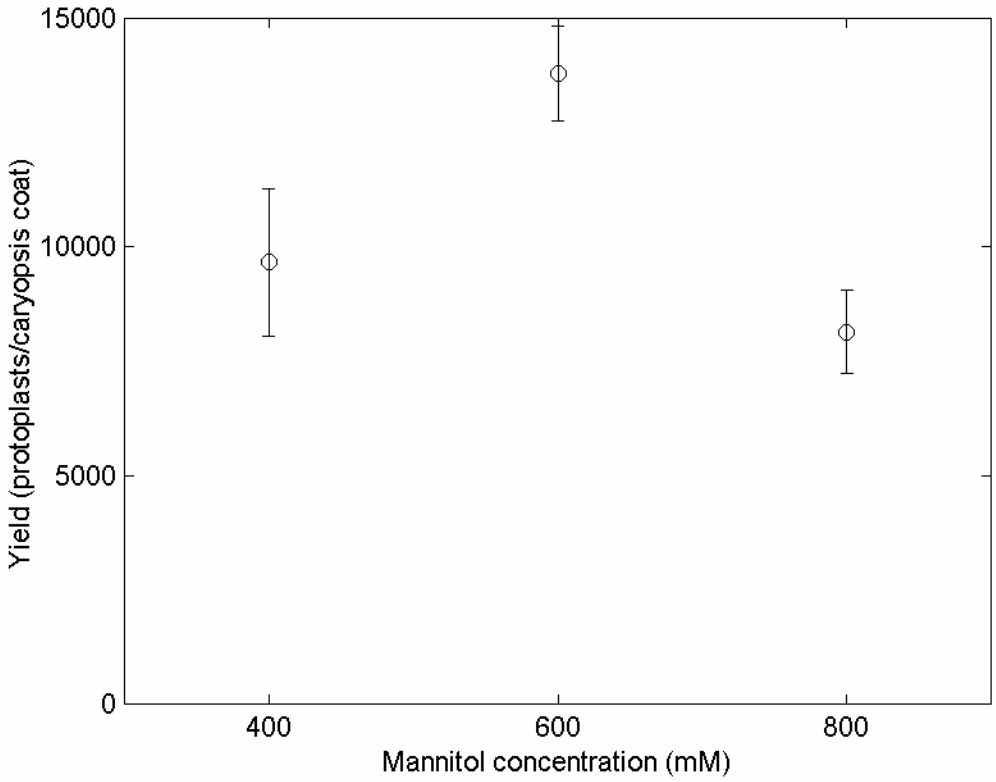

Figure 33 Effect of mannitol concentration on yield of endosperm protoplasts from ripening caryopsis coats of *Oryza sativa* L. cv. Jefferson. Procedures were the same as those of Figure 32 except that mannitol concentration instead of incubation time (90 minutes) was varied for the cellulase incubation. Bars are the standard error of a mean of three replicates.

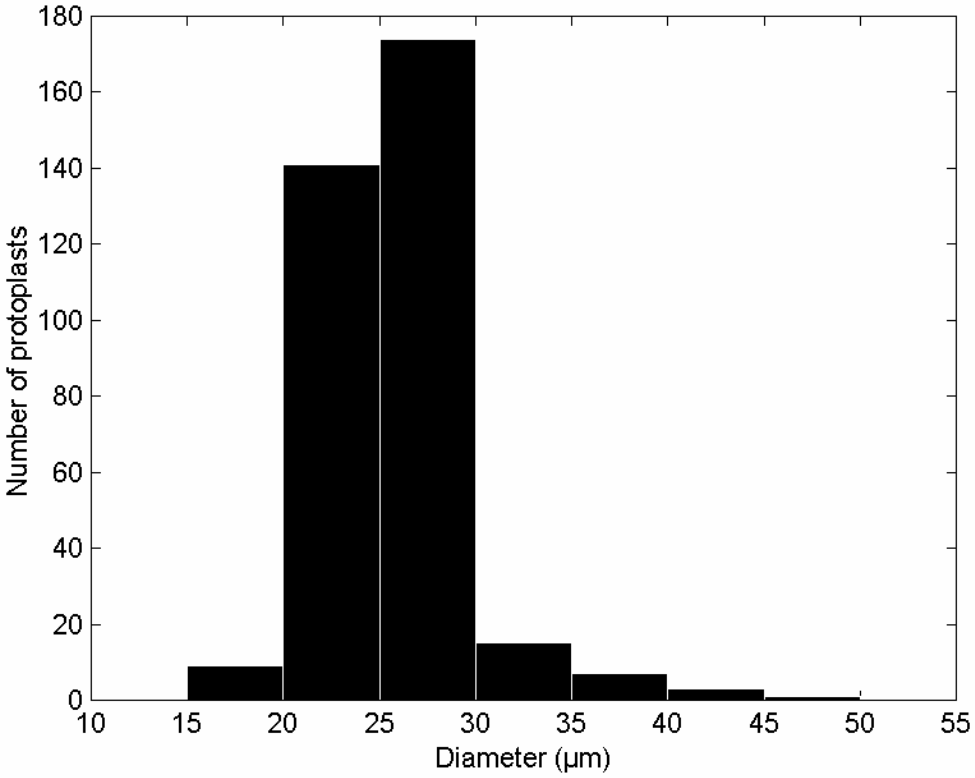

Figure 34 Diameter histogram for endosperm protoplasts isolated from ripening caryopsis coats of *Oryza sativa* L. cv. Jefferson. The diameters of 350 protoplasts were measured. The minimum, maximum and average diameters were 18, 48 and 26 µm, respectively.

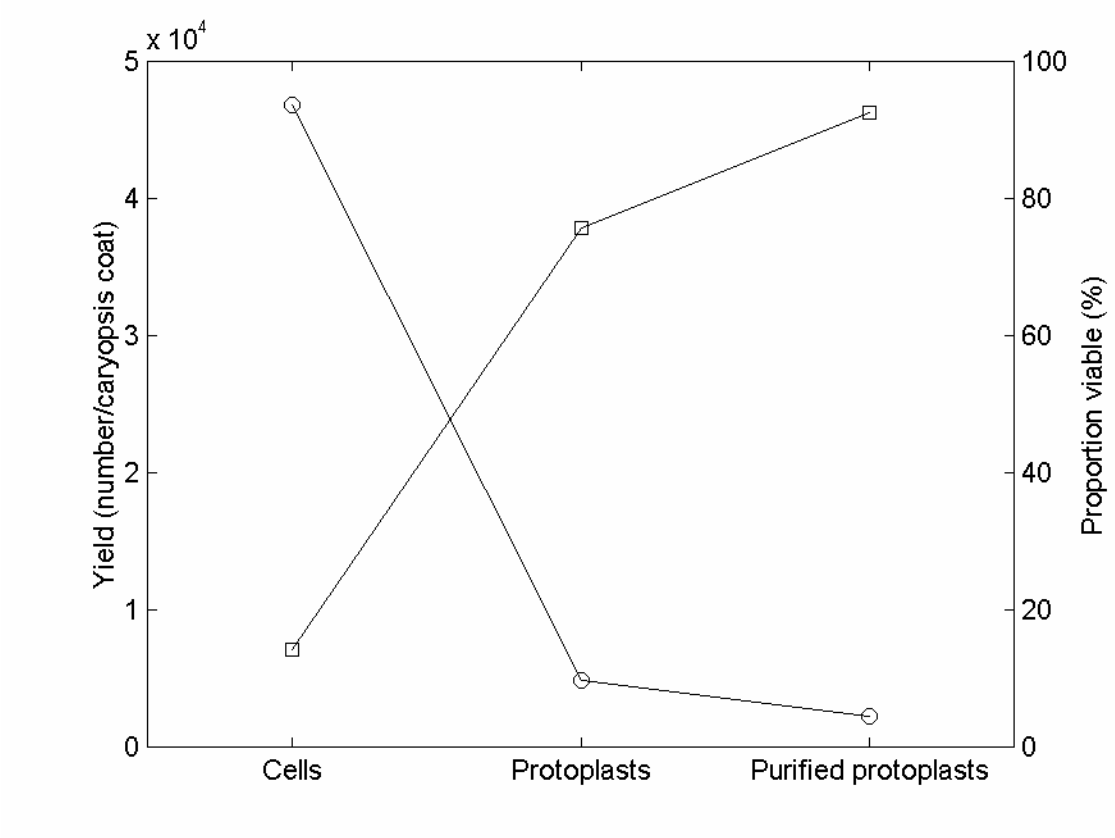

Figure 35 Yield and viability of endosperm cells, protoplasts and purified protoplasts isolated from ripening caryopsis coats of *Oryza sativa* L. cv. Jefferson. Symbols are averages of three replicates and indicate yield (○) and proportion viable (□).

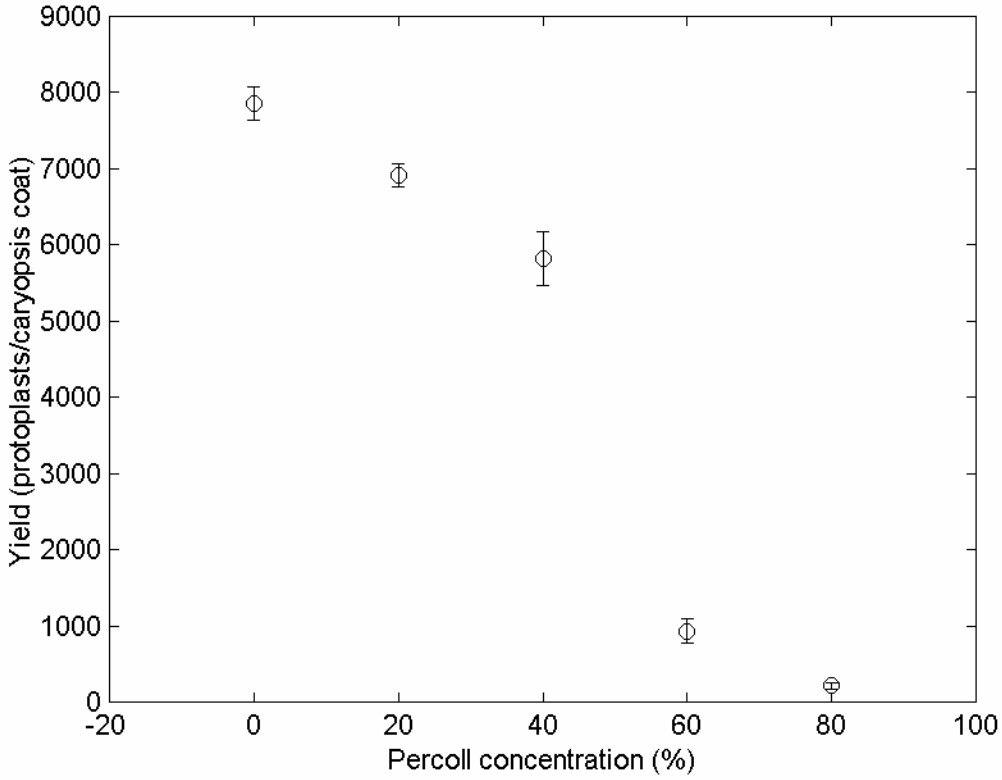

Figure 36 Effect of Percoll concentration on yield of overlaid, centrifuged endosperm protoplasts from the ripening caryopsis coat of *Oryza sativa* L. cv. Jefferson. Protoplasts in IM were overlaid on an equal volume of PIM containing various Percoll concentrations. After centrifugation, completely spherical protoplasts in the pellet were counted. Bars are the standard error of a mean of three replicates.

Shearing caryopsis coats after incubation in Pectolyase Y-23 and cellulase for eight hours yielded giant aleurone protoplasts and maternal tissue protoplasts. Giant aleurone protoplasts had diameters greater than ten times normal. Maternal tissue protoplasts were smaller than normal aleurone protoplasts, clear and not as granular. Some maternal protoplasts were vacuolated.

Discussion

The most time consuming step for protoplast isolation involves the preparation of caryopsis coats. The aleurone is a difficult tissue to obtain in abundance (Phillips and Paleg, 1970). Techniques for high throughput isolation of caryopsis coats from ripening rice grains are needed. Some techniques have been developed for other grains in the imbibed state (Phillips and Paleg, 1970; Murthy, 1989). For ripening rice, the main difficulties to circumvent are detaching grains from the panicle and removing the tight hulls that enclose the ripening caryopses.

Cellulase alone was not effective for isolating aleurone protoplasts. However, digestions viewed under the microscope suggested that it was effective at degrading cell wall since protoplasm was released from the cells.

Sequential cell and protoplast isolation is the best method for isolating aleurone protoplasts from the isolated caryopsis coat of ripening rice (Figure 31). There are other reports of aleurone protoplasts that have been isolated from isolated cells (Taiz and Jones, 1971; Eastwood, 1977). Cell isolation as a first step may have a few advantages. First, it prevents large-scale spontaneous fusion of protoplasts by separating them. Cell death could also contribute to reducing fusion among cells in isolated clumps. Furthermore, there is easy access of the cellulase to the suspended cells (Cocking, 1972). It takes less than two hours to digest away the cell walls of suspended aleurone cells. In addition, since it is easy to partition cell suspensions, this decreases variability in studies of factors that affect protoplast isolation.

Only approximately 10% of the isolated cells yielded protoplasts (Figure 35). This is an extremely low yield. It has been reported that over 90% of the cells of oat aleurone yield protoplasts (Hooley, 1982). The low yield from cells is not surprising since the viability of the isolated cells is very low, also approximately 10%. Hence, low viability of the isolated cells is the major limitation to protoplast yield. Maceration is associated with cell death that can be prevented with plasmolysis (Bateman and Millar, 1966). It may be that the methods described here do not adequately plasmolyze the cells. Aleurone cells are embryonic and densely cytoplasmic. These cells fit criteria for cells that do not easily plasmolyze (Lee-Stadelmann and Stadelmann, 1989). Membrane damage can occur during wall degradation when cells are not plasmolyzed (Bateman and Basham, 1976). This may be responsible for the low viability of isolated aleurone cells. Mechanical damage due to shearing of aleurone cells from the maternal tissues may also be responsible. Still, it seems likely that there should be a way to isolate aleurone cells that are more viable from ripening rice aleurone. Aleurone cells isolated from oat were over 75% viable (Eastwood, 1977). Longer incubation times and shearing by shaking might be helpful. However, for the purposes of quickly isolating aleurone protoplasts to be used in uptake studies, long incubation times are not desirable. More protoplasts can be isolated with more caryopsis coat tissue, but again there is a big trade off in time.

The aleurone is prone to spontaneous fusion of protoplasts. Spontaneous fusion of developing maize endosperm cells, with giant protoplasts containing more than approximately 50 nuclei, has been observed (Usui et al., 1974). The giant protoplasts observed in this study, with diameters greater than ten times normal, assuming conservation of surface area during fusion, would have at least that many nuclei. Spontaneous fusion, as opposed to the fusion between isolated protoplasts, occurs when partitioning cell walls are degraded. This type of fusion occurs *in vivo* during the

formation of giant cells in galls formed by root-knot nematodes (Dropkin, 1969). *In vitro* it is common during protoplast isolation, and depends on the cell wall degrading enzymes used (Ye and Earle, 1991). Spontaneous fusion results from expansion of plasmodesmata that symplasmically connect protoplasts (Power et al., 1970). Numerous plasmodesmata cross the lateral walls of aleurone cells (Oparka and Gates, 1981a; Hoshikawa, 1993). Plasmolysis is thought to isolate cells symplasmically from each other (Cocking, 1972). Fusion is probably common in the aleurone due to a difficulty in breaking plasmodesmatal connections. Aleurone cells do not plasmolyze appreciably in the range of mannitol where protoplasts are most stable. Not all cells, especially embryonic cells, plasmolyze, and other cells are very difficult to plasmolyze and require high concentrations of salts (Lee-Stadelmann and Stadelmann, 1989). Even for cells that do plasmolyze appreciably, plasmodesmata do not necessarily break (Oparka, 1994).

It is interesting that maternal cell protoplasts were observed after longer incubation times. A procedure for the isolation of nucellar protoplasts would be very useful. The vacuolated protoplasts that were observed are probably not from the nucellus. These protoplasts looked different than the cells of the intact nucellus exposed after aleurone protoplast isolation. Nucellar epidermis vacuoles decrease early in ripening (Ishimaru et al., 2003). Since they were clear, lacking chloroplasts, they cannot be from the cross cell layer. Instead, they may be from the inner integument or possibly vascular tissue. Smaller protoplasts without vacuoles may be of nucellus origin. Since aleurone protoplasts are quite dense (Figure 36), it should not be difficult to separate maternal tissues from aleurone protoplasts. It may also be possible to isolate maternal protoplasts after shearing off the aleurone. Further work is needed to develop optimal methods for maternal protoplast isolation.

CHAPTER 7

SUCROSE UPTAKE BY RIPENING RICE ALEURONE PROTOPLASTS

Abstract

The aleurone is the first tissue in a position to retrieve apoplasmic sucrose that is released into the endosperm by the maternal nucellus. It was hypothesized that the aleurone layer has sucrose transporter activity used in the transit of sucrose across plasma membranes. The concentration-dependence of uptake rate was expected to show a saturable component, consistent with carrier-mediated transport. The mechanism of sucrose transport across the plasma membranes of this tissue was investigated in isolated aleurone protoplasts with the silicone oil centrifugation technique. Uptake was dependent on time, sucrose concentration and protoplast integrity. The concentration-dependence of uptake was biphasic. A function that depended nonlinearly on three parameters fitted the data. These results are consistent with the aleurone having saturable and nonsaturable components of sucrose uptake.

Introduction

The rice fruit, or caryopsis, originates from an ovary following double fertilization. At its inception, the caryopsis occupies a very small amount of the space enclosed by the palea and lemma. From the surface inwards, the caryopsis has a pericarp, outer integument, inner integument, nucellus and a single embryo sac.

External dynamics of caryopsis ripening include expansion in length and girth. Initially, length, width and thickness increase simultaneously, however, length substantially has the greatest growth rate and reaches a maximum in approximately 5 days, approximately 10 days before maximum girth (Hoshikawa, 1989). Here, the period of growth in caryopsis length is termed early ripening.

Internal dynamics of early ripening include endosperm development from the fertilized central cell of the embryo sac. The endosperm is completely cellular by the

time early ripening is finished. Cell division and expansion occur beyond this time. Maximum number of endosperm cells is reached when the nucellus is disintegrated (Ishimaru et al., 2003).

Being heterotrophic, the endosperm is dependent on a supply of sugars from the maternal tissues. The transfer of assimilates between maternal tissues and endosperm of wheat involves symplasmic unloading from the phloem, diffusion through the maternal tissues, efflux across the plasma membrane into the endosperm cavity and uptake by the aleurone (Wang et al., 1994; Wang et al., 1995a; Wang et al., 1995b). The maternal tissues passively release sucrose into the apoplasm and may be more important than the endosperm in regulating partitioning of sucrose to the ripening caryopsis (Wang and Fisher, 1994a, 1995). There is supporting evidence for the diffusion of sucrose into the apoplasm via protein pores in peas (Van Dongen et al., 2001).

Sucrose is the major translocated carbohydrate in rice (Fukumorita and Chino, 1982) and is unloaded symplasmically from sieve elements of the dorsal vascular bundle. Some distance away from the vascular bundle is a symplasmic discontinuity at the maternal/embryonic interface (Oparka and Gates, 1981a, b). Sucrose is detected in apoplasmic fluid at this interface in species where it is possible to sample the fluid. Apoplasmic sucrose, during early rice caryopsis ripening, may be cleaved, resulting in monosaccharides that can be retrieved by the endosperm. Evidence for this includes the pattern of expression and activity of cell wall invertases (Hirose et al., 2002).

Later stages of ripening emphasize sucrose uptake and starch deposition by the endosperm. Sucrose transporters are involved in retrieval of sucrose from the apoplasm. A number of studies have shown that sucrose transporters are expressed in ripening caryopses of rice, wheat, and barley and are localized in both embryonic and maternal tissues (Hirose et al., 1997; Bagnall et al., 2000; Weschke et al., 2000;

Furbank et al., 2001; Aoki et al., 2002). Transgenic approaches have demonstrated the importance of sucrose transporters in the control of caryopsis ripening (Scofield et al., 2002) and starch accumulation in seeds of other species (Rosche et al., 2002).

Kinetic studies of sucrose uptake by ripening caryopses are few in number. Two sucrose transporters of barley expressed in yeast have K_m values of 5 and 7.5 mM (Weschke et al., 2000). As far as mechanisms of uptake, the aleurone of wheat has a saturable and a linear component, and the starchy endosperm has only the latter (Niemietz and Jenner, 1993). In rice, *p*-chloromercuribenzene-sulphonic acid (PCMBS) inhibits sucrose uptake by caryopsis segments (Furbank et al., 2001).

The aleurone is expected to retrieve apoplasmic sucrose released by the nucellus. However, this has not been clearly demonstrated. Sucrose uptake during ripening has been assessed only with caryopsis segments (Furbank et al., 2001). The objectives of this study are to demonstrate uptake of sucrose specifically by the aleurone and to assess the mechanism of uptake. One approach could be through the isolation of plasma membrane vesicles (De Jong and Borstlap, 2000a, b). Plasma membrane vesicles from the aleurone of imbibed (germinating) caryopses have been isolated (Walker et al., 1993; Robbins et al., 1999). Another approach uses protoplasts as an experimental system (Niemietz and Jenner, 1993). Protoplasts were isolated from the aleurone of ripening rice, and uptake of radioactive sucrose was assessed by the silicone oil centrifugation technique.

Materials and Methods

Aleurone Protoplast Isolation and Purification

Aleurone protoplasts were isolated according to the procedure previously described (Aleurone Protoplast Isolation, page 85) except the incubation medium (IM) contained 0.8 M mannitol, 10 mM sucrose, 5 mM MES and was adjusted to pH 6 with KOH. Protoplasts were suspended in 3 ml IM with 66% Percoll (PIM) and overlaid

with 3 ml 50% PIM, 3 ml 15% PIM and 3 ml IM. After centrifuging for 10 minutes, the protoplasts between the 50% PIM and 15% PIM layers were resuspended in 15 ml IM with no sucrose and then centrifuged again for 10 minutes. Centrifugation was as previously described (Protoplast Density Estimation, page 85). The protoplast pellet was resuspended in IM with no sucrose.

Protoplast Uptake

Protoplast suspension was added to an equal volume of radioactive IM containing Gamborg's B-5 salts, various sucrose concentrations and specific activities. The composition of the resulting uptake solutions are listed in Table 4. Protoplasts were shaken at room temperature. At various times a 150-µl sample of uptake solution was placed on top of a 100-µl silicone oil (AP 100, Fluka) layer in a 250-µl tube and then centrifuged (Eppendorf 5415) for 1.5 minutes at 9000 rpm. After freezing, the tube tip was cut within the silicone oil layer and the protoplast pellet was extracted into scintillation fluid. Uptake rate was determined by computing the amount of sucrose in the pellet after uptake for 1.5 and 10 minutes and computing the slope.

Curve Fitting

The data were fit with the biphasic kinetics function:

$$V = [V_m S/(S + K_m)] + kS$$

where V is the sucrose uptake rate (nmol/hr/10^5 protoplasts), V_m the maximum saturable uptake rate (nmol/hr/10^5 protoplasts), S the external sucrose concentration (mM), K_m the S where the saturable V is half of V_m and k a constant (nmol/mM/hr/10^5 protoplasts). Units were chosen according to Niemietz and Jenner (1993). After making an educated, initial guess of the parameters, the Gauss-Newton method was used to converge on the parameters (Chapra and Canale, 1998).

Table 4 Uptake solutions used for the determination of the concentration dependence of rate of sucrose uptake by protoplasts isolated from *Oryza sativa* L. cv. Jefferson. Each contained half-strength Gamborg's B-5 salts and was pH 6. Uptake solution was sampled at various times, overlaid on silicone oil and protoplasts centrifuged to the bottom.

Sucrose (mM)	Specific activity (mCi/mol sucrose)	Mannitol (mM)	Volume (ml)	Protoplasts/ml
0.49	0.0156	768.75	0.52	48,077
0.97	0.0079	768.27	0.52	48,077
2.90	0.0027	766.35	0.52	48,077
4.82	0.0016	764.42	0.52	48,077
9.63	0.0008	759.62	0.52	48,077
28.86	0.0003	740.38	0.52	48,077

Results

Centrifugation of purified protoplasts through silicone oil separated them from the radioactive uptake solution. Since the purified protoplasts were obtained from the 15%/50% PIM interface, they were denser than 15% PIM. The silicone oil used was less dense than the 15% PIM and denser than radioactive protoplast suspension. The silicone oil at the bottom of the tube became radioactive when the silicone oil was overlaid with radioactive uptake solution and centrifuged. Microscopic inspection of the contents of the pellet showed that intact protoplasts precipitated.

Sucrose taken up by protoplasts generally increased with time. Sucrose was found in the pellet directly after centrifuging protoplasts suspended in radioactive uptake solution. The time course for uptake of sucrose by protoplasts was linear for approximately at least 10 minutes (Figure 37).

Compared to the control protoplasts, frozen and thawed protoplasts took up less sucrose after 20 minutes and had a minor uptake rate. Some sucrose was found in the pellet immediately after centrifugation of both types of protoplasts (Figure 38).

Sucrose uptake rate was positively correlated with external sucrose concentration (Figure 39). Optimal values of the parameters that best fit the biphasic kinetics function to the data were found using nonlinear regression with the following educated guesses: 1 nmol/hr/10^5 protoplasts (V_m), 0.1 mM (K_m) and 2 nmol/mM/hr/10^5 protoplasts (k). These guesses converged on 2.37 nmol/hr/10^5 protoplasts (V_m), 0.23 mM (K_m) and 2.08 nmol/mM/hr/10^5 protoplasts (k).

Discussion

Centrifugation of protoplasts through silicone oil is an efficient way to separate them from the rest of the radioactive uptake solution. When radioactivity associates with dense enough objects, it is centrifuged to the bottom of the tube. In this way, it is possible to measure uptake. The radioactivity measured in the pellet after immediate

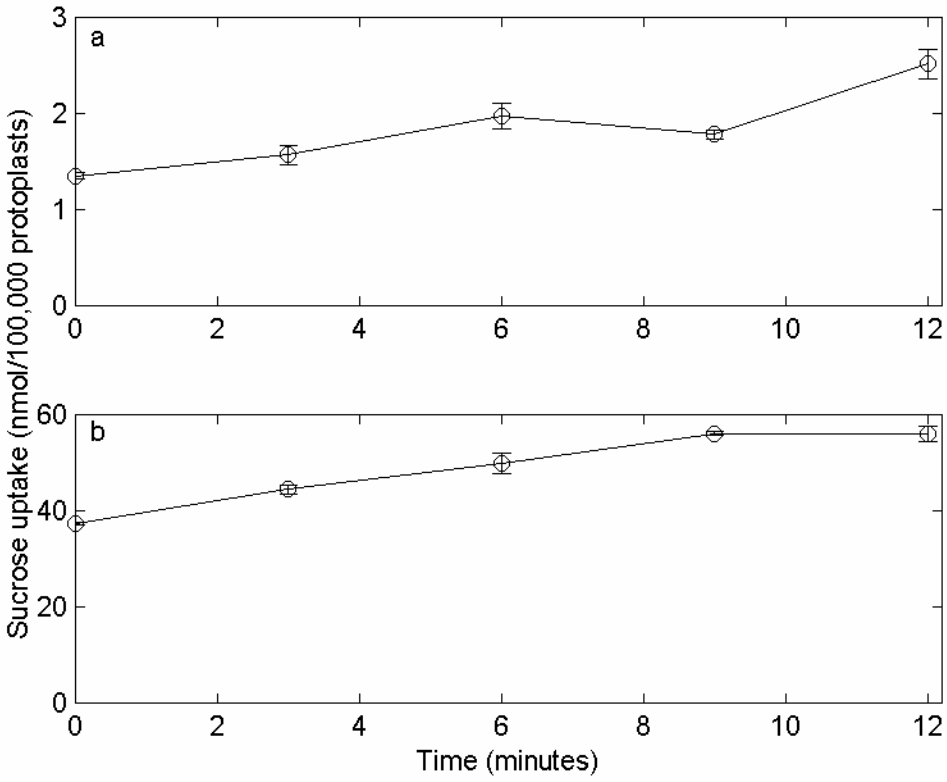

Figure 37 Relationship between sucrose uptake by aleurone protoplasts isolated from ripening caryopses of *Oryza sativa* L. cv. Jefferson and time. Sucrose concentrations are 1 mM (a) and 20 mM (b). Bars are the standard error of a mean of three replicates.

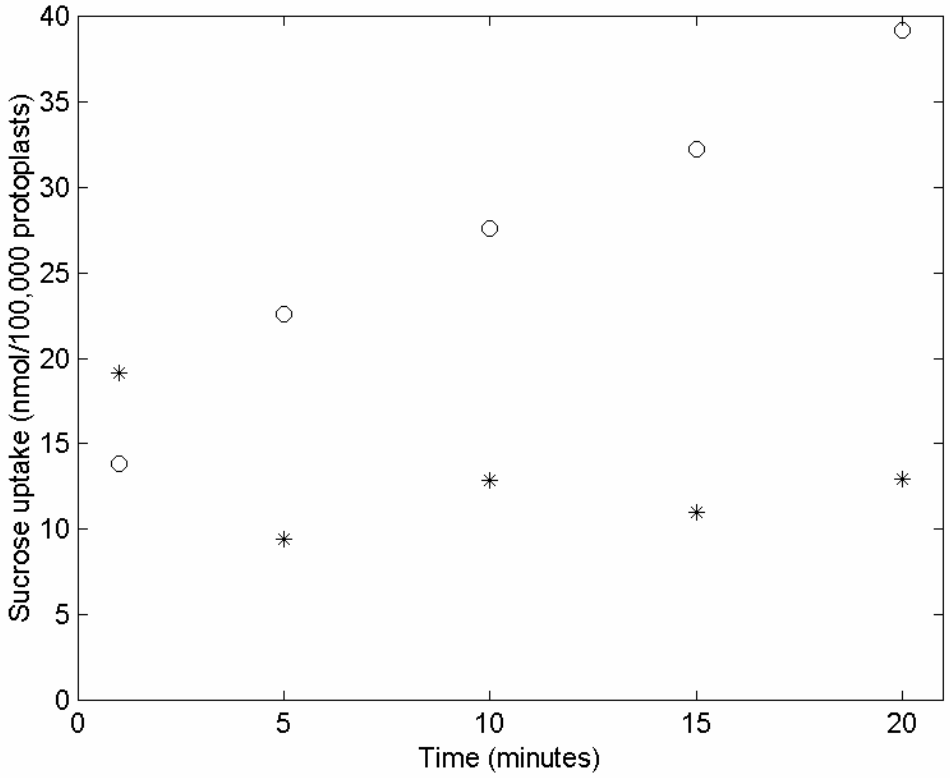

Figure 38 The effect of protoplast intactness on uptake of sucrose by aleurone protoplasts isolated from ripening caryopses of *Oryza sativa* L. cv. Jefferson. Symbols indicate frozen and thawed (*) and control (○) protoplasts. The sucrose concentration was 10 mM.

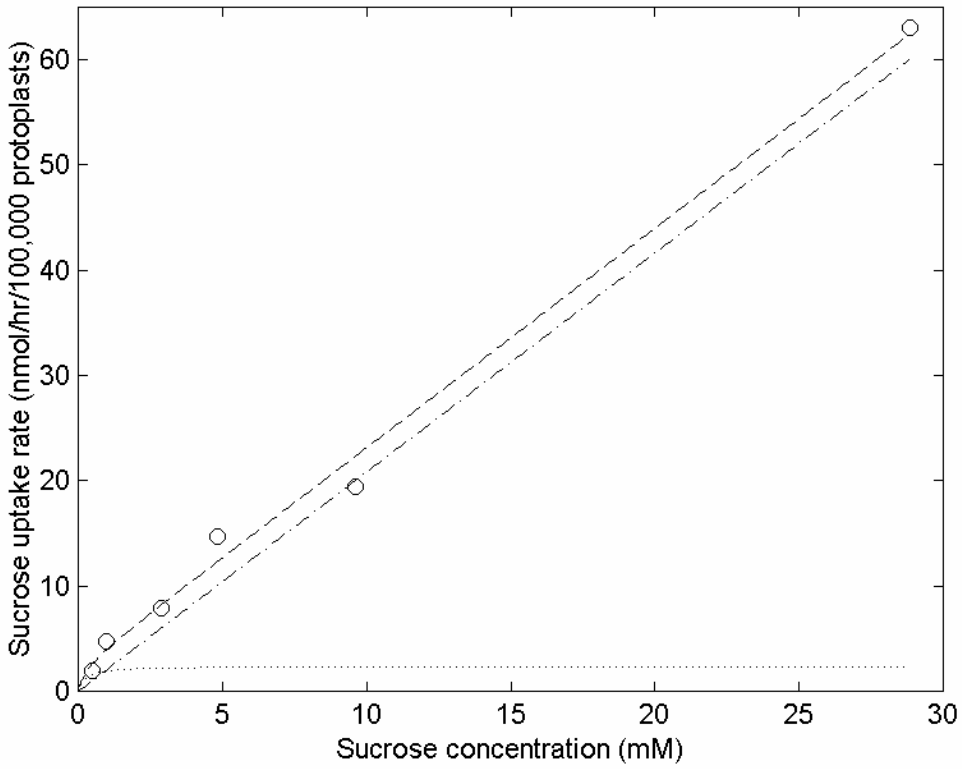

Figure 39 The effect of sucrose concentration on uptake rate of sucrose by aleurone protoplasts isolated from ripening caryopses of *Oryza sativa* L. cv. Jefferson. The constants 2.37 nmol/hr/10^5 protoplasts (V_m), 0.23 mM (K_m) and 2.08 nmol/mM/hr/10^5 protoplasts (k) were determined using nonlinear regression and used to graph uptake rate (– –), nonsaturable uptake rate (· –) and the saturable uptake rate (·). The sum of the squares of the residuals is 16.02. Uptake solutions are listed in Table 4.

centrifugation, or 0 minutes of uptake, is that carried with the protoplasts, not necessarily within the protoplasts.

Since purified protoplasts are denser than 15% PIM, which is denser than the silicone oil used, it can be assumed that all the protoplasts overlaid on silicone oil are centrifuged to the bottom of the tube. Protoplasts after centrifugation appear intact, hence protoplast lysis is likely negligible. Freezing and thawing of protoplasts inhibited uptake (Figure 38). This suggests that uptake does correspond to sucrose crossing intact plasma membranes of purified protoplasts.

The time-dependence of sucrose uptake is initially linear (Figure 37). If there is a plateau, uptake levels off around 10 minutes. The uptake rate of sucrose can be accurately determined from protoplasts sampled during the first ten minutes of uptake. The slope between sucrose uptakes at two time points was used to calculate uptake rate. The assumptions for calculating uptake rate in this way include constant background radioactivity and radioactivity from solution adhered to protoplasts.

The relationship between sucrose uptake rate of protoplasts and sucrose concentration is biphasic (Figure 39). The nonlinear relationship at low sucrose concentrations implies a saturable, protein-mediated mechanism of uptake. Sucrose transporters likely form the basis of this component. It would be interesting to test the hypothesis that OsSUT1 is responsible for the saturable component of uptake. If this were true, the kinetics of uptake would be predicted to be linear in the antisense plant (Scofield et al., 2002). Furthermore, sucrose transporter inhibitors such as PCMBS would be expected to mimic the effects of the antisense mutation. Likewise, inhibitors of respiration should inhibit transport, since sucrose transporters harness the potential energy of proton gradients established by ATP hydrolyzing proton pumps to transport sucrose against its concentration gradient.

The linear component of uptake is not well understood. The lack of uptake by freeze/thawed protoplasts suggests that the linear component, like the saturable component requires intact plasma membranes. Plasma membrane vesicles from tobacco leaves do not have a linear component (Borstlap and Schuurmans, 2004). Protoplasts from wheat showed a linear component (Niemietz and Jenner, 1993). The linear component may be mediated by proteins that have a mechanism of sucrose transport different from that of sucrose transporters.

Nonlinear regression was useful to find values of parameters that best fit the biphasic kinetics function to the data. This method required an understanding of the saturable and nonsaturable components of uptake to make educated guesses of the parameters. The biphasic kinetics function made a good fit to the data. However, the precision of the parameter estimates is surely low. More data would need to be collected, especially data that define the nonlinear portion of the curve. Niemietz and Jenner (1993) reported a V_m and K_m of 22 nmol/hr/10^5 protoplasts and 5 mM respectively. Although k was not reported, it could be estimated from their results as approximately 1 nmol/mM/hr/10^5 protoplasts. The constants they reported were from linearized, inverted, data. Using the constants they reported and the estimate of k, the curve does not make a good fit to the data. Using nonlinear regression, the parameters for their data come out to be 6.21 nmol/hr/10^5 protoplasts (V_m), 0.95 mM (K_m) and 1.08 nmol/mM/hr/10^5 protoplasts (k). These constants are closer to those determined in this study (Figure 39). The sucrose concentration in the endosperm cavity of wheat was reported as 65 mM (Fisher and Gifford, 1986). The saturable uptake rate is approximately 2%, 8% and 24% of the total uptake rate at this external sucrose concentration for rice aleurone protoplasts (this study), wheat aleurone protoplasts (parameters from nonlinear regression) and wheat aleurone protoplasts (reported parameters and estimated k), respectively. Hence, the saturable component of uptake

appears to be relatively small compared to the nonsaturable component. Contribution of the saturable component to the influx in cereals appears to be smaller than that in dicots at the same concentration (Lichtner and Spanswick, 1981b).

CHAPTER 8

ELECTROPHYSIOLOGY OF THE RIPENING CARYOPSIS COAT OF RICE

Abstract

Sucrose transporters are important in the partitioning of assimilated carbon to the developing rice grain. It has been demonstrated that there is a saturable mechanism that mediates sucrose influx by isolated aleurone protoplasts. It was hypothesized that this component is associated with a sucrose/proton cotransporter. It was expected that sucrose would depolarize the membrane potential of aleurone cells. The membrane potential of the aleurone exposed on the surface of isolated caryopsis coats was assessed with microelectrode techniques. Potentials were low in magnitude, around 60 mV. Sucrose negligibly depolarized the membrane potential. The potential varied spatially with depth of microelectrode insertion. There was a sharp depolarization below the surface of the caryopsis coat. The nucellus, assumed centripetal to this depolarization, had a potential around –80 mV. The maximum value of the potential magnitude centripetal to the depolarization was not greatly dependent on potassium concentration, mannitol concentration or pH. Potentials recorded from imbibed caryopses were similar. The results did not support the aleurone having sucrose/proton cotransporter activity. The reason may be related to membrane potentials that are small in magnitude.

Introduction

The ripening rice caryopsis accumulates dry matter for the most part by the synthesis and storage of starch in endosperm amyloplasts. The caryopsis is supplied with assimilated carbon in the form of sucrose, which can be allocated for the synthesis of nucleotide sugars, substrates for starch synthases (James et al., 2003).

Plasmodesmata, being absent at the junction between maternal and embryonic tissues, do not accommodate symplasmic transport of sucrose from phloem sieve

elements to endosperm. Hence, uptake of apoplasmic sucrose by the endosperm and flux of sucrose across plasma membranes are important steps in the pathway leading to starch (Oparka and Gates, 1981a, b). The maternal nucellus and embryonic aleurone form an interface and are sites of sucrose efflux and influx, respectively. Many layers of endosperm cells probably accommodate the flux of sucrose from endosperm apoplasm to symplasm.

Sucrose retrieval by the aleurone is particularly of interest because of much evidence that suggests an important role of sucrose/proton cotransporters. The dependence of sucrose influx on sucrose concentration is biphasic. Investigations using aleurone protoplasts have demonstrated saturable and nonsaturable mechanisms (Chapter 7). Sucrose transporters localize to the aleurone, sucrose uptake by caryopsis segments is inhibited by PCMBS and proton pumps localize to the nucellus/aleurone interface (Furbank et al., 2001). Caryopses of OsSUT1 antisense plants have reduced dry weight (Scofield et al., 2002). All these results suggest an important contribution by sucrose/proton cotransporters to the control of the flux of sucrose to starch. Hence, the saturable mechanism of uptake is expected to be associated with the activity of sucrose transporters.

One mechanism of sucrose transport is cotransport with protons and depends on the electrochemical gradient of protons established by proton pumps (Spanswick, 1981). Hence, electrophysiology is a useful tool to assess the activity of sucrose/proton cotransporters. Electrophysiological studies of the rice caryopsis are few if any. There are few studies on the aleurone of other grains. The first objective of this study was to characterize the membrane potentials of tissues in the ripening caryopsis.

It is well established that the saturable component of sucrose uptake by legume cotyledon surface tissue, which is analogous in terms of sucrose uptake to the aleurone,

is associated with sucrose/proton cotransport (Lichtner and Spanswick, 1981a, b). However, cotransport has not been demonstrated in the aleurone. The second objective of this study was to test the hypothesis that the saturable component of uptake is a sucrose/proton cotransporter. Sucrose-induced and sucrose concentration-dependent depolarization of membrane potential were expected. Membrane potentials were recorded using microelectrode techniques.

Materials and Methods

Caryopsis coats from ripening rice 10-14 days after heading were fastened (aleurone side up) with waterproof tape to the bottom of a recording chamber (RC 16, Warner Instruments). Some caryopsis coats were heat killed by boiling in water for over an hour. The standard incubation medium (IM) contained 200 mM mannitol, 0.1 mM KCl, 0.1 mM $MgCl_2$, 0.1 mM $CaCl_2$ and 1 mM MES and was adjusted to pH 6 with NaOH. Reference electrodes were fabricated with 2 mm glass and filled with 3 M KCl/2% agar and held with a holder (MEH1R20, WPI). Microelectrodes were fabricated from glass capillaries (1B100F-4, WPI) with a puller (PP-83, Narishige), filled with 3 M KCl, and held with a holder (MEH1S10, WPI). Microelectrodes were positioned at a 45° angle or perpendicular to the caryopsis coat with a micromanipulator that was calibrated for distance. Cells and microelectrode tip were visualized with an inverted microscope (DIAPHOT-TMD, Nikon). Everything was mounted on a vibration isolation table (Micro-g, TMC) inside a Faraday cage. A vacuum pump controlled the drain. Data were recorded with a potentiometric strip chart recorder (MFE).

Results

Microelectrodes could be positioned at 45° relative to the caryopsis coat and next to specific aleurone cells using the micromanipulator and inverted microscope. Potential recordings from those cells were less than 100 mV in magnitude, typically

around –50 mV and stable for over 20 minutes (Figure 40). Perfusion with sucrose concentrations up to 100 mM resulted in a depolarization of only a few mV (data not shown).

Cells could be impaled blindly at 90° relative to the dorsal region of the caryopsis coat. As the microelectrode advanced through the caryopsis coat, electrical potential increased in magnitude. Dead caryopsis coats had smaller electrical potential magnitudes. A sharp, transient depolarization occurred, on average, approximately 100 μm below the inner surface of the dorsal region of the caryopsis coat (Figure 41). The location of the depolarization was closer to the inner surface of lateral regions of the caryopsis coat. Potassium concentration, mannitol concentration and pH did not greatly affect the maximum membrane potential magnitude recorded to the inside of the depolarization (Table 5). Maximum potential magnitudes were all less than 100 mV. Caryopsis coats 10 days after imbibition had a maximum potential magnitude of 76 ± 1.3 mV (n = 20).

For a very small proportion of prepared caryopsis coats, the sharp depolarization was followed by a sharp hyperpolarization (Figure 42). Some potentials on the centrifugal side of the depolarization were well over 100 mV in magnitude. To the centripetal side, there was a region less than 25 μm thick with potential as great as 80 mV in magnitude. Centripetal to that region, was a region approximately 50 μm thick, with a potential around –60 mV.

Discussion

Potentials were negative, as expected for the membrane potential of plant cells. Initial results from impaling specific aleurone cells on the surface of the caryopsis coat suggest that they have low magnitude electrical potentials. These small magnitude potentials are consistent with potential measurements of barley aleurone protoplasts (Heimovaara-Dijkstra et al., 1994; Van Duijn and Heimovaara-Dijkstra, 1994).

Figure 40 Membrane potential trace of an aleurone cell of a caryopsis coat of ripening rice *Oryza sativa* L. cv. Jefferson. Horizontal bar, from left to right, equals 12 minutes. Vertical bar, down to up, equals −10 mV. The microelectrode was withdrawn 17 minutes after insertion when the potential was −48 mV.

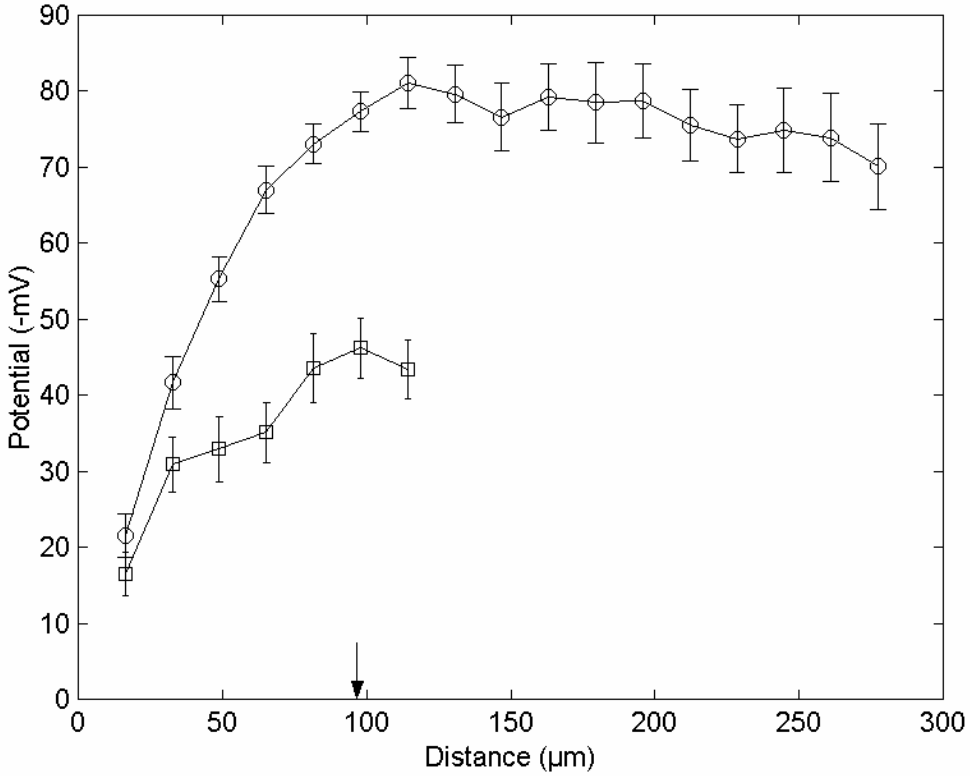

Figure 41 Relationship between electrical potential and depth of microelectrode insertion into the caryopsis coat isolated from ripening rice *Oryza sativa* L. cv. Jefferson. The microelectrode was positioned 90° relative to the inner surface of dorsal regions of heat killed caryopsis coats (□) and control caryopsis coats (○) and advanced in increments. The arrow marks the average position of a sharp depolarization. Bars are the standard error of a mean of at least 20 replicates. Potentials were aligned at the position of first contact with the microelectrode.

Table 5 Effect of potassium concentration, pH and mannitol concentration on electrical potential recording from the caryopsis coat isolated from ripening rice *Oryza sativa* L. cv. Jefferson. Average maximum potential magnitudes recorded as the microelectrode passed though all the layers of cells centripetally positioned relative to the sharp depolarization and standard errors are listed (n = 20).

pH	5	6	8
Potential (–mV)	79.4	76.0	74.7
±	1.0	1.6	3.0
Mannitol (mM)	200	400	600
Potential (–mV)	87.0	82.7	82.8
±	1.3	1.1	1.8
Potassium (mM)	0.01	0.1	1
Potential (–mV)	88.0	89.1	80.1
±	2.0	1.1	1.9

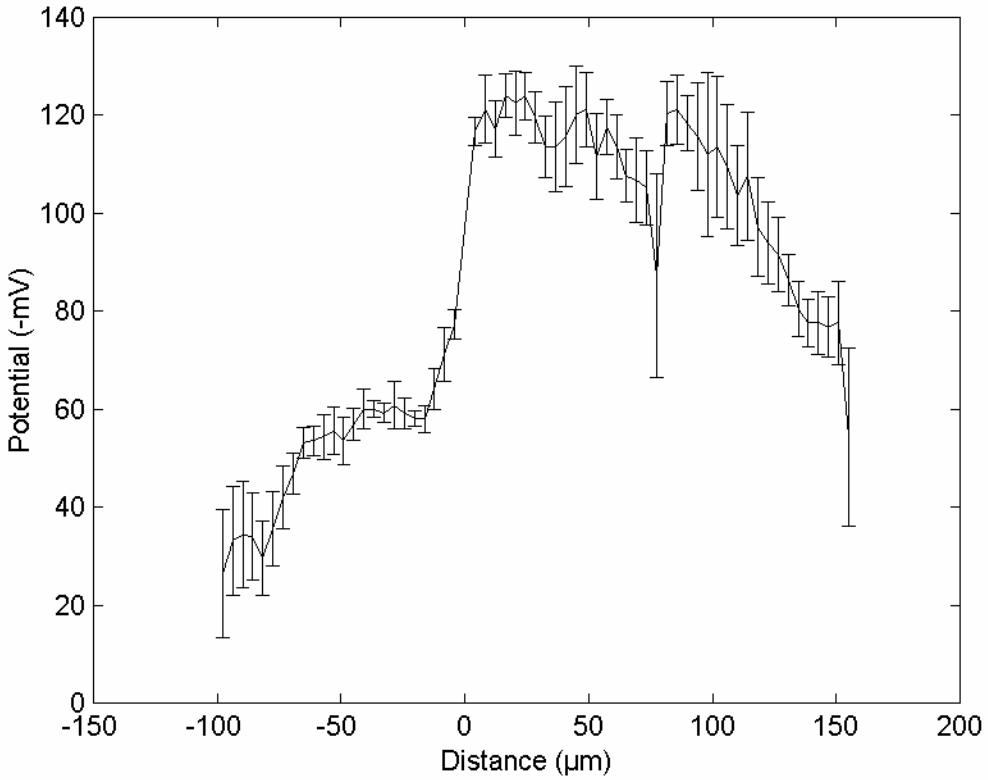

Figure 42 Spatial distribution of electrical potential of the caryopsis coat isolated from ripening rice *Oryza sativa* L. cv. Jefferson. Potentials were aligned relative to the position of a sharp depolarization followed by hyperpolarization (0 μm), which was observed for a very small proportion of prepared caryopsis coats. Bars are the standard error of a mean of five replicates.

However, there are reports of potentials well over 100 mV in magnitude for the aleurone tissue of germinating wheat in 0.01-0.1 mM KCl (Kazaryan et al., 1981).

Depolarizations due to sucrose perfusion are very small. Depolarization by sucrose has been shown to be dependent on sucrose concentration and the concentration at which half the maximum depolarization results is consistent with the K_m for sucrose influx (Lichtner and Spanswick, 1981a, b). Even though sucrose uptake by isolated aleurone protoplasts has a saturable component (Figure 39) and the aleurone is equipped with sucrose transporters (Furbank et al., 2001), the depolarizations demonstrated in this study were minor and not favorable for comparison at various sucrose concentrations. The small depolarizations by sucrose may be caused by a factor related to the small magnitude of membrane potentials. One possible reason for the small magnitude of potentials could be the ionic composition of the bath medium. Membrane potential is often similar to the diffusion potential, which can be usually determined by the Nernst potential for potassium because the permeability coefficient for potassium is usually large (Spanswick, 1981). Interestingly, potentials have been previously shown to be dependent on potassium concentration (Kazaryan et al., 1981). However, data of this study do not support this. This, together with the small effect of mannitol concentrations and pH, suggests that the membrane potential of aleurone cells really is small in magnitude.

Potential magnitude increases as the microelectrode advances through the caryopsis coat. Killing the cells inhibited this trend. It is unlikely that there is that great a variation among cell layers of the dorsal aleurone. Instead the rise in potential may be attributed to movement of the caryopsis coat when contacted with the microelectrode. Another factor may be the presence of subaleurone which is a patchy tissue variable in thickness (Figure 25). Furthermore, the potential distributions were aligned at the point of contact of the microelectrode with the caryopsis coat surface,

which may not be an optimal alignment for computing average potential with caryopsis coat thickness.

There is a characteristic sharp depolarization when the microelectrode encounters an internal region of the caryopsis coat. This depolarization might be caused by the inner cuticle that is located between the nucellus and inner integument (Figure 1). Evidence for this includes a longer advance of the microelectrode needed to encounter the depolarization in the dorsal region of the caryopsis coat compared to the lateral region. What causes the hyperpolarization beyond this position (Figure 42) is not understood. It could be an inner integument cell with large potential magnitude. The layer of inner integument cells is patchy in viability (Chapter 4, page 64). Hence, there may be a small chance of impaling a living one. However, it would not explain why the region of high potential magnitude is so large in thickness, much thicker than the inner integument. Another possibility may be that it is an artifact. However, an artifact of this sort could be assumed to affect only the portion of the coat outwardly adjacent to the depolarization since the inner portion behaves normally.

Alignment of potential distributions at the position of the sharp depolarization followed by hyperpolarization (Figure 42) appears to be more optimal than that at the position of initial contact with the microelectrode (Figure 41). The reason for this is that instead of a smooth gradation in potential, there are identifiable regions, of specific thickness, that vary in potential. The region of –60 mV corresponds well with the thickness of the aleurone. The smaller region that has potentials greater in magnitude and is directly to the inside of the depolarization corresponds well with the thickness of the nucellus. From these data, it can be inferred that the nucellus has a greater membrane potential magnitude than the aleurone.

CHAPTER 9

SUMMARY AND FUTURE RESEARCH OBJECTIVES

Summary

Caryopsis ripening is essential for the life cycle and yield of rice. It is complex because it covers multiple levels in the structural hierarchy from gene to whole plant. Advances and remaining problems in our understanding of this important process resulted from the structural and functional studies of this dissertation.

Caryopses do not ripen in isolation. The first problem that was addressed was the description of asynchronous ripening of multiple caryopses on a single panicle. The major outcome of this work was an alternative to manual drawings of this complex process. The arrangement and degree of ripening of caryopses on a panicle were reduced to a numerical array. This format could be easily stored, and after imported into Matlab, analyzed and graphically represented. Furthermore, the format made a way to generate a consensus panicle for a given cultivar.

Caryopsis ripening is governed by structural/functional relationships. Structural features of biological material can hinder experimentation. The second problem that was addressed was the need for experimental systems for the study of sucrose transport at the maternal/embryonic interface of ripening caryopses. As a first approach to the problem, caryopsis dissection was considered. The analysis clearly showed that the mechanical separability of caryopsis tissues was limited by tissue adhesion. Dissection was not sufficient to separate the maternal nucellus and embryonic aleurone. A clear description of component cell types was made for the parts of the caryopsis that were mechanically separable. Anatomical terms such as seed coat were shown to be unclear when applied to the caryopsis after dissection. An alternative, mechanically-based terminology was put forth that did not ignore the problem of tissue adhesion. As another attempt to separate aleurone from nucellus,

enzymatic approaches were considered. The major outcome was the successful separation of the maternal/embryonic interface. This circumvented the problem of tissue adhesion and the absence of an endosperm cavity in rice. This enzymatic maceration method is attractive because it is quick and easy. However, a disadvantage is that only a small percentage of the isolated aleurone cells is viable. This is not too surprising given the delicate nature of the aleurone and the harshness of maceration.

Sucrose retrieval by the endosperm is necessary because of the symplasmic discontinuity between aleurone and nucellus. The ability to isolate aleurone protoplasts paved the way for the study of the mechanism of sucrose retrieval. Protoplasts could be isolated in high enough yield to conduct uptake experiments. However, since protoplast isolation was a very inefficient way to acquire the tissue, it limited the number of experiments for which a single batch of protoplasts could be used. Nevertheless, the analysis did suggest some characteristics of the mechanism of uptake. The concentration dependence of uptake rate indicates the presence of saturable and nonsaturable components of uptake.

It was expected that sucrose would depolarize the membrane potential of aleurone cells. The results of this analysis were negative. This may be due to an incompatibility between the microelectrode techniques and the way the tissue was prepared. It is not uncommon to have difficulty impaling small cells with microelectrodes. However, the caryopsis coat preparation was amenable for an analysis of the spatial variation of membrane potential. The results clearly demonstrate variation in potential as the electrode is advanced into the caryopsis coat. Furthermore, the results demonstrate an electrical landmark, a sharp depolarization, which is useful in keeping track of the general location of the microelectrode when it is used to blindly impale the cells.

Future Research Objectives

The computational, spatiotemporal analysis of panicle ripening is descriptive. Many questions concerning ripening asynchrony remain. While spatial variation in the characteristics of caryopses on a single panicle has been considered (Mohapatra et al., 1993; Ishimaru et al., 2003), the regulation of ripening asynchrony is still unclear. Genomic and proteomic techniques (Koller et al., 2002; Zhu et al., 2003; Tanaka et al., 2004) that account for spatiotemporal variation in ripening on the panicle may provide new insights into these problems.

While tissue adhesion was looked upon as problematic from an experimental standpoint, it may have an importance *in vivo*. Tissue adhesion may contribute to the regulation of carbon flow into the endosperm. It would be interesting to assess the effect of compromising the adhesion at the maternal/embryonic interface *in vivo*.

In general, the exact functions of the various maternal tissues in transporting sucrose along its cellular pathway are still unclear. Questions concerning the development of each caryopsis tissue remain. For example, the temporal dynamics of cell viability, especially for maternal cell types, are unclear. Furthermore, in depth, spatiotemporal expression analysis (to the level of each caryopsis cell type) of sucrose transporters is still needed. The exact functions of the various sucrose transporter genes (Aoki et al., 2003) still need to be uncovered.

Better understanding of the development and functions of the various cell types could lead to targeted genetic modification of caryopsis ripening. Although some caryopsis cell-type-specific promoters have been discovered (Chen and Foolad, 1997; Linnestad et al., 1998; Chen and Foolad, 1999; Qu and Takaiwa, 2004), a better understanding of the regulation of gene expression in each of the tissues is needed. It should be possible to modify key tissues in the cellular pathway for sucrose transport, such as the small population of pigment strand cells, which comprise the gateway

through which sucrose moves on its way to the endosperm from the phloem. Another example would be modification of the nucellar epidermis to assess directly the function of its cuticle. Furthermore, modifications to the maternal/embryonic interface may allow for a better understanding of sucrose efflux and influx.

The studies of maternal and endosperm protoplast isolation and aleurone sucrose influx are first steps toward better understanding the mechanisms of sucrose transport that operate at the plasma membranes on either side of the maternal/embryonic interface. With separation of the maternal/embryonic interface and their corresponding functions of efflux and influx, respectively, now possible, the question of relative contributions of these transport steps to the control of caryopsis ripening can be assessed. One approach to the problem is metabolic control analysis which quantifies rate limitation of steps by the calculation of flux control coefficients (ap Rees and Hill, 1994). The questionable nature of the mechanism behind the linear component of aleurone influx remains. In addition, it has not yet been demonstrated whether influx is bidirectional or not. This needs to be clarified because net influx is important for metabolic control analysis. The mechanism of efflux is still poorly understood. The idea that sucrose transporters may actually be involved in efflux is interesting, but remains to be demonstrated. Methods to assess efflux from the enzymatically exposed nucellus need to be worked out. An *in vivo* system consisting of caryopses still attached to the panicle should be considered, although this would require extreme technical ingenuity. It is tempting to envision systems analogous to those in legumes or wheat (Wang and Fisher, 1994a) in terms of their convenience for the assessment of sucrose efflux. Attached caryopses would have milky endosperm mechanically and aleurone enzymatically removed.

Further work on maternal tissue protoplast isolation would be useful for transport studies. In addition, isolation of plasma membrane vesicles from the ripening

rice caryopsis should be considered as it has been for imbibed caryopses of other species (Walker et al., 1993; Robbins et al., 1999). Perhaps isolated endosperm cells from maceration of the endosperm of caryopsis coats, though low in viability, could be used as starting material. This might circumvent frustratingly low protoplast yield due to the low viability of isolated cells. Plasma membrane preparations from inner caryopsis coats with exposed nucellus (aleurone lacking) should also be considered.

Sucrose transport by caryopses from *OsSUT1* antisense plants (Ishimaru et al., 2001; Scofield et al., 2002) should be investigated. The structure of the caryopses and sucrose transport by various tissues should be compared between antisense and wild type plants. It would be interesting to see the phenotype of a caryopsis with sucrose transporters inhibited specifically in the nucellus, aleurone and other tissues.

The electrophysiological analysis of caryopsis coats has established that it may be difficult to assess sucrose/proton cotransport with microelectrode techniques. Hence, electrophysiological support for sucrose/proton cotransporters as the basis for saturable sucrose influx by endosperm is still lacking. Perhaps conventional microelectrode membrane potential recording and patch clamping of protoplasts should be explored.

APPENDIX

MATLAB SCRIPTS AND FUNCTIONS

Functions for Creating the Annotated Panicle Array

```
%getpm.m is a function that imports a text file of a panicle array into Matlab. The
%input argument is the name of a text file (tab-delimited) and the output argument is a
%Matlab array (m x 12).
function [Y]=getpm(x)
Y=dlmread(x,'\t');

%insert.m is a function that inserts elements into an annotated panicle vector. The
%input arguments are an annotated panicle vector, the index where elements are to be
%inserted, and the elements to be inserted.
function [x]=insert(pva,n,a)
x=[pva(1:n) a pva(n+1:length(pva))];

%pva.m is a function that annotates a panicle array. The input argument is a Matlab
%panicle array (m x 12) and the output argument is an annotated panicle array (1 x n).
function [Y]=pva(x)
%Transform a (m x 12) panicle array to a 1 x n panicle vector.
x=nonzeros(reshape(flipud(x)', 1, prod(size(x))))';
%rachis node counter, primary branch node counter, panicle vector index
nc=0; pnc=1; c=1;
%Read the panicle vector from left to right.
while c<= length(x);
%Annotate a grain that sank.
if x(c)==1;
```

```
c=c+1;
%Annotate a spikelet/grain that did not sink.
elseif x(c)==2;
c=c+1;
%Annotate the lack of a primary branch at the first rachis node.
elseif x(c)==3 & x(c+1)==3 & x(c+2)==3 & x(c+3)==3 & x(c+4)==3
x(c)=nc; nc=nc+10; x(c+1)=nc; x(c+2:c+4)=0; c=c+5;
%Annotate a jump to a secondary branch on the next rachis node.
elseif x(c)==3 & x(c+1)==3 & x(c+2)==3 & x(c+3)==3;
pnc=1; x(c)=nc; nc=nc+10; x(c+1)=nc+pnc; x(c+2)=0; x(c+3)=0; c=c+4;
%Annotate a jump to a primary branch on the next rachis node.
elseif x(c)==3 & x(c+1)==3 & x(c+2)==3;
x(c)=nc; nc=nc+10; x(c+1)=nc; x(c+2)=0; c=c+3;
%Annotate a jump to the next secondary branch on the same rachis node.
elseif x(c)==3 & x(c+1)==3;
x(c)=nc+pnc; pnc=pnc+1; x(c+1)=(nc+pnc); c=c+2;
%Annotate a jump from a secondary to primary branch on the same rachis node.
else
x=insert(x,c,nc); x(c)=nc+pnc; c=c+2;
end; end; Y=nonzeros(x)'; l=length(Y); Y(l+1)=nc;
```

Functions for Analyzing the Annotated Panicle Array

```
%nfs.m is a function that returns the number of filled spikelets in an annotated panicle
%vector (the input argument).
function y=nfs(pva)
y=sum(pva==1);
```

```
%ns.m is a function that returns the number of spikelets in an annotated panicle vector.
function y=ns(pva)
pva=or(pva==1,pva==2); y=sum(pva);

%numnodes.m is a function that returns the number of rachis nodes.
function y=numnodes(pva)
y=floor(max(pva)/10);

%numpbs.m is a function that returns the number of primary branches in an annotated
%panicle vector.
function n=numpbs(pva)
if(and(pva(1)==10, pva(2)==10))
n=floor(max(pva)/10)-1;
else
n=floor(max(pva)/10);
end;

%numsbs.m is a function that returns the number of secondary branches in an
%annotated panicle vector.
function n=numsbs(pva)
n=find(pva>2 & rem(pva,10)>0);
n=sum(length(n))/2;

%pbnfs.m is a function that returns the number of filled primary spikelets.
function a=pbnfs(pva)
a=nfs(pva)-sbnfs(pva);
```

```
%pbns.m is a function that returns the number of primary spikelets.
function a=pbns(pva)
a=ns(pva)-sbns(pva);

%sbnfs.m is a function that returns the number of filled secondary spikelets.
function y=sbnfs(pva)
on=-1;
for c=1:length(pva)
if and(pva(c)>10,rem(pva(c),10)>0)
on=on*-1;
elseif pva(c)==1 & on==1
pva(c)=3;
end
end
pva=pva==3;
y=sum(pva);

%sbns.m is a function that returns the number of secondary spikelets.
function [a]=sbns(pva)
on=-1;
for c=1:length(pva)
if and(pva(c)>10,rem(pva(c),10)>0)
on=on*-1;
elseif and(or(pva(c)==1, pva(c)==2),on==1)
pva(c)=3;
end
```

```
end
pva=pva==3;
a=sum(pva);
```

Function and Scripts for Drawing the Panicle Plot

```
%draw.m is a function that draws an annotated panicle array. The input argument is an
%annotated panicle array.
function x=draw(pva)
axis off; hold;
r=35; %distance between rachis nodes
s=5; %distance between secondary branches and primary spikelets
t=5; %distance between secondary spikelets
xo=0; yo=0; %first rachis node coordinates
xp=xo; yp=yo-r; %pen coordinates
yn=-r; %rachis node y
plot (xo,yo, 'ks'); %Plot first rachis node.
plot ([xp, xp], [yp, yp+r], 'k-'); %Draw peduncle.
i=1; %annotated panicle array index.
%Interpret the annotated panicle array from left to right.
while i<length(pva)
%Interpret a grain that sank.
if pva(i)==1
dfs; i=i+1;
%Interpret a spikelet/grain that did not sink.
elseif pva(i)==2
dufs; i=i+1;
%Interpret a jump to a secondary spikelet on the next rachis node.
```

```
elseif rem(pva(i),10)==1 & (sum(pva(i:length(pva))==pva(i))==2)
gtn; drf; dpbf; dsbf; i=i+1;
%Interpret a jump to the next secondary branch on the same rachis node.
elseif rem(pva(i),10)>1 & (sum(pva(i:length(pva))==pva(i))==2)
gbtpb; dpbf; dsbf; i=i+1;
elseif rem(pva(i),10)==0 & (sum(pva(i:length(pva))==pva(i))==2) & i>1 & ...
(pva(i)-pva(i-1))<1
gbtpb; i=i+1;
elseif rem(pva(i),10)==0 & (sum(pva(i:length(pva))==pva(i))==2)
gtn; drf; i=i+1;
else
i=i+1;
end; end;

%dfs.m is a script that draws a grain that sinks and a connecting short primary branch
%or secondary branch segment.
if opb==1 %Pen is on a primary branch.
plot([xp+s], [yp], 'ko'); %Plot a black o for a filled spikelet on a primary branch.
plot([xp xp+s],[yp yp],'k-'); %Draw a black primary branch segment.
xp=xp+s; %Advance the pen in x direction by length s.
end
if opb==0 %Pen is on a secondary branch.
plot([xp], [yp+t], 'ko'); %Plot a black o for a filled spikelet on a primary branch.
plot([xp xp],[yp yp+t],'k-') %Draw a black secondary branch segment.
yp=yp+t; %Advance the pen in the y direction by length t.
end
```

```
%dpbf.m draws a primary branch as a black line. It is used to connect a secondary
%branch to the rachis or it is used to connect sequential secondary branches.
opb=1; %Pen is on a primary branch.
plot([xp xp+s],[yp yp],'k-'); %Draw the primary branch as a black line of length s.
xp=xp+s; %Advance pen by length s.

%drf.m is a script that draws a rachis internode of length r.
opb=1; %Pen is on primary branch.
plot([xp xp],[yp yp+r],'k-'); %Draw the rachis branch as a black line of length r.
yp=yp+r; %Advance the pen by length r.
yn=yn+r; %Advance the node y coordinate by length r.

%dsbf.m draws a secondary branch fragment connected to a primary branch. The
%fragment will be drawn over when draw filled spikelet is called.
opb=0; %Pen is not on a primary branch.
plot([xp xp],[yp yp+t],'k-') %Draw the secondary branch fragment with a black line.
yp=yp+t; %Advance the pen in the y direction by length t.

%dufs.m is a script that draws a spikelet/grain that does not sink and a connecting
%short primary branch or secondary branch segment.
if opb==0
plot([xp], [yp+t], 'k*');
plot([xp xp],[yp yp+t],'k-')
yp=yp+t;
end
if opb==1
```

```
plot([xp+s], [yp], 'k*');
plot([xp xp+s],[yp yp],'k-');
xp=xp+s;
end

%gbtpb.m sets the pen y coordinate to the coordinate of the current rachis node.
opb=1; %Pen is on the primary branch.
yp=yn; %Pen y coordinate is set to the y coordinate of the connecting rachis node.

%gtn.m puts the pen back at the rachis node coordinates.
xp=xo;
yp=yn;
```

Functions for Aligning Annotated Panicle Arrays

```
%getbranch.m is a function that returns spikelets between their borders. The input
%arguments are an annotated panicle array and the border.
function [Y]=getbranch(x, b)
a=find(x==b);
Y=x(a(1):a(2));

%pvap.m transforms an annotated panicle array into an array that can be aligned. The
%input argument is an annotated panicle array.
function [A]=pvap(pva)
for b=10:10:10
T=[b+1 0 0 0 0 0 0 0 0 b+1 b+2 0 0 0 0 0 0 0 0 b+2 b+3 0 0 0 0 0 0 0 0 ...
b+3 b+4 0 0 0 0 0 0 0 0 b+4 b+5 0 0 0 0 0 0 0 0 b+5 b 0 0 0 0 0 0 0 0 0 0 0 b];
end
```

```
for b=20:10:200
Tn=[b+1 0 0 0 0 0 0 0 0 b+1 b+2 0 0 0 0 0 0 0 0 b+2 b+3 0 0 0 0 0 0 0 0 b+3 b+4 ...
0 0 0 0 0 0 0 0 b+4 b+5 0 0 0 0 0 0 0 0 b+5 b 0 0 0 0 0 0 0 0 0 0 0 0 b];
T=[T Tn];
end
x=find(pva>2);
for c=1:2:length(x)
wT=find(T==pva(x(c)));
wT=wT(1);
border=pva(x(c));
branch=getbranch(pva, border);
branchseg=branch(1:(length(branch)-1));
T(wT:(wT+length(branchseg)-1))=branchseg;
end
A=T;
```

REFERENCES

Abe T, Niiyama H, Sasahara T (2002) Cloning of cDNA for UDP-glucose pyrophosphorylase and the expression of mRNA in rice endosperm. Theoretical and Applied Genetics **105:** 216-221

Aoki N, Hirose T, Scofield GN, Whitfeld PR, Furbank RT (2003) The sucrose transporter gene family in rice. Plant and Cell Physiology **44:** 223-232

Aoki N, Hirose T, Takahashi S, Ono K, Ishimaru K, Ohsugi R (1999) Molecular cloning and expression analysis of a gene for a sucrose transporter in maize (*Zea mays* L.). Plant and Cell Physiology **40:** 1072-1078

Aoki N, Whitfeld P, Hoeren F, Scofield G, Newell K, Patrick J, Offler C, Clarke B, Rahman S, Furbank RT (2002) Three sucrose transporter genes are expressed in the developing grain of hexaploid wheat. Plant Molecular Biology **50:** 453-462

ap Rees TA, Hill SA (1994) Metabolic control analysis of plant metabolism. Plant, Cell and Environment **17:** 587-599

Asano T, Kunieda N, Omura Y, Ibe H, Kawasaki T, Takano M, Sato M, Furuhashi H, Mujin T, Takaiwa F, Wu C-Y, Tada Y, Satozawa T, Sakamoto M, Shimada H (2002) Rice SPK, a calmodulin-like domain protein kinase, is required for storage product accumulation during seed development: phosphorylation of sucrose synthase is a possible factor. The Plant Cell **14:** 619-628

Bacic A, Stone BA (1981a) Isolation and ultrastructure of aleurone cell walls from wheat and barley. Australian Journal of Plant Physiology **8:** 453-474

Bacic A, Stone BA (1981b) Chemistry and organization of aleurone cell wall components from wheat and barley. Australian Journal of Plant Physiology **8:** 475-495

Bagnall N, Wang X-D, Scofield GN, Furbank RT, Offler CE, Patrick JW (2000) Sucrose transport-related genes are expressed in both maternal and filial tissues of developing wheat grains. Australian Journal of Plant Physiology **27:** 1009-1020

Basham HG, Bateman DF (1975) Killing of plant cells by pectic enzymes: the lack of direct injurious interaction between pectic enzymes or their soluble reaction products and plant cells. Phytopathology **65:** 141-153

Bateman DF, Basham HG (1976) Degradation of plant cell walls and membranes by microbial enzymes. *In* R Heitefuss, PH Williams, eds, Encyclopedia of Plant Physiology, Vol 4. Springer-Verlag, New York, pp 317-355

Bateman DF, Millar RL (1966) Pectic enzymes in tissue degradation. Annual Review of Phytopathology **14:** 119-146

Bechtel DB, Pomeranz Y (1977) Ultrastructure of the mature ungerminated rice (*Oryza sativa*) caryopsis. The caryopsis coat and the aleurone cells. American Journal of Botany **64:** 966-973

Bethke PC, Hillmer S, Jones RL (1996) Isolation of intact protein storage vacuoles from barley aleurone- identification of aspartic and cysteine proteases. Plant Physiology **110:** 521-529

Bethke PC, Jones RL (2001) Cell death of barley aleurone protoplasts is mediated by reactive oxygen species. The Plant Journal **25:** 19-29

Bethke PC, Lonsdale JE, Fath A, Jones RL (1999) Hormonally regulated programmed cell death in barley aleurone cells. The Plant Cell **11:** 1033-1045

Bethke PC, Lonsdale JE, Swanson SJ, Jones RL (1997) GA and ABA regulate cell death in barley aleurone protoplasts. Plant Physiology **114:** 782-782

Borstlap AC, Schuurmans JAMJ (2004) Sucrose transport into plasma membrane vesicles from tobacco leaves by H^+ symport or counter exchange does not display a linear component. The Journal of Membrane Biology **198:** 31-42

Brown RC, Lemmon BE, Olsen OA (1996) Development of the endosperm in rice (*Oryza sativa* L.): cellularization. Journal of Plant Research **109:** 301-313

Buckhout TJ, Tubbe A (1996) Structure, mechanisms of catalysis, and regulation of sugar transporters in plants. *In* E Zamski, AA Schaffer, eds, Photoassimilate Distribution in Plants and Crops: Source-Sink Relationships. Marcel Dekker, Inc., New York, pp 229-260

Bush DR (1999) Sugar transporters in plant biology. Current Opinion in Plant Biology **2:** 187-191

Champagne ET, Wood DF, Juliano BO, Bechtel DB (2004) The rice grain and its gross composition. *In* ET Champagne, ed, Rice: Chemistry and Technology, Ed 3rd. American Association of Cereal Chemists, Inc., St. Paul, pp 77-107

Chapra SC, Canale RP (1998) Numerical Methods for Engineers, Ed 3rd. McGraw-Hill, Boston

Chen F, Foolad MR (1997) Molecular organization of a gene in barley which encodes a protein similar to aspartic protease and its specific expression in nucellar cells during degeneration. Plant Molecular Biology **35:** 821-831

Chen F, Foolad MR (1999) Nucellar-cell-specific expression of a lipid transfer protein gene in barley (*Hordeum vulgare* L.). Plant Cell Reports **18:** 445-450

Chino M, Hayashi H, Fukumorita T (1987) Chemical composition of rice phloem sap and its fluctuation. Journal of Plant Nutrition **10:** 1651-1661

Cochrane MP (1994) Observations on the germ aleurone of barley. Morphology and histochemistry. Annals of Botany **73:** 113-119

Cocking EC (1972) Plant cell protoplasts- isolation and development. Annual Review of Plant Physiology **23:** 29-50

Counce PA, Keisling TC, Mitchell AJ (2000) A uniform, objective, and adaptive system for expressing rice development. Crop Science **40:** 436-443

Darussalam, Cole MA, Patrick JW (1998) Auxin control of photoassimilate transport to and within developing grains of wheat. Australian Journal of Plant Physiology **25:** 69-77

Davies TGE, Steele SH, Walker DJ, Leigh RA (1996) An analysis of vacuole development in oat aleurone protoplasts. Planta **198:** 356-364

De Jong A, Borstlap AC (2000a) Transport of amino acids (L-valine, L-lysine, L-glutamic acid) and sucrose into plasma membrane vesicles isolated from cotyledons of developing pea seeds. Journal of Experimental Botany **51:** 1663-1670

De Jong A, Borstlap AC (2000b) A plasma membrane-enriched fraction isolated from the coats of developing pea seeds contains H^+-symporters for amino acids and sucrose. Journal of Experimental Botany **51:** 1671-1677

De Boer AH, Van Duijn B, Giesberg P, Wegner L, Obermeyer G, Kohler K, Linz KW (1994) Laser microsurgery: a versatile tool in plant (electro) physiology. Protoplasma **178:** 1-10

Díaz I (1994) Optimization of conditions for DNA uptake and transient GUS expression in protoplasts for different tissues of wheat and barley. Plant Science **96:** 179-187

Domínguez F, Moreno J, Cejudo FJ (2001) The nucellus degenerates by a process of programmed cell death during the early stages of wheat grain development. Planta **213:** 352-360

Dropkin VH (1969) Cellular responses of plants to nematode infections. Annual Review of Phytopathology **7:** 101-122

Eastwood D (1977) Responses of enzymically isolated aleurone cells of oat to gibberellin A_3. Plant Physiology **60:** 457-459

Echeverria E, Boyer C, Liu K-C, Shannon J (1985) Isolation of amyloplasts from developing maize endosperm. Plant Physiology **77:** 513-519

Ellis JR, Chaffey NJ (1987) Structural differentiation of the nucellar epidermis in the caryopsis of rice (*Oryza sativa*). Annals of Botany **60:** 671-675

Ellis JR, Gates PJ, Boulter D (1987) Storage-protein deposition in the developing rice caryopsis in relation to the transport tissues. Annals of Botany **60:** 663-670

Entwistle G, Tyson RH, ap Rees T (1988) Isolation of amyloplasts from wheat endosperm. Phytochemistry **27:** 993-996

Farrar JF (1996) Sinks- integral parts of a whole plant. Journal of Experimental Botany **47:** 1273-1279

Felker FC, Thomas PA, Crawford CG (1991) Isolation and sugar uptake characteristics of protoplasts from maize endosperm suspension cultures. Physiologia Plantarum **81:** 83-88

Fisher DB, Cash-Clark CE (2000a) Sieve tube unloading and post-phloem transport of fluorescent tracers and proteins injected into sieve tubes via severed aphid stylets. Plant Physiology **123:** 125-137

Fisher DB, Cash-Clark CE (2000b) Gradients in water potential and turgor pressure along the translocation pathway during grain filling in normally watered and water-stressed wheat plants. Plant Physiology **123:** 139-147

Fisher DB, Gifford RM (1986) Accumulation and conversion of sugars by developing wheat grains. VI. Gradients along the transport pathway from the peduncle to the endosperm cavity during grain filling. Plant Physiology **82:** 1024-1030

Fisher DB, Oparka KJ (1996) Post-phloem transport: principles and problems. Journal of Experimental Botany **47:** 1141-1154

Fisher DB, Wang N (1993) A kinetic and microautoradiographic analysis of [^{14}C] sucrose import by developing wheat grains. Plant Physiology **101:** 391-398

Fisher DB, Wang N (1995) Sucrose concentration gradients along the post-phloem transport pathway in the maternal tissues of developing wheat grains. Plant Physiology **109:** 587-592

Fry SC (1986) Cross-linking of matrix polymers in the growing cell walls of angiosperms. Annual Review of Plant Physiology **37:** 165-186

Fukumorita T, Chino M (1982) Sugar, amino acid and inorganic contents in rice phloem sap. Plant and Cell Physiology **23:** 273-283

Furbank RT, Scofield GN, Hirose T, Wang X-D, Patrick JW, Offler CE (2001) Cellular localisation and function of a sucrose transporter *OsSUT1* in developing rice grains. Australian Journal of Plant Physiology **28:** 1187-1196

Gilroy S, Jones RL (1994) Perception of gibberellin and abscisic acid at the external face of the plasma membrane of barley (*Hordeum vulgare* L.) aleurone protoplasts. Plant Physiology **104:** 1185-1192

Gopalakrishnan B, Sonthayanon B, Rahmatullah R, Muthukrishnan S (1991) Barley aleurone layer cell protoplasts as a transient expression system. Plant Molecular Biology **16:** 463-467

Hayama R, Coupland G (2004) The molecular basis of diversity in the photoperiodic flowering responses of *Arabidopsis* and rice. Plant Physiology **135:** 677-684

Hayashi H, Chino M (1990) Chemical composition of phloem sap from the uppermost internode of the rice plant. Plant and Cell Physiology **31:** 247-251

He Z, Zhu Q, Dabi T, Li D, Weigel D, Lamb C (2000) Transformation of rice with the *Arabidopsis* floral regulator *LEAFY* causes early heading. Transgenic Research **9:** 223-227

Heimovaara-Dijkstra S, Van Duijn B, Libbenga KR, Heidekamp F, Wang M (1994) Abscisic acid-induced membrane potential changes in barley aleurone protoplasts: a possible relevance for the regulation of rab gene expression. Plant and Cell Physiology **35:** 743-750

Hillmer S, Bush DS, Robinson DG, Zingen-Sell I, Jones RL (1990) Barley aleurone protoplasts are structurally and functionally similar to the walled cells of aleurone layers. European Journal of Cell Biology **52:** 169-173

Hirose T, Endler A, Ohsugi R (1999) Gene expression of enzymes for starch and sucrose metabolism and transport in leaf sheaths of rice (*Oryza sativa* L.) during the heading period in relation to the sink to source transition. Plant Production Science **2:** 178-183

Hirose T, Imaizumi N, Scofield GN, Furbank RT, Ohsugi R (1997) cDNA cloning and tissue specific expression of a gene for sucrose transporter from rice (*Oryza sativa* L.). Plant and Cell Physiology **38:** 1389-1396

Hirose T, Takano M, Terao T (2002) Cell wall invertase in developing rice caryopsis: molecular cloning of *OsCIN1* and analysis of its expression in relation to its role in grain filling. Plant and Cell Physiology **43:** 452-459

Hooley R (1982) Protoplasts isolated from aleurone layers of wild oat (*Avena fatua* L.) exhibit the classic response to gibberellic acid. Planta **154:** 29-40

Horigane AK, Engelaar WMHG, Maruyama S, Yoshida M, Okubo A, Nagata T (2001) Visualisation of moisture distribution during development of rice caryopses (*Oryza sativa* L.) by nuclear magnetic resonance microimaging. Journal of Cereal Science **33:** 105-114

Hoshikawa K (1989) The Growing Rice Plant. Nobunkyo, Tokyo

Hoshikawa K (1993) Anthesis, fertilization and development of the caryopsis. *In* T Matsuo, K Hoshikawa, eds, Science of the Rice Plant, Vol 1. Food and Agricultural Policy Research Center, Tokyo, pp 339-376

Ishii S (1976) Enzymatic maceration of plant tissues by endo-pectin lyase and endo-polygalacturonase from *Aspergillus japonicus*. Phytopathology **66:** 281-289

Ishimaru K, Hirose T, Aoki N, Takahashi S, Ono K, Yamamoto S, Wu J, Saji S, Baba T, Ugaki M, Matsumoto T, Ohsugi R (2001) Antisense expression of a rice sucrose transporter OsSUT1 in rice (*Oryza sativa* L.). Plant and Cell Physiology **42:** 1181-1185

Ishimaru T, Matsuda T, Ohsugi R, Yamagishi T (2003) Morphological development of rice caryopses located at the different positions in a panicle from early to middle stage of grain filling. Functional Plant Biology **30:** 1139-1149

Itoh J-I, Hasegawa A, Kitano H, Nagato Y (1998) A recessive heterochronic mutation, *plastochron1*, shortens the plastochron and elongates the vegetative phase in rice. The Plant Cell **10:** 1511-1521

Iwai H, Masaoka N, Ishii T, Satoh S (2002) A pectin glucuronyltransferase gene is essential for intercellular attachment in the plant meristem. Proceedings of the National Academy of Sciences of the United States of America **99:** 16319-16324

Izawa T, Oikawa T, Sugiyama N, Tanisaka T, Yano M, Shimamoto K (2002) Phytochrome mediates the external light signal to repress *FT* orthologs in photoperiodic flowering of rice. Genes and Development **16:** 2006-2020

Izawa T, Oikawa T, Tokutomi S, Okuno K, Shimamoto K (2000) Phytochromes confer the photoperiodic control of flowering in rice (a short-day plant). The Plant Journal **22:** 391-399

Izawa T, Takahashi Y, Yano M (2003) Comparative biology comes into bloom: genomic and genetic comparison of flowering pathways in rice and *Arabidopsis*. Current Opinion in Plant Biology **6:** 113-120

Jacobsen JV, Zwar JA, Chandler PM (1985) Gibberellic-acid-responsive protoplasts from mature aleurone of Himalaya barley. Planta **163:** 430-438

James MG, Denyer K, Myers AM (2003) Starch synthesis in the cereal endosperm. Current Opinion in Plant Biology **6:** 215-222

Jarvis MC, Briggs SPH, Knox JP (2003) Intercellular adhesion and cell separation in plants. Plant, Cell and Environment **26:** 977-989

Jenner CF (1970) Relationship between levels of soluble carbohydrate and starch synthesis in detached ears of wheat. Australian Journal of Biological Sciences **23:** 991-1003

Jenner CF (1974) Factors in the grain regulating the accumulation of starch. *In* RL Bieleski, AR Ferguson, MM Cresswell, eds, Mechanisms of Regulation of Plant Growth. The Royal Society of New Zealand, Wellington, pp 901-908

Jenner CF, Rathjen AJ (1972a) Factors limiting the supply of sucrose to developing wheat grain. Annals of Botany **36:** 729-741

Jenner CF, Rathjen AJ (1972b) Limitations to the accumulation of starch in the developing wheat grain. Annals of Botany **36:** 743-754

Jenner CF, Rathjen AJ (1975) Factors regulating the accumulation of starch in ripening wheat grain. Australian Journal of Plant Physiology **2:** 311-322

Jenner CF, Rathjen AJ (1977) Supply of sucrose and its metabolism in developing grains of wheat. Australian Journal of Plant Physiology **4:** 691-701

Jenner CF, Ugalde TD, Aspinall D (1991) The physiology of starch and protein deposition in the endosperm of wheat. Australian Journal of Plant Physiology **18:** 211-226

Jennings PR, Coffman WR, Kauffman HE (1979) Rice Improvement. International Rice Research Institute, Los Baños

Kato T, Takeda K (1993) Endogenous abscisic acid in developing grains on primary and secondary branches of rice (*Oryza sativa* L.). Japanese Journal of Crop Science **62:** 636-637

Kazaryan GT, Artsruni IG, Panosyan GA (1981) Membrane potential in cells of the aleurone layer of wheat seeds. Soviet Plant Physiology **28:** 851-855

Keeling PL, Baird S, Tyson RH (1989) Isolation and properties of protoplasts from endosperm of developing wheat grain. Plant Science **65:** 55-62

Klepper B, Rickman RW, Peterson CM (1982) Quantitative characterization of vegetative development in small cereal grains. Agronomy Journal **74:** 789-792

Kobayasi K, Imaki T (1997) Varietal differences of rice in differentiation and degeneration of secondary rachis-branches and spikelets in terms of their nodal distribution on a rachis. Japanese Journal of Crop Science **66:** 578-587

Kobayasi K, Imaki T, Horie T (2001) Relationship between the size of the apical dome at the panicle initiation and the panicle components in rice. Plant Production Science **4:** 81-87

Kojima S, Takahashi Y, Kobayashi Y, Monna L, Sasaki T, Araki T, Yano M (2002) *Hd3a*, a rice ortholog of the *Arabidopsis FT* gene, promotes transition to flowering downstream of *Hd1* under short-day conditions. Plant and Cell Physiology **43:** 1096-1105

Koller A, Washburn MP, Lange BM, Andon NL, Deciu C, Haynes PA, Hays L, Schieltz D, Ulaszek R, Wei J, Wolters D, Yates III JR (2002) Proteomic survey of metabolic pathways in rice. Proceedings of the National Academy of Sciences of the United States of America **99:** 11969-11974

Komatsu M, Maekawa M, Shimamoto K, Kyozuka J (2001) The *LAX1* and *FRIZZY PANICLE 2* genes determine the inflorescence architecture of rice by controlling rachis-branch and spikelet development. Developmental Biology **231:** 364-373

Krishnan S, Dayanandan P (2003) Structural and histochemical studies on grain-filling in the caryopsis of rice (*Oryza sativa* L.). Journal of Biosciences **28:** 455-469

Krishnan S, Ebenezer GAI, Dayanandan P (2001) Histochemical localization of storage components in caryopsis of rice (*Oryza sativa* L.). Current Science **80:** 567-571

Kurkdjian A, Leitz G, Manigault P, Harim A, Greulich KO (1993) Non-enzymatic access to the plasma membrane of *Medicago* root hairs by laser microsurgery. Journal of Cell Science **105:** 263-268

Kyozuka J, Konishi S, Nemoto K, Izawa T, Shimamoto K (1998) Down-regulation of *RFL*, the *FLO/LFY* homolog of rice, accompanied with panicle branch initiation. Proceedings of the National Academy of Sciences of the United States of America **95:** 1979-1982

Lalonde S, Tegeder M, Throne-Holst M, Frommer WB, Patrick JW (2003) Phloem loading and unloading of sugars and amino acids. Plant, Cell and Environment **26:** 37-56

Lalonde S, Wipf D, Frommer WB (2004) Transport mechanisms for organic forms of carbon and nitrogen between source and sink. Annual Review of Plant Biology **55:** 341-372

Lee B, Murdoch K, Topping J, Kreis M, Jones MG (1989) Transient gene expression in aleurone protoplasts isolated from developing caryopses of barley and wheat. Plant Molecular Biology **13:** 21-29

Lee-Stadelmann O, Stadelmann EJ (1989) Plasmolysis and deplasmolysis. *In* S Fleisher, B Fleisher, eds, Methods in Enzymology, Vol 174. Academic Press, New York, pp 225-246

Li X, Qian Q, Fu Z, Wang Y, Xiong G, Zeng D, Wang X, Liu X, Teng S, Hiroshi F, Yuan M, Luo D, Han B, Li J (2003) Control of tillering in rice. Nature **422:** 618-621

Lichtner FT, Spanswick RM (1981a) Electrogenic sucrose transport in developing soybean cotyledons. Plant Physiology **67:** 869-874

Lichtner FT, Spanswick RM (1981b) Sucrose uptake by developing soybean cotyledons. Plant Physiology **68:** 693-698

Lingle SE, Chevalier P (1985) Development of the vascular tissue of wheat and barley caryopsis as related to the rate and duration of grain filling. Crop Science **25:** 123-128

Linnestad C, Doan DNP, Brown RC, Lemmon BE, Meyer DJ, Jung R, Olsen O-A (1998) Nucellain, a barley homolog of the dicot vacuolar-processing protease, is localized in nucellar cell walls. Plant Physiology **118:** 1169-1180

Matsukura C-A, Saitoh T, Hirose T, Ohsugi R, Perata P, Yamaguchi J (2000) Sugar uptake and transport in rice embryo. Expression of companion cell-specific sucrose transporter (*OsSUT1*) induced by sugar and light. Plant Physiology **124:** 85-93

Matsushima S (1967) Crop Science in Rice: Theory of Yield Determination and its Application. Fuji Publishing Co., Ltd., Tokyo

McClung AM, Marchetti MA, Webb BD, Bollich CN (1997) Registration of 'Jefferson' rice. Crop Science **37:** 629-630

Mitra S, Bera AK (2003) Influence of grain density on some qualitative characters of rice (*Oryza sativa* L.). Crop Research **25:** 400-405

Miyoshi K, Ahn B-O, Kawakatsu T, Ito Y, Itoh J-I, Nagato Y, Kurata N (2004) *PLASTOCHRON1*, a timekeeper of leaf initiation in rice, encodes cytochrome P450. Proceedings of the National Academy of Sciences of the United States of America **101:** 875-880

Mohapatra PK, Masamoto Y, Morita S, Takanashi J, Kato T, Itani T, Adu-Gyamfi JJ, Shunmugasundaram M, Nguyen NT, Saneoka H, Fujita K (2004) Partitioning of ^{13}C-labelled photosynthate varies with growth stage and panicle size in high-yielding rice. Functional Plant Biology **31:** 131-139

Mohapatra PK, Naik PK, Patel R (2000) Ethylene inhibitors improve dry matter partitioning and development of late flowering spikelets on rice panicles. Australian Journal of Plant Physiology **27:** 311-323

Mohapatra PK, Patel R, Sahu SK (1993) Time of flowering affects grain quality and spikelet partitioning within the rice panicle. Australian Journal of Plant Physiology **20:** 231-241

Mollet J-C, Park S-Y, Nothnagel EA, Lord EM (2000) A lily stylar pectin is necessary for pollen tube adhesion to an *in vitro* stylar matrix. The Plant Cell **12:** 1737-1749

Mori S, Nishizawa N, Hayashi H, Chino M, Yoshimura E, Ishihara J (1991) Why are young rice plants highly susceptible to iron deficiency? Plant and Soil **130:** 143-156

Mu C, Yamagishi J (2001) Effects of gibberellic acid application on panicle characteristics and size of shoot apex in the first bract differentiation stage in rice. Plant Production Science **4:** 227-229

Murai M, Iizawa M (1994) Effects of major genes controlling morphology of panicle in rice. Breeding Science **44:** 247-255

Murai M, Sato S, Nagayama A, Ishii N, Ihashi S (2002) Effects of a major gene *Ur1* characterized by undulation of rachis branches on yield and its related traits in rice. Breeding Science **52:** 299-307

Murthy PPN (1989) A fast and easy technique for the isolation of aleurone layers. Plant Physiology **90:** 388-389

Nakamura T, Hours RA, Sakai T (1995) Enzymatic maceration of vegetables with protopectinases. Journal of Food Science **60:** 468-472

Nemoto K, Morita S, Baba T (1995) Shoot and root development in rice related to the phyllochron. Crop Science **35:** 24-29

Niemietz C, Jenner CF (1993) Mechanisms of sugar uptake into endosperm and aleurone protoplasts isolated from developing wheat grains. Australian Journal of Plant Physiology **20:** 371-378

Nishimura M, Hara-Nishimura I, Akazawa T (1987) Preparation of protoplasts from plant tissues for organelle isolation. *In* L Packer, R Douce, eds, Methods in Enzymology, Vol 148. Academic Press, San Diego, pp 27-34

Okano K, Kono Y (1993) Partitioning of ^{15}N applied at reproductive stages among grains and in grain tissues of rice plants. Japanese Journal of Crop Science **62:** 577-584

Okawa S, Makino A, Mae T (2002) Shift of the major sink from the culm to the panicle at the early stage of grain filling in rice (*Oryza sativa* L. cv. Sasanishiki). Soil Science and Plant Nutrition **48:** 237-242

Olsen O-A (2001) Endosperm development: cellularization and cell fate specification. Annual Review of Plant Physiology and Plant Molecular Biology **52:** 233-267

Oparka KJ (1994) Plasmolysis: new insights into an old process. New Phytologist **126:** 571-591

Oparka KJ, Gates P (1981a) Transport of assimilates in the developing caryopsis of rice (*Oryza sativa* L.). Ultrastructure of the pericarp vascular bundle and its connections with the aleurone layer. Planta **151:** 561-573

Oparka KJ, Gates P (1981b) Transport of assimilates in the developing caryopsis of rice (*Oryza sativa* L.). The pathways of water and assimilated carbon. Planta **152:** 388-396

Oparka KJ, Gates PJ (1982) Ultrastructure of the developing pigment strand of rice (*Oryza sativa* L.) in relation to its role in solute transport. Protoplasma **113:** 33-43

Oparka KJ, Prior DAM (1992) Direct evidence for pressure-generated closure of plasmodesmata. The Plant Journal **2:** 741-750

Pao SS, Paulsen IT, Saier Jr. MH (1998) Major facilitator superfamily. Microbiology and Molecular Biology Reviews **62:** 1-34

Park S-Y, Jauh G-Y, Mollet J-C, Eckard KJ, Nothnagel EA, Walling LL, Lord EM (2000) A lipid transfer-like protein is necessary for lily pollen tube adhesion to an *in vitro* stylar matrix. The Plant Cell **12:** 151-163

Patel R, Mohapatra PK (1996) Assimilate partitioning within floret components of contrasting rice spikelets producing qualitatively different types of grains. Australian Journal of Plant Physiology **23:** 85-92

Patrick JW, Offler CE (1996) Post-sieve element transport of photoassimilates in sink regions. Journal of Experimental Botany **47:** 1165-1177

Patrick JW, Offler CE, Wang HL, Wang X-D, Jin S-P, Zhang W-C, Ugalde TD, Jenner CF, Wang N, Fisher DB, Felker FC, Thomas PA, Crawford CG (1991) Assimilate transport in developing cereal grain. *In* JL Bonnemain, S Delrot, WJ Lucas, J Dainty, eds, Recent Advances in Phloem Transport and Assimilate Compartmentation. Quest Editions, Nantes

Paul MJ, Foyer CH (2001) Sink regulation of photosynthesis. Journal of Experimental Botany **52:** 1383-1400

Phillips M, Paleg LG (1970) The isolated aleurone layer. *In* International Conference on Plant Growth Substances, pp 396-406

Power JB, Cummins SE, Cocking EC (1970) Fusion of isolated plant protoplasts. Nature **225:** 1016-1018

Qu LQ, Takaiwa F (2004) Evaluation of tissue specificity and expression strength of rice seed component gene promoters in transgenic rice. Plant Biotechnology Journal **2:** 113-125

Regierer B, Fernie AR, Springer F, Perez-Melis A, Leisse A, Koehl K, Willmitzer L, Geigenberger P, Kossmann J (2002) Starch content and yield increase as a result of altering adenylate pools in transgenic plants. Nature Biotechnology **20:** 1256-1260

Robbins KM, Bhuvarahamurthy N, Pliska-Matyshak G, Murthy PPN (1999) The isolation and characterization of right-side-out plasma membrane vesicles from barley aleurone cells. Lipids **34:** 75-82

Rosche E, Blackmore D, Tegeder M, Richardson T, Schroeder H, Higgins TJV, Frommer WB, Offler CE, Patrick JW (2002) Seed-specific overexpression of a potato sucrose transporter increases sucrose uptake and growth rates of developing pea cotyledons. The Plant Journal **30:** 165-175

Sadasivam R, Kailasam C, Chandrababu R, Arjunan A, Nagarajan M, Rangasamy SRS (1990) Developing a functional model of rice panicle growth. International Rice Research Newsletter **15:** 9

Sadasivam S, Gallie DR (1994) Isolation and transformation of rice aleurone protoplasts. Plant Cell Reports **13:** 394-396

Sasaki T (2003) Rice genome analysis: understanding the genetic secrets of the rice plant. Breeding Science **53:** 281-289

Sato S, Ishikawa S, Shimono M, Shinjyo C (1996) Genetic studies on an awnness gene *An-4* on chromosome 8 in rice, *Oryza sativa* L. Breeding Science **46:** 321-327

Scofield GN, Hirose T, Gaudron JA, Upadhyaya NM, Ohsugi R, Furbank RT (2002) Antisense suppression of the rice sucrose transporter gene, *OsSUT1*, leads to impaired grain filling and germination but does not affect photosynthesis. Functional Plant Biology **29:** 815-826

Shibuya N, Nakane R (1984) Pectic polysaccharides of rice endosperm cell walls. Phytochemistry **23:** 1425-1429

Shimada H, Koishihara H, Saito Y, Arashima Y, Furukawa T, Hayashi H (2004) A rice antisense SPK transformant that lacks the accumulation of seed storage substances shows no correlation between sucrose concentration in phloem sap and demand for carbon sources in the sink organs. Plant and Cell Physiology **45:** 1105-1109

Sikka VK, Choi S-B, Kavakli IH, Sakulringharoj C, Gupta S, Ito H, Okita TW (2001) Subcellular compartmentation and allosteric regulation of the rice endosperm ADP-glucose pyrophosphorylase. Plant Science **161:** 461-468

Singh BK, Jenner CF (1982) Association between concentrations of organic nutrients in the grain, endosperm cell number and grain dry weight within the ear of wheat. Australian Journal of Plant Physiology **9:** 83-95

Singh R, Juliano BO (1977) Free sugars in relation to starch accumulation in developing rice grain. Plant Physiology **59:** 417-421

Smidansky ED, Clancy M, Meyer FD, Lanning SP, Blake NK, Talbert LE, Giroux MJ (2002) Enhanced ADP-glucose pyrophosphorylase activity in wheat endosperm increases seed yield. Proceedings of the National Academy of Sciences of the United States of America **99:** 1724-1729

Smidansky ED, Martin JM, Hannah LC, Fischer AM, Giroux MJ (2003) Seed yield and plant biomass increases in rice are conferred by deregulation of endosperm ADP-glucose pyrophosphorylase. Planta **216:** 656-664

Smirnova TA, Kintsurashvili LN, Manamsh'yan TA, Noskov VA, Kir'yanov GI (1989) Isolated cells of barley aleurone layer as a model for investigating changes in the chromatin structure of individual genes during induction of expression by phytohormones. Biochemistry-Moscow **54:** 350-357

Spanswick RM (1981) Electrogenic ion pumps. Annual Review of Plant Physiology **32:** 267-289

Sung H-Y, Huang W-C (1994) Purification and characterization of cell-wall-bound invertase from rice (*Oryza sativa*) grains. Biotechnology and Applied Biochemistry **19:** 75-83

Suzuki Y, Kitagawa M, Knox JP, Yamaguchi I (2002) A role for arabinogalactan proteins in gibberellin-induced α-amylase production in barley aleurone cells. The Plant Journal **29:** 733-741

Taiz L, Jones RL (1971) The isolation of barley-aleurone protoplasts. Planta **101:** 95-100

Takebe I, Otsuki Y, Aoki S (1968) Isolation of tobacco mesophyll cells in intact and active state. Plant and Cell Physiology **9:** 115-124

Takeoka Y, Shimizu M, Wada T (1993) Panicles. *In* T Matsuo, K Hoshikawa, eds, Science of the Rice Plant, Vol 1. Food and Agricultural Policy Research Center, Tokyo, pp 295-338

Tanaka N, Fujita M, Handa H, Murayama S, Uemura M, Kawamura Y, Mitsui T, Mikami S, Tozawa Y, Yoshinaga T, Komatsu S (2004) Proteomics of the rice cell: systematic identification of the protein populations in subcellular compartments. Molecular Genetics and Genomics **271:** 566-576

Tivet F, Pinheiro BD, De Raïssac M, Dingkuhn M (2001) Leaf blade dimensions of rice (*Oryza sativa* L. and *Oryza glaberrima* Steud.). Relationships between tillers and the main stem. Annals of Botany **88:** 507-511

Trebacz K, Schonknecht G (2000) Simple method to isolate vacuoles and protoplasts for patch-clamp experiments. Protoplasma **213:** 39-45

Tsukaguchi T, Horie T, Koshioka M (1999) Dynamics of abscisic acid levels during grain-filling in rice: comparisons between superior and inferior spikelets. Plant Production Science **2:** 223-226

Usui H, Maeda M, Ito M (1974) High frequency of spontaneous fusion in protoplasts from various plant tissues. Botanical Magazine-Tokyo **87:** 179-182

Van Dongen JT, Laan RGW, Wouterlood M, Borstlap AC (2001) Electrodiffusional uptake of organic cations by pea seed coats. Further evidence for poorly selective pores in the plasma membrane of seed coat parenchyma cells. Plant Physiology **126:** 1688-1697

Van Duijn B, Heimovaara-Dijkstra S (1994) Intracellular microelectrode membrane potential measurements in tobacco cell-suspension protoplasts and barley aleurone protoplasts: interpretation and artifacts. Biochimica et Biophysica Acta **1193:** 77-84

Vergara BS, Chang TT (1985) The Flowering Response of the Rice Plant to Photoperiod: a Review of the Literature. IRRI, Los Baños

Walker RP, Waterworth WM, Hooley R (1993) Preparation and polypeptide composition of plasma membrane and other subcellular fractions from wild oat (*Avena fatua*) aleurone. Physiologia Plantarum **89:** 388-398

Wang HL, Offler CE, Patrick JW (1995a) The cellular pathway of photosynthate transfer in the developing wheat grain. II. A structural analysis and histochemical studies of the pathway from the crease phloem to the endosperm cavity. Plant, Cell and Environment **18:** 373-388

Wang HL, Offler CE, Patrick JW, Ugalde TD (1994) The cellular pathway of photosynthate transfer in the developing wheat grain. I. Delineation of a potential transfer pathway using fluorescent dyes. Plant, Cell and Environment **17:** 257-266

Wang HL, Patrick JW, Offler CE, Wang XD (1995b) The cellular pathway of photosynthate transfer in the developing wheat grain. III. A structural analysis and physiological studies of the pathway from the endosperm cavity to the starchy endosperm. Plant, Cell and Environment **18:** 389-407

Wang HL, Patrick JW, Offler CE, Wardlaw IF (1993) A novel experimental system for studies of photosynthate transfer in the developing wheat grain. Journal of Experimental Botany **44:** 1177-1184

Wang N, Fisher DB (1994a) Monitoring phloem unloading and post-phloem transport by microperfusion of attached wheat grains. Plant Physiology **104:** 7-16

Wang N, Fisher DB (1994b) The use of fluorescent tracers to characterize the post-phloem transport pathway in maternal tissues of developing wheat grains. Plant Physiology **104:** 17-27

Wang N, Fisher DB (1995) Sucrose release into the endosperm cavity of wheat grains apparently occurs by facilitated diffusion across the nucellar cell membranes. Plant Physiology **109:** 579-585

Wang Q, Chen J, Wang X, Sun J, Sha W (2002) Molecular cloning and expression analysis of the rice triose phosphate/phosphate translocator gene. Plant Science **162:** 785-790

Weschke W, Panitz R, Sauer N, Wang Q, Neubohn B, Weber H, Wobus U (2000) Sucrose transport into barley seeds: molecular characterization of two transporters and implications for seed development and starch accumulation. The Plant Journal **21:** 455-467

Withers LA, Cocking EC (1972) Fine-structural studies on spontaneous and induced fusion of higher plant protoplasts. Journal of Cell Science **11:** 59-75

Wright KM, Oparka KJ (1994) Physicochemical properties alone do not predict the movement and compartmentation of fluorescent xenobiotics. Journal of Experimental Botany **45:** 35-44

Xu XB, Vergara BS (1986) Morphological changes in rice panicle development. A review of literature. IRRI Research Paper Series **117:** 1-13

Yamagishi J, Nemoto K, Mu C (2003) Diversity of the rachis-branching system in a panicle in japonica rice. Plant Production Science **6:** 59-64

Yamaki S, Nagato Y (2001) *GYPSY EMBRYO* gene controls embryo position by regulating integument development. Rice Genetics Newsletter **18:** 24-26

Yang J, Peng S, Visperas RM, Sanico AL, Zhu Q, Gu S (2000) Grain filling pattern and cytokinin content in the grains and roots of rice plants. Plant Growth Regulation **30:** 261-270

Yang J, Zhang J, Huang Z, Wang Z, Zhu Q, Liu L (2002) Correlation of cytokinin levels in the endosperms and roots with cell number and cell division activity during endosperm development in rice. Annals of Botany **90:** 369-377

Yang J, Zhang J, Wang Z, Zhu Q, Liu L (2003) Activities of enzymes involved in sucrose-to-starch metabolism in rice grains subjected to water stress during filling. Field Crops Research **81:** 69-81

Yang J, Zhang J, Wang Z, Zhu Q, Wang W (2001) Hormonal changes in the grains of rice subjected to water stress during grain filling. Plant Physiology **127:** 315-323

Yang JC, Zhang JH, Ye YX, Wang ZQ, Zhu QS, Liu LJ (2004) Involvement of abscisic acid and ethylene in the responses of rice grains to water stress during filling. Plant, Cell and Environment **27:** 1055-1064

Yano M, Katayose Y, Ashikari M, Yamanouchi U, Monna L, Fuse T, Baba T, Yamamoto K, Umehara Y, Nagamura Y, Sasaki T (2000) *Hd1*, a major photoperiod sensitivity quantitative trait locus in rice, is closely related to the *Arabidopsis* flowering time gene *CONSTANS*. The Plant Cell **12:** 2473-2483

Yano M, Kojima S, Takahashi Y, Lin H, Sasaki T (2001) Genetic control of flowering time in rice, a short-day plant. Plant Physiology **127:** 1425-1429

Ye G-N, Earle ED (1991) Effect of cellulases on spontaneous fusion of maize protoplasts. Plant Cell Reports **10:** 213-216

Yin X, Kropff MJ (1998) The effect of photoperiod on interval between panicle initiation and flowering in rice. Field Crops Research **57:** 301-307

Yokota T, Nakayama M, Harasawa I, Sato M, Katsuhara M, Kawabe S (1994) Polyamines, indole-3-acetic acid and abscisic acid in rice phloem sap. Plant Growth Regulation **15:** 125-128

Yoshida S (1972) Physiological aspects of grain yield. Annual Review of Plant Physiology **23:** 437-464

Young TE, Gallie DR (2000) Programmed cell death during endosperm development. Plant Molecular Biology **44:** 283-301

Zaitlin M (1959) Isolation of tobacco leaf cells capable of supporting virus multiplication. Nature **184:** 1002-1003

Zaitlin M, Coltrin D (1964) Use of pectic enzymes in a study of the nature of intercellular cement of tobacco leaf cells. Plant Physiology **39:** 91-95

Zee S-Y (1972) Vascular tissue and transfer cell distribution in the rice spikelet. Australian Journal of Biological Sciences **25:** 411-414

Zhu Q, Cao X, Luo Y (1988) Growth analysis on the process of grain filling in rice. Acta Agronomica Sinica **14:** 182-193

Zhu T, Budworth P, Chen W, Provart N, Chang H-S, Guimil S, Su W, Estes B, Zou G, Wang X (2003) Transcriptional control of nutrient partitioning during rice grain filling. Plant Biotechnology Journal **1:** 59-70